Report 2142

DEPARTMENT OF THE NAVY

DAVID TAYLOR MODEL BASIN
WASHINGTON, D.C.

HYDROMECHANICS

o

AERODYNAMICS

o

STRUCTURAL MECHANICS

o

APPLIED MATHEMATICS

o

ACOUSTICS AND VIBRATION

TRANSIENT RESPONSE OF A DAMPED MECHANICAL OSCILLATOR ATTACHED TO A SHOCK-WAVE-EXCITED, SUBMERGED CYLINDRICAL SHELL

by

Thomas L. Geers

and

Miguel C. Junger

Cambridge Acoustical Associates, Inc.

Distribution of this document is unlimited.

STRUCTURAL MECHANICS LABORATORY
RESEARCH AND DEVELOPMENT REPORT

March 1966

Report 2142

DAVID TAYLOR MODEL BASIN
WASHINGTON, D. C. 20007

TRANSIENT RESPONSE OF A DAMPED MECHANICAL OSCILLATOR ATTACHED TO A SHOCK-WAVE-EXCITED, SUBMERGED CYLINDRICAL SHELL

by

Thomas L. Geers

and

Miguel C. Junger

Cambridge Acoustical Associates, Inc.

March 1966 Report 2142

TABLE OF CONTENTS

LIST OF FIGURES

LIST OF TABLES

Page

NOTATION

A	Cross-sectional area of stiffened hull of length ℓ_S divided by $h\ell_S$ (Equation [B.1])
A_0	Equipment foundation-hull interface area (Equation [A.14])
a	Radius of hull
c	Velocity of sound in fluid
c_h	Equivalent plate velocity appropriate to hull material of a stiffened hull, $[E_0/\rho_0(1-\nu^2/A)]^{1/2}$
c_0	Plate velocity of hull material, $[E_0/\rho_0(1-\nu^2)]^{1/2}$
c_s	Velocity of shear waves in hull material, $[E_0/2(1+\nu)\rho_0]^{1/2}$
D_x, D_θ	Bending stiffnesses of stiffened hull in axial and circumferential directions, respectively (Equation [IV.7])
d	Effective diameter of equipment foundation-hull interface, $2\sqrt{A_0/\pi}$
E_0	Young's modulus of hull material
F_e	Oscillator driving force per unit oscillator mass due to response of shock-wave-excited bare hull for $t<t_e$ (Equation [IV.12])
$\hat{F}_e$	Dimensionless force per unit oscillator mass for $t\gtrsim t_e$ (Equation [IV.31]), $F_e a/c^2$
F_r	Oscillator driving force per unit oscillator mass due to response of shock-wave-excited bare hull for $t>>t_e$ (Equation [IV.24])
f	Frequency, $\omega/2\pi$
f_0	Oscillator undamped natural frequency on fixed base, $\omega_0/2\pi$
f_r	Pressure on rigid hull using Mindlin-Bleich approximation (Equation [III.7])
h	Thickness of hull plating
I_S	Moment of inertia associated with circumferential bending of stiffened hull

I_U	Moment of inertia associated with bending of unstiffened hull
I_n'	Derivative of I_n with respect to its argument
I_n	Modified Bessel function of order n, equal to $j^n J_n(-jz)$, where J_n is the Bessel function of order n
j	$\sqrt{-1}$
K	Oscillator spring constant (Equation [IV.2])
K_H	Experimentally determined low-frequency, steady-state effective spring constant of hull (Equation [IV.16])
K_n	MacDonald function, or modified Bessel function of the second kind, of order n, equal to $(\pi/2)(-j)^{n+1} H_n^{(2)}(-jz)$, where $H_n^{(2)}$ is the Hankel function of the second kind, of order n
K_n'	Derivative of K_n with respect to its argument
k_{mn}	Generalized stiffness of (m, n) hull mode (Equation [II.3]), $m_{mn}\,\omega_{mn}^2$
L	Lagrangian ~~equation~~
$\mathfrak{L}$	Length of hull
ℓ	Length of hull compartment
ℓ_E	Effective length of hull plating associated with one ring stiffener (Equation [B.4])
ℓ_S	Distance between adjoining ring stiffeners
M	Oscillator mass (Equation [IV.2])
$\hat{M}_0$	Dimensionless oscillator mass, $\frac{M}{K_H}\left(\frac{c}{a}\right)^2$
m	Axial mode number of hull compartment (Equations [II.1] and [III.14])
m_{mn}	Generalized mass of (m, n) hull mode (Equation [II.3])

n	Circumferential mode number of hull compartment (Equations [II.1] and [III.1])
P_i	Laplace transform of p_i (Equation [II.7])
P_r	Laplace transform of p_r (Equation [II.21])
P_s	Laplace transform of p_s (Equation [II.8])
p	Pressure
p_i	Pressure of the Heaviside (or step) incident wave (Equation [II.3])
p_0	Pressure amplitude of the Heaviside (or step) incident wave
p_r	Radiated (or relief) pressure, i.e.,pressure radiated by hull in response to (p_i+p_s) (Equation [II.3])
p_s	Pressure scattered by a rigid hull (Equation [II.3])
Q_{mn}, R_{mn}	Generalized forces of (m, n) hull mode associated with (p_i+p_s) and p_r, respectively, (Equations [II.6])
Q_1, R_1	Generalized forces of $n=1$; rigid body hull mode associated with (p_i, p_s) and p_r, respectively (Equations [III.5] and [III.6])
R	Oscillator damping constant (Equation [IV.2])
R_H	Point mechanical impedance of infinite orthotropic plate (Equations [IV.7] and [IV.8])
r	Radial coordinate measured from hull axis
$\hat{r}$	Effective radius of gyration associated with circumferential bending of the stiffened hull divided by the radius of gyration associated with bending of the unstiffened hull (Equation [B.3])
r_g	Radius of gyration of a plate cross section (Equation [A.2])
T	Kinetic energy of hull
t	Time
t_e	Envelopment time of hull by normally incident shock wave, $2a/c$

t_ℓ	Travel time of shear waves along length of hull compartment (Equation [IV.4])
u	Axial displacement of a point on the hull
u_{mn}, v_{mn}, w_{mn}	Generalized coordinates of (m, n) hull mode (Equations [II.1] and [III.14])
$\left(\frac{U}{W}\right)_{mn}$, $\left(\frac{V}{W}\right)_{mn}$	Ratios defining a mode shape of the hull (Equation [B.9])
V	Potential energy of hull
V_i, V_r, V_s	Laplace transforms of radial particle velocities associated with incident, radiated, and scattered waves, respectively, (Equations [II.7], [II.8] and [II.22])
$\hat{V}_0$	Dimensionless step velocity input at oscillator attachment point required to produce a specified peak oscillator response (Equation [V.1])
v	Circumferential displacement of a point on the hull
W_0	Weight of equipment component (Equation [A.17])
w	Radial displacement of a point on the hull
w_M	Displacement of oscillator mass (Equation [IV.2])
w_R	Relative displacement between oscillator mass and oscillator attachment point (Equation [IV.15])
w_0	Radial displacement of hull at oscillator attachment point (Equation [IV.1])
w_{0sc}	Displacement of hull at oscillator attachment point in response to oscillator reaction (Equation [IV.1])
w_s	Radial displacement of shock-wave-excited bare hull at oscillator attachment point (Equation [IV.1])
w_c	Displacement of oscillator attachment point, for $t > t_e$, associated with the approach to its final equilibrium state of the hull exclusive of w_1, time-averaged over time intervals commensurate with the natural periods of the randomly-phased, fluid-coupled, x-dependent hull modes (Equation [IV.26])

$\hat{w}_M$	Dimensionless displacement of oscillator mass, w_M/a
$\hat{w}_R$	Dimensionless relative displacement between oscillator mass and oscillator attachment point, w_R/a
w_1	Generalized coordinate of $n=1$, rigid body hull mode (Equation [III.11])
x'	Displaced axial coordinate, $x - \frac{\ell}{2}$
x	Axial coordinate
Z_H	Mechanical impedance of hull at oscillator attachment point (Equation [IV.3])
Z_{He}	Value of Z_H for $t<t_e$ (Equation [IV.7])
Z_{Hr}	Value of Z_H for $t>>t_e$ (Equation [IV.16])
z_{mn}, $\bar{z}_{mn}$, z_e, $\bar{z}_e$	Dimensionless decay constants (Equations [III.22], [III.32], and [IV.33])
z_1	Positive buoyancy factor, $\rho a/2\rho_0 hA$ (Equation [III.11])
α	Envelopment parameter, $\cos^{-1}(1-\tau)$ (Equation [III.7])
α_{mn}, α_e	Dimensionless decay constants (Equations [III.25], [III.35], and [IV.31])
β_e	Effective critical damping ratio of oscillator mounted in hull compartment for $t \leq t_e$ (Equation [IV.12])
β_{mn}	Critical damping ratio of (m, n) hull mode (Equations [III.23] and [III.32])
β_0	Oscillator critical damping ratio on fixed base, $R/2M\omega_0$
β_r	Effective critical damping ratio of oscillator mounted in hull compartment for $t>t_e$ (Equation [IV.21])
γ_{mn}, γ_e	Dimensionless damped natural frequencies (Equations [III.25], [III.35], and [IV.31])

δ	Square of the ratio (c_s/c_n); $\frac{1}{2}(1-\nu^2/A)/(1+\nu)$
ϵ_m	Neumann factor; 1 for $m=0$; 2 for $m\neq 0$.
ϵ_x, ϵ_y, ϵ_{xy}	Strain components
ζ	Modified transform variable, defined after (Equation [II.21])
η	Dimensionless integral parameter, $\hat{\omega}_0/2\beta_0$ (Equation [IV.35])
θ	Circumferential angle
κ_1, κ_2, κ_{12}	Changes in curvature (Equations [A.7] and [A.8])
λ	Axial mode parameter of hull compartment, $m\pi a/\ell$
λ_{ac}	Acoustic wavelength in water
λ_f	Flexural wavelength in hull (Equation [A.5])
μ_{mn}	Dimensionless generalized mass of (m, n) hull mode (Equations [B.10] to [B.12])
ν	Poisson ratio of hull material
ρ	Mass density of fluid
ρ_0	Density of hull material
σ_x, σ_y, σ_{xy}	Stress components
τ	Dimensionless time parameter, ct/a
χ	Radiation loading factor (Equation [A.1])
ψ_m	Axial characteristic function (Equation [II.1])
ω	Circular frequency
ω_c	Coincidence frequency (Equation [A.2])
ω_e	Effective undamped natural circular frequency of oscillator mounted in hull compartment for $t \lesssim t_e$ (Equation [IV.12])
ω_0	Natural circular frequency of oscillator on fixed base, $\sqrt{K/M}$

ω_{mn}	Undamped natural circular frequency of (m, n) hull mode (Equations [B.10] to [B.12])
ω_r	Effective undamped natural circular frequency of oscillator mounted in hull compartment for $t > t_e$ (Equation [IV.21])
$\hat{\omega}$	Dimensionless frequency, $\omega a/c$
$\hat{\omega}_c, \hat{\omega}_e, \hat{\omega}_0, \hat{\omega}_r$	Dimensionless frequencies given by a/c times $\omega_c, \omega_e, \omega_0$, and ω_r, respectively

wave with waves.

Page 18, last line – replace "$0 \leq t \leq 2\ a/c$" with "for $0 \leq t \leq 2\ a/c$."

Page 19, third line after Equation [III.11] – replace "$z - 1$" with "$z_1 = 1$."

Page 22, Equation [III.21] – replace "u_{m0}" with "μ_{m0}."

Page 28, lines 1 and 2 after "**A. GOVERNING EQUATIONS**" – replace "the radial displacement into two components at the point of oscillator attachment w_0" with "up the radial displacement at the point of oscillator attachment, w_0, into two components."

Page 38, last line before Equation [IV.41] – replace "rather" with "either."

Page 40, line 1 in last paragraph – replace "shown" with "shows."

Page 41, line 4 in second to last paragraph – replace "of" with "or."

Page 60, lines 3 and 4 after Equation [A.3] – replace "alternating current" with "a/c."

Page 61, last line before Equation [A.5] – insert asterisk after "follows" and add the footnote at the bottom of the page: "The second of these equations follows from the first since $\lambda_{ac} = 2\pi c/\omega = 2\pi a/\hat{\omega}$."

Page 61, lines 10–11 – replace "the membrane stresses become important only after standing waves are established" with "membrane stresses are not produced, the response of the plate being inextensional."

Note: The first paragraph on page 35, including Equations [IV.27] and [IV.28], is incorrect and should be replaced by:

"Now relative displacement is given by $w_R = w_M - w_0$, so that combining Equations [IV.1] and [IV.17] and neglecting incoherent bare hull motion yields

$$w_M = \frac{R}{K_H}\,\dot{w}_R + \left(1 + \frac{K}{K_H}\right) w_R + w_1 + w_c \qquad \text{[IV.27]}$$

Differentiating this twice, and combining the result with Equation [IV.2], (using $w_R = w_M - w_0$), we obtain

$$R\,\frac{M}{K_H}\,\dddot{w}_R + M\left(1 + \frac{K}{K_H}\right)\ddot{w}_R + R\,\dot{w}_R + K\,w_R = -M\,(\ddot{w}_1 + \ddot{w}_c) \qquad \text{[IV.28]}$$

The assumption is now made that for $t > t_e$, both $\ddot{w}_1$ and $\ddot{w}_c$ are very low-frequency, small amplitude motions so that the right side of Equation [IV.28] can be set equal to zero. Then, using the same reasoning which produced Equation [IV.23] from Equation [IV.19], we neglect the first term on the left side of Equation [IV.28]. Under these conditions, it is conservative to neglect the small damping term in Equation [IV.28], ($\beta_r \tilde{<} 10^{-2}$), so that, from the initial conditions at $t = t_e$, maximum relative displacement for $t > t_e$ is given by"

ABSTRACT

This report presents a simple analytical technique for investigating the response of a linear single degree-of-freedom mechanical oscillator mounted in a frame-stiffened cylindrical compartment of a shock-wave-excited submarine hull. Computations are performed to explore the dependence of peak oscillator response on oscillator fixed-base natural frequency, mass, and damping. It is found that damping is not a significant variable for lightly damped oscillators and that peak oscillator response can be correlated with reasonable accuracy in terms of two simple parameters. The general characteristics of experimental shock spectra measured in model tests and in tests on operational submarines are found to be predictable by means of two different mathematical models. Suggestions are made for further use of the analytical technique developed here, possibly in combination with experimental studies.

I. INTRODUCTION

A. PURPOSE OF THIS STUDY

For many years, the Navy has been seeking to design effectively submarine equipment that will better withstand the shock caused by a noncontact underwater explosion. Tests have shown that static design concepts alone are inadequate, and the need for a realistic and dynamic design method has been recognized. In recent years, Belsheim and O'Hara[1, 2] at the Naval Research Laboratory have formulated such a design method based on the normal modes of vibration of submarine equipment. This method is basically empirical, and the data used to produce the design criteria have shown considerable scatter. Model-scaled test data have shown less scatter, but the method still suffers from absence of an analytic investigation. It is the purpose of this report to attempt such an investigation.

B. PREVIOUS RELATED STUDIES

Several fairly thorough analyses have been published dealing with the two-dimensional response of a uniform cylindrical shell to a pressure pulse in a fluid medium.* These analyses fall into two classes, one, a modal approach, in which the time histories of different shell modes are evaluated separately and, two, an integral transform approach, which yields a closed form solution for the total shell response during the early stages of the envelopment

---

[1]References are listed on page 74.

*Two-dimensional response as used herein denotes x-independent motion.

of the shell by the shock wave and which can be extended to longer time periods if a branch cut line integral is evaluated numerically. The modal approach is used by Sette[3] and others to evaluate the response of the cylinder in the breathing mode ($n = 0$), the translational mode ($n = 1$), and the lowest lobar mode ($n = 2$), as well as by Murray[4] for the translational ($n = 1$) mode. The integral transform approach in its simpler form, i.e., confined to the early stages of development, is used by Payton[5] and by Peralta, et al.[6] The more cumbersome solution for later times is presented by Friedlander.[7] Two approximate analyses of the two-dimensional response of a uniform cylindrical shell to a pressure pulse have been published. The first, developed by Mindlin and Bleich,[8] uses a plane-wave approximation and is rigorously correct at early times. The second, developed by Haywood,[9] uses a cylindrical wave approximation and gives excellent results for $n = 0$ and $n = 1$ responses, even at late times.

The only rigorous solutions known to the authors for the three-dimensional response* of a cylindrical shell to a pressure pulse in a fluid medium are by Herman and Klosner,[10] by Murray,[4] and by Junger et al.[11] Herman and Klosner consider the response of an infinite, compartmented cylinder to an axially symmetric longitudinally sinusoidal Heaviside pressure pulse. Their solution is of theoretical interest but has little application to common shock problems since it cannot be used in a Fourier series approach to such shock problems. Murray considers the ($n = 1$) beam response to a spherical pressure wave in a fluid medium. In a subsequent analysis, Junger et al. attempt to extend the Murray three-dimensional analysis to other shell modes. Even though it is possible to obtain several alternative formulations for the response of a frame-stiffened shell to an incident wave (including the interaction with an oscillator attached to the shell), the numerical evaluation of the solutions is felt to be far too cumbersome for practical use. The approximate analysis by Forrestal and Herrmann[12] of an axially propagating shock wave exciting an infinite cylinder neglects entirely the axially dependent nature of the radiated wave in the fluid and is felt to be of very limited value in treating the present problem. The same conclusion applied to the analyses by Bhuta[13] and by Brogan[14] who ignore the radiated (or relief) pressure entirely in their studies of the response of a cylindrical shell to an axially propagating shock wave. For situations involving other than axial shock-wave propagation, scattered waves are generated which cannot be neglected, rendering the solution by Cottis[15] for the incidence of a shock wave on a cylinder at an oblique angle subject to criticism.

C. MATHEMATICAL MODEL USED IN THIS STUDY

In view of the inherent complexity of the interaction problem and of the structure involved, we see that a highly rigorous analysis is extremely difficult. In order to proceed at all, therefore, it is necessary to make rather drastic physical assumptions which must be

*Three-dimensional response as used herein denotes x-dependent motion, although, strictly speaking, θ-dependent response is also only two-dimensional.

justified on the basis of experimental agreement. The key to success, then, is to select a model that lends itself to analytic investigation but that also includes the essential behavior of the physical interaction. The model selected is shown in Figure 1. It consists of a long series of simply supported, orthotropic, cylindrical shells having the same shell-area density. Mounted at a point halfway along the center shell is a single degree-of-freedom mechanical oscillator. The incident shock-wave propagation vector is parallel to the line of motion of the oscillator. The shock wave is taken to be an acoustic traveling Heaviside function so that the entire analysis is linear. The boundaries of the fluid medium are assumed to be located too far from the hull to affect the hull-shock wave interaction.

Each hull compartment in the mathematical model is based on an experimental model used by the Underwater Explosions Research Division (UERD) of the David Taylor Model Basin[16] to study sound radiation from PERMIT-Class submarines. This experimental model (UERD Model VS-1, long model) embodies the structural characteristics of the PERMIT-Class hull in the vicinity of Frame 45. The structure of each compartment of the mathematical model differs from that of the UERD shell in that it is orthotropic rather than frame stiffened, but the orthotropic elastic constants are selected in accordance with the structural characteristics of the stiffened shell. Another difference results from the manner in which neutral buoyancy is achieved in the UERD shell, where the required ballast is in the form of heavy end bells. This uneven axial mass distribution produces, under shock excitation, transverse ($n = 1$) response characterized by nearly stationary ends. In contrast, the mass distribution in an actual hull produces transverse ($n = 1$) responses of the bow and stern regions which tend to exceed the response of the amidship region. Two different idealizations of the actual hull are used in the mathematical model; both assume the mass to be equally distributed along the entire length of the hull. These idealizations are that (1) items of equipment other than the oscillator are assumed to possess foundations with negligible mass and are assumed to be mounted at extremely low frequencies so that the elastic-mode responses in the absence of the oscillator for times less than the envelopment time ($t_e = 2a/c$) are not affected by the presence of the equipment and (2) items of equipment other than the oscillator are assumed to be rigidly attached to the hull, producing an effective increase in the area density of the hull sufficient to achieve neutral buoyancy. It is felt that Case 1 grossly overestimates transverse motion, especially in the amidship region, and that Case 2 tends to overestimate the transverse response of the amidship region and to underestimate the transverse responses of the bow and stern regions.

Elastic mode responses, i.e., those of the breathing ($n = 0$) and the lobar $n \geq 2$ modes, are investigated by means of the two idealizations indicated above and by the additional idealization that (3) uniformly distributed equipment components and their foundations are assumed to contribute to both hull stiffness and area density in such a way that neutral buoyancy for each compartment is achieved, while the *in vacuo* natural frequencies of each compartment are the same as those of an identical compartment devoid of any equipment.

D. APPROXIMATIONS USED IN THIS STUDY

The interaction is divided into two parts. First, the response of the hull with the oscillator removed is investigated. Second, resulting hull responses are used in determining the response of the oscillator in the coupled interaction.

Boundary conditions at the end of each compartment for the elastic modes are approximated by those of a simply supported cylinder. It will be seen that no appreciable errors are introduced by this approximation. The presence of the fluid is accounted for by using the Mindlin-Bleich approximation. It will be seen that for the shell modes considered, this approximation does not introduce unacceptable errors for $t < t_e$. Finally, since the mathematical model is long, end effects are ignored.

Oscillator response in the coupled interaction for $t < t_e$ is related to the response of the hull with the oscillator removed by approximating the point impedance of the hull and of the fluid beyond by that of a fluid-backed infinite orthotropic plate. Oscillator response for $t > t_e$ is obtained by approximating the point impedance of the hull and of the fluid beyond by that of a spring, an approximation based upon experimental impedance data for submarines. Also for $t > t_e$, oscillator response to forcing produced by the transiently decaying motion of the shock-wave-excited hull is neglected, an approximation based largely on experimental shock response data.[17]

E. DISCUSSION OF THE MATHEMATICAL MODEL AND OF THE APPROXIMATIONS USED IN THIS STUDY

It is admitted that a linear, lightly damped, single degree-of-freedom, point-attached oscillator mounted alone in an orthotropic cylindrical shell with rotational motion precluded by the use of symmetry is a highly simplified model of a realistic equipment configuration encountered in a full-scale submarine. It is felt, however, that this model does embody the essential elements of the real situation while avoiding, as much as possible, the very great complexity of the real situation. Moreover, it has been observed that response data of model-scale equipment in situations involving large rotational motion appear to be correlated almost as well in terms of equipment translational parameters as in terms of equipment rotational parameters, and that peak response for heavy equipment may be very insensitive to the presence of other heavy equipment located nearby.[17] It is clear that heavy equipment is insensitive to light equipment mounted nearby but not the reverse. Thus our analysis is limited to heavy equipment. Also, a point-attachment approximation will be shown to be reasonable for a broad class of submarine equipment which at the same time lends itself to normal mode analysis, being essentially linear and very lightly damped.

Linear acoustic theory and the assumption of a Heaviside pressure-wave input are felt to be sufficiently general for a beginning study of this type. Nonlinear acoustic phenomena and pressure waves having other that this time dependence may be considered later.

Regarding the orthotropic shell approximation, since the stiffened experimental model has many identical frames, it seems logical to effect an orthotropic cylinder approximation by using most of these stiffeners rather than using the more complicated method of treating each ring singly. The dynamic parameters obtained via the orthotropic shell analysis are felt to be within 10 percent of the true values for the experimental stiffened shell.

Equipment mass distribution along the length of the hull for $n = 1$ motion is very difficult to handle. One might be tempted to deal with $n = 1$ motion in the manner of Chertock,[18] which would take into account variations in equipment mass and hull stiffness along the length of the hull. This is not completely satisfactory, however, because the equipment which contributes to the weight to be accounted for is not rigidly attached to the hull. The only truly accurate approach would account for the dynamic characteristics of all the equipment mounted inside the submarine, a very difficult undertaking. It is felt that the rigid body motion obtained in this report by assuming a uniform mass distribution along the length of the model serves as an indication of the type of motion associated with the $n = 1$ response. The equipment mass distribution is also a problem for the elastic modes. It will be seen, however, that the responses of the elastic modes on oscillator motion are too small to be considered an important factor.

The interaction of the shell fluid even without the oscillator is also a difficult problem. The problem of two-dimensional interaction is in a more advanced state of development than is the three-dimensional, but even the former leaves many matters untreated. For example, shell response for intermediate times and the effects of cavitation have not been determined. Also, potentially significant nonlinear coupling between $n = 0$ extensional motion and high-n inextensional motion has not been investigated in the two-dimensional problem.[19, 20]

Finally, approximations for the oscillator-hull interaction are crude, but the level of crudeness does not appear inconsistent with the level of approximation tolerated in other areas. The assumptions used in the analysis of oscillator response for $t < t_e$ are examined quantitatively in Appendix A. The assumption of a springlike input point impedance of the hull for $t > t_e$ is a result of the low-frequency (below 200 cps, full scale) nature of oscillator response for $t > t_e$. Neglecting oscillator response to forcing produced by the transiently decaying motion of the shock-wave-excited hull modes for $t > t_e$ is actually a result of two approximations. The first of these assumes that the responses of the large number of x-dependent, coupled (through the fluid) hull modes are incoherent and largely self canceling at the point of oscillator attachment. A more refined analysis which would solve for the motions of the x-dependent modes presents great analytical difficulties because of modal coupling through the fluid. Taking the motion of the point of oscillator attachment (with the oscillator removed) as a random process also results in no simplification, because such a process would be nonstationary in time. Since experimental data[17] have shown little evidence

of this complicated forcing in oscillator response records, the analytical effort required to account for the incoherent motions of the x-dependent modes for $t > t_e$ is not considered justified. The second approximation conerns the motion of the shock-wave-excited hull exclusive of the above incoherent motion. It is assumed that the acceleration of the point of oscillator attachment (with the oscillator removed) due to such motion is low frequency and small amplitude, resulting in negligible oscillator forced response. The fundamental assumption underlying the toleration of all the simplifications and approximations is, of course, that the shock spectra produced will be very insensitive to perturbations in the approximate relations used.

II. FLUID-SHELL INTERACTION

Consider a very long, orthotropic, thin cylindrical shell having a uniform area density and containing rigid bulkheads at intervals of length ℓ. For radial forcing symmetrical about $\theta = 0$, radial response of the shell is given by

$$w(x, \theta, t) = \sum_{n=0}^{\infty} \sum_{m=0}^{\infty} w_{mn}(t)\, \psi_m(x) \cos n\theta \qquad \text{[II.1]}$$

where $\psi_m(x)$ is periodic in x, and is normalized as follows

$$\int_0^{\ell} \psi_m^2(x)\, dx = \frac{\ell}{\epsilon_m} \qquad \text{[II.2]}$$

A. DYNAMIC EXCITATION BY A TRANSIENT PRESSURE PULSE

For transient radial forcing by an x-independent pressure pulse, the response $w_{mn}(t)$ of each mode of the shell is determined by the solution of the Lagrange equation for a mode of a compartment of the shell

$$m_{mn}\, \ddot{w}_{mn} + k_{mn}\, w_{mn} = \int_{-\pi}^{\pi} \int_0^{\ell} [p_i(r, \theta, t) + p_s(r, \theta, t)$$

$$+ p_r(x, r, \theta, t)]_{r=a}\, \psi_m(x)\, a \cos n\theta\, dx d\theta \qquad \text{[II.3]}$$

in which m_{mn} and $k_{mn} = m_{mn}\, \omega_{mn}^2$ are the generalized mass and stiffness, respectively, of the shell vibrating *in vacuo*; they are derived in Appendix B. In Equation [II.3], p_i is the pressure of the incident wave; the other two pressures are due to the presence of the cylinder,

p_s being the pressure generated by a rigid, immovable cylinder (the scattered pressure) and p_r being the pressure generated by the response $w(x, \theta, t)$ of the shell (the radiated pressure).*

The exact solution to Equation [II.3] is difficult to obtain; to find an approximate solution, we will seek approximate relations for the scattered and radiated pressures. In doing this, it is convenient to express p_i, p_s, and p_r as follows

$$p = \sum_{n=0}^{\infty} p_n \cos n\theta \qquad \text{[II.4]}$$

Using this in Equation [II.3] and making use of orthogonality among cosine functions, we obtain

$$m_{mn}\, \ddot{w}_{mn} + k_{mn}\, w_{mn} = Q_{mn}(t) + R_{mn}(t) \qquad \text{[II.5]}$$

in which the generalized forces $Q_{mn}(t)$ and $R_{mn}(t)$ are given by

$$Q_{mn}(t) = \frac{2\pi a}{\epsilon_n} \left[p_{in}(a, t) + p_{sn}(a, t)\right] \int_0^{\ell} \psi_m(x)\, dx$$

$$R_{mn}(t) = \frac{2\pi a}{\epsilon_n} \int_0^{\ell} p_{rn}(x, a, t)\, \psi_m(x)\, dx \qquad \text{[II.6]}$$

B. GENERALIZED FORCES ASSOCIATED WITH THE INCIDENT AND SCATTERED WAVES

Since $p_i(r, \theta, t)$ is given $p_{in}(a, t)$ is easily obtained by using Equation [II.4]. To determine $p_{sn}(a, t)$, we make use of the following facts regarding the scattering problem: (1) p_i and p_s must satisfy the wave equation everywhere in the fluid and (2) the sum of the radial particle velocities of the incident and scattered waves must vanish at the surface of the shell. The method of the Laplace transform will be used to obtain the desired relations.

Remembering that incident radial particle velocity is taken positive in the direction of decreasing r, the Laplace transformed modal incident pressure and radial particle velocity appropriate to an x-independent Heaviside plane wave are

*See for example, Reference 4.

$$P_{in}(r, s) = p_0 \epsilon_n \frac{e^{-sa/c}}{s} I_n\left(\frac{sr}{c}\right)$$

$$V_{in}(r, s) = \frac{1}{\rho s} \frac{\partial P_{in}}{\partial r} = \frac{p_0 \epsilon_n}{\rho c} \frac{e^{-sa/c}}{s} I_n'\left(\frac{sr}{c}\right) \qquad \text{[II.7]}$$

where the prime denotes differentiation with respect to the argument $\left(\frac{sr}{c}\right)$. The solution to the Laplace transformed x-independent wave equation in cylindrical coordinates for outgoing waves yields for the Laplace transformed modal scattered pressure and radial particle velocity

$$P_{sn}(r, s) = A_n(s) K_n\left(\frac{sr}{c}\right)$$

$$V_{sn}(r, s) = -\frac{1}{\rho s} \frac{\partial P_{sn}}{\partial r} = -\frac{1}{\rho c} A_n(s) K_n'\left(\frac{sr}{c}\right) \qquad \text{[II.8]}$$

Since $V_{in} - V_{sn}$ must vanish at $r = a$, the second of Equations [II.7] and the second of Equations [II.8] give

$$A_n(s) = -p_0 \epsilon_n \frac{e^{-sa/c}}{s} \frac{I_n'\left(\frac{sa}{c}\right)}{K_n'\left(\frac{sa}{c}\right)} \qquad \text{[II.9]}$$

Using Equation [II.9] and the second of Equations [II.7] in the first of Equations [II.8] then yields

$$P_{sn}(a, s) = -\rho c \frac{K_n\left(\frac{sa}{c}\right)}{K_n'\left(\frac{sa}{c}\right)} V_{in}(a, s) \qquad \text{[II.10]}$$

For solutions at very early times, $K_n\left(\frac{sa}{c}\right)$ and $K'_n\left(\frac{sa}{c}\right)$ in Equation [II.10] can be expressed in terms of their large argument asymptotic expansions to obtain

$$\frac{K_n(z)}{K'_n(z)} = -1 + \frac{1}{2z} + \frac{4n^2-3}{8z^2} - \frac{8n^2-3}{8z^3} - \frac{48n^4-232n^2+63}{128z^4} + \ldots \qquad \text{[II.11]}$$

Using Equation [II.11] in Equation [II.10], multiplying both sides of the resulting equation by $\cos n\theta$, and then summing over n yields

$$P_s(a, \theta, s) = \rho c \left[\left(1 - \frac{1}{2}\frac{c}{as}\right) V_i(a, \theta, s) - \frac{1}{8}\left(\frac{c}{as}\right)^2 \sum_{n=0}^{\infty} (4n^2-3)\, V_{in}(a, s) \cos n\theta + \frac{1}{8}\left(\frac{c}{as}\right)^3 \sum_{n=0}^{\infty} (8n^2-3)\, V_{in}(a, s) \cos n\theta + \ldots\right] \qquad \text{[II.12]}$$

For the incident plane wave, the Laplace transformed incident pressure and radial particle velocity are related by

$$V_i(r, \theta, s) = \frac{1}{\rho c} P_i(r, \theta, s) \cos \theta \qquad \text{[II.13]}$$

Using this relation in Equation [II.12], multiplying both sides of the resulting equation by $\cos n\theta$, and integrating over θ then yields

$$P_{sn}(a, s) = \left(1 - \frac{1}{2}\frac{c}{as}\right) \frac{\epsilon_n}{2\pi} \int_{-\pi}^{\pi} P_i(a, \theta, s) \cos \theta \cos n\theta \, d\theta - \rho c \left[\frac{1}{8}\left(\frac{c}{as}\right)^2 (4n^2-3)\, V_{in}(a, s) - \frac{1}{8}\left(\frac{c}{as}\right)^3 (8n^2-3)\, V_{in}(a, s) - \ldots\right] \qquad \text{[II.14]}$$

Now the large argument aymptotic expansion for $I'_n(z)$ is

$$I'_n(z) = \frac{e^z}{\sqrt{2\pi z}} \left[1 - \frac{4n^2+3}{8z} + \frac{(4n^2-1)(4n^2+15)}{2!(8z)^2} - \ldots\right] \qquad \text{[II.15]}$$

so that using this and the second of Equations [II.7] in Equation [II.14] yields for early times

$$P_{sn}(a, s) = \left(1 - \frac{1}{2}\frac{c}{as}\right) \frac{\epsilon_n}{2\pi} \int_{-\pi}^{\pi} P_i(a, \theta, s) \cos\theta \cos n\theta \, d\theta$$

$$- \frac{p_0 \epsilon_n}{8\sqrt{2\pi}} \left[(4n^2-3)\left(\frac{c}{a}\right)^{5/2} s^{-7/2}\right.$$

$$\left. - \frac{1}{8}(16n^4-64n^2+33)\left(\frac{c}{a}\right)^{7/2} s^{-9/2+\ldots}\right] \qquad \text{[II.16]}$$

Inverse transforming then gives

$$p_{sn}(a, t) = \frac{\epsilon_n}{2\pi} \int_{-\pi}^{\pi} \left[p_i(a, \theta, t)\right.$$

$$\left. - \frac{c}{2a} \int_0^t p_i(a, \theta, t_1)\, dt_1\right] \cos\theta \cos n\theta \, d\theta$$

$$- \frac{\sqrt{2} p_0 \epsilon_n}{16\pi} \left[\frac{8}{15}(4n^2-3)\left(\frac{ct}{a}\right)^{5/2}\right.$$

$$\left. - \frac{2}{105}(16n^4-64n^2+33)\left(\frac{ct}{a}\right)^{7/2} + \ldots\right] \qquad \text{[II.17]}$$

C. GENERALIZED FORCE ASSOCIATED WITH THE RADIATED WAVE

To determine $p_{rn}(x, a, t)$, we make use of the following facts regarding the radiation problem: (1) p_r must satisfy the wave equation everywhere in the fluid and (2) the radial particle velocity of the radiated wave at the surface of the shell must equal the shell velocity. The method of the Laplace transform will again be used to obtain the desired relations.

Since p_r depends upon the response of the shell, we take

$$p_{rn}(x, r, t) = \sum_{m=0}^{\infty} p_{rmn}(r, t)\, \psi_m(x) \qquad \text{[II.18]}$$

Now $\psi_m(x)$ is symmetrical about $x = \ell/2$ and is periodic in ℓ, so we can write, letting $x' = x - \ell/2$

$$\psi_m(x) = \sum_{q=0}^{\infty} a_{mq} \cos \frac{2q\pi x'}{\ell} \qquad \text{[II.19]}$$

Using Equation [II.19] in Equation [II.18] yields

$$p_{rn}(x, r, t) = \sum_{q=0}^{\infty} p_{rqn}(r, t) \cos \frac{2q\pi x'}{\ell} \qquad \text{[II.20]}$$

in which $p_{rqn}(r, t) = \sum_{m=0}^{\infty} a_{mq}\, p_{rmn}(r, t)$.

The solution to the Laplace transformed wave equation in cylindrical coordinates for outgoing waves then yields for the Laplace transformed radiation pressure "component"

$$P_{rqn}(r, s) = A_{qn}(s)\, K_n\left(\frac{\zeta r}{c}\right) \qquad \text{[II.21]}$$

in which $\zeta = \left[s^2 + \left(\frac{2q\pi c}{\ell}\right)^2\right]^{1/2}$. Thus the Laplace transformed radiation radial particle velocity "component" is given by

$$V_{rqn}(r, s) = -\frac{1}{\rho s} \frac{\partial P_{rqn}}{\partial r} = -A_{qn}(s) \frac{\zeta}{\rho c s} K_n'\left(\frac{\zeta r}{c}\right) \qquad \text{[II.22]}$$

We now use Equation [II.19] in Equation [II.1] to obtain for each n

$$w_n(x, t) = \sum_{q=0}^{\infty} w_{qn}(t) \cos \frac{2q\pi x'}{\ell} \qquad [II.23]$$

in which $w_{qn}(t) = \sum_{m=0}^{\infty} a_{mq} w_{mn}(t)$. Since $V_{rqn}(a, s) + sW_{qn}(s)$ must vanish, Equations [II.22] and [II.23] yield

$$A_{qn}(s) = \rho c \frac{s}{\zeta} \frac{sW_{qn}(s)}{K_n'\left(\frac{\zeta a}{c}\right)} \qquad [II.24]$$

Using Equation [II.24] in Equation [II.21] gives

$$P_{rqn}(a, s) = \rho c \frac{s}{\zeta} \frac{K_n\left(\frac{\zeta a}{c}\right)}{K_n'\left(\frac{\zeta a}{c}\right)} s W_{qn}(s) \qquad [II.25]$$

Now s/ζ can be expressed in a binomial series as

$$\frac{s}{\zeta} = 1 - \frac{1}{2}\left(\frac{2q\pi c}{\ell s}\right)^2 + \frac{3}{8}\left(\frac{2q\pi c}{\ell s}\right)^4 - \ldots \qquad [II.26]$$

so that using Equations [II.11] and [II.26] in Equation [II.25] yields

$$P_{rqn}(a, s) = -\rho c s W_{qn}(s) \left[1 - \frac{1}{2\frac{sa}{c}} - \frac{4n^2 - 3 + 4\left(2q\pi \frac{a}{\ell}\right)^2}{8\left(\frac{sa}{c}\right)^2} + \frac{8n^2 - 3 + 4\left(2q\pi \frac{a}{\ell}\right)^2}{8\left(\frac{sa}{c}\right)^3}\right.$$

$$\left. + \frac{48n^4 - 232n^2 + 63 + 24(4n^2 - 3)\left(2q\pi \frac{a}{\ell}\right)^2 + 48\left(2q\pi \frac{a}{\ell}\right)^4}{128\left(\frac{sa}{c}\right)^4} + \ldots\right] \qquad [II.27]$$

Inverse transforming then gives

$$p_{rqn}(a, t) = -\rho c \left\{ \dot{w}_{qn}(t) - \frac{c}{2a} w_{qn}(t) \right.$$

$$- \left[\frac{1}{2} n^2 - \frac{3}{8} + \frac{1}{2}\left(2\pi q \frac{a}{\ell}\right)^2 \right] \left(\frac{c}{a}\right)^2 \int_0^t w_{qn}(t_1)\, dt_1$$

$$\left. + \left[n^2 - \frac{3}{8} + \frac{1}{2}\left(2q\pi \frac{a}{\ell}\right)^2 \right] \left(\frac{c}{a}\right)^3 \int_0^t \int_0^{t_1} w_{qn}(t_2)\, dt_2\, dt_1 + \ldots \right\} \qquad \text{[II.28]}$$

Multiplying this equation through by $\cos 2q\pi x'/\ell$, summing over q, using Equations [II.19], [II.20], and [II.23], and remembering the definition of $w_{qn}(t)$, we obtain

$$p_{rn}(x, a, t) = -\rho c \left\{ \sum_{m=0}^{\infty} \left[\dot{w}_{mn}(t) - \frac{c}{2a} w_{mn}(t) \right] \psi_m(x) \right.$$

$$- \left(\frac{c}{a}\right)^2 \sum_{q=0}^{\infty} \left[\frac{1}{2} n^2 - \frac{3}{8} + \frac{1}{2}\left(2q\pi \frac{a}{\ell}\right)^2 \right] \cos \frac{2q\pi x'}{\ell} \int_0^t w_{qn}(t_1)\, dt_1 \qquad \text{[II.29]}$$

$$\left. + \left(\frac{c}{a}\right)^3 \sum_{q=0}^{\infty} \left[n^2 - \frac{3}{8} + \frac{1}{2}\left(2q\pi \frac{a}{\ell}\right)^2 \right] \cos \frac{2q\pi x'}{\ell} \int_0^t \int_0^{t_1} w_{qn}(t_2)\, dt_2\, dt_1 + \ldots \right\}$$

We see that after the second term on the right side of Equation [II.29], $\psi_m(x)$ cannot be completely recovered by using the definition of $w_{qn}(t)$ and Equation [II.19]. This shows the coupling which arises between the shell modes because each function $\psi_m(x)$ cannot itself be a part of a solution to the wave equation in the infinite fluid.

D. APPROXIMATE FORMS OF THE SHELL LAGRANGE EQUATIONS

We now use Equations [II.2], [II.17], [II.19], [II.29] and the definition of $w_{qn}(t)$ in Equations [II.5] and [II.6] to obtain

$$m_{mn}\,\ddot{w}_{mn} + \frac{2\pi a\ell}{\epsilon_m \epsilon_n}\,\rho c\dot{w}_{mn} + k_{mn}\,w_{mn} - \frac{\pi\ell}{\epsilon_m \epsilon_n}\,\rho c^2 w_{mn}$$

$$= \frac{2\pi a}{\epsilon_n}\,p_{in}(a,\,t)\int_0^{\ell}\psi_m(x)\,dx + a\int_{-\pi}^{\pi}p_i(a,\,\theta,\,t)\cos\theta\cos n\theta\,d\theta\int_0^{\ell}\psi_m(x)\,dx$$

$$- \frac{c}{2}\int_{-\pi}^{\pi}\int_0^{t}p_i(a,\,\theta,\,t_1)\,dt_1\cos\theta\cos n\theta\,d\theta\int_0^{\ell}\psi_m(x)\,dx$$

$$- \frac{\sqrt{2}p_0\,a\ell}{8}\left[\frac{8}{15}(4n^2-3)\left(\frac{ct}{a}\right)^{5/2} - \frac{2}{105}(16n^4-64n^2+33)\left(\frac{ct}{a}\right)^{7/2} + \cdots\right] \qquad \text{[II.30]}$$

$$+ \frac{2\pi\ell}{\epsilon_m \epsilon_n}\rho\,\frac{c^3}{a}\left(\frac{1}{2}n^2-\frac{3}{8}\right)\int_0^{t}w_{mn}(t_1)\,dt_1$$

$$+ \frac{4\pi}{\epsilon_n}\left(\frac{\pi a}{\ell}\right)^2\rho\,\frac{c^3}{a}\int_0^{t}\sum_{m_1=0}^{\infty}w_{m_1 n}(t_1)\int_0^{\ell}\psi_m(x)\sum_{q=1}^{\infty}a_{m_1 q}\,q^2\cos\frac{2q\pi x'}{\ell}\,dx\,dt_1 + \cdots$$

For $m = q = 0$ (i.e., x-independent motion) neglecting the last term on the left side and all except the first two terms on the right side of Equation [II.30] produces the Mindlin-Bleich solutions for x-independent motion.[8] For $m = q = 0$, neglecting all terms except the first three on the right side of Equation [II.30] produces solutions similar to the Haywood solutions for x-independent motion.[9] These solutions for a Heaviside incident wave are, of course, accurate for a longer period after $t = 0$ than are the Mindlin-Bleich solutions.

That the equation obtained by neglecting all terms except the first three on the right side of Equation [II.30] for $m = q = 0$ yields solutions similar to the Haywood solutions is seen by examining the exact equation for x-independent motion. From Equations [II.5], [II.6], [II.10], and [II.25], the Laplace transformed governing equation for x-independent motion is

$$\left[m_n s^2 - \frac{2\pi a}{\epsilon_n}\,\rho c\,\frac{K_n\left(\frac{sa}{c}\right)}{K_n'\left(\frac{sa}{c}\right)}s + k_n\right]\,W_n(s) = \frac{2\pi a}{\epsilon_n}\left[P_{in}(a,\,s) - \rho c\,\frac{K_n\left(\frac{sa}{c}\right)}{K_n\left(\frac{sa}{c}\right)}V_{in}(a,\,s)\right] \qquad \text{[II.31]}$$

Taking $K_n(sa/c)/K_n'(sa/c) \approx -1$ in this equation yields the Mindlin-Bleich equation. Taking $K_n(sa/c)/K_n'(sa/c) \approx -1 + c/2as$ in this equation yields the equation referred to above. Multiplying Equation [II.31] through by $sK_n'(sa/c)/K_n(sa/c)$ and taking $K_n'(sa/c)/K_n(sa/c) \approx -1 - c/2as$ yields an equation of the Haywood type. Since the last two types involve the same degree of approximation in the K-function ratio, their accuracies as time progresses should be comparable.

For x-dependent motion, it is seen from Equation [II.27] that when $\left(2\pi q \frac{a}{\ell}\right)^2 > |n^2 - 1|$, x-independent approximations begin to fail. This failure is described by Herman and Klosner[10] in terms of "nonradiating" solutions for an axially symmetric, longitudinally sinusoidal Heaviside pressure pulse. However, the response of a mode whose x-dependence $\psi_m(x)$ is such that the a_{mq}'s in Equation [II.19] for $q > \frac{\ell}{2\pi a}|n^2 - 1|^{1/2}$ are negligible should be described with reasonable accuracy by the Mindlin-Bleich and Haywood solutions for early times. Thus, accepting shell response errors of as much as 20 percent, we shall use the Mindlin-Bleich approximation for these modes up to time $t_e = 2a/c$.

As pointed out earlier, taking $K_n(sa/c)/K_n'(sa/c) \approx -1 + c/2as$ in Equation [II.31] (for the x-independent problem) should produce solutions whose accuracy is comparable to that of the Haywood solutions. It is seen, however, that these solutions are much easier to obtain than the Haywood solutions since the latter must be obtained from a third-order differential equation while the former are obtained from a second-order differential equation. One might argue that, in a strict sense, the Haywood approximation is not actually a high-frequency approximation but is a kind of averaging approximation, and therefore might be superior to a high-frequency approximation of comparable complexity. Herman and Klosner did not find this to be the case for their problem however; thus the argument remains largely unresolved. If one is willing to solve a third-order differential equation, one might take $K_n(sa/c)/K_n'(sa/c) = -1 + c/2as + (4n^2 - 3)\ c^2/8a^2\ s^2$ in Equation [II.31]; this should yield solutions of greater accuracy than the Haywood solutions and require no significantly greater effort.

The x-dependent problem remains virtually unsolved, even in an approximate sense. The complexity of the problem is indicated by the governing equation for a shell mode

$$m_{mn}\, s^2 W_{mn}(s) - \frac{2\pi a}{\epsilon_n}\, \rho c \sum_{m_1=0}^{\infty} s W_{m_1 n}(s) \int_0^{\ell} \psi_m(x) \sum_{q=0}^{\infty} \frac{s}{\zeta} \frac{K_n\left(\frac{\zeta a}{c}\right)}{K_n'\left(\frac{\zeta a}{c}\right)}\, a_{m_1 q} \cos \frac{2q\pi x'}{\ell}\, dx$$

[II.32]

$$+ k_{mn} W_{mn}(s) = \frac{2\pi a}{\epsilon_n} \left[P_{in}(a, s) - \rho c \frac{K_n\left(\frac{sa}{c}\right)}{K_n'\left(\frac{sa}{c}\right)} V_{in}(a, s) \right] \int_0^{\ell} \psi_m(x)\, dx$$

where coupling between shell modes results from ζ being a function of q. The earlier discussion served only as a criterion for deciding when x-independent approximations should be valid. As stated earlier, the x-dependent solution by Herman and Klosner has little application to common shock problems since it cannot be used in a Fourier series approach to such shock problems.

III. RESPONSE OF THE HULL ALONE

Let us first remove the oscillator from the cylinder. We are then left with a very long, orthotropic, thin cylindrical shell having a uniform area density and containing rigid bulkheads at intervals of length ℓ. Because shock-wave forcing is symmetric about $\theta = 0$, we see that radial motion is given by

$$w(x, \theta, t) = \sum_{n=0}^{\infty} w_n(x, t) \cos n\theta \qquad \text{[III.1]}$$

We now investigate the motion of the shell for each value of n.

A. n = 1 MODES

One $n = 1$ mode is obviously an x-independent rigid body motion for the entire shell; this mode will be orthogonal to all other $n = 1$ modes. Since the area density is independent of x, this orthogonality statement is of the form:

$$\int_{-1/2\mathfrak{L}}^{+1/2\mathfrak{L}} \psi_1(x)\, dx = 0 \qquad \text{[III.2]}$$

in which $\psi_1(x)$ is an x-dependent $n = 1$ mode. The generalized force for such a mode is of the form:

$$F_1(t) = \int_{-1/2\mathfrak{L}}^{+1/2\mathfrak{L}} f_1(x, t)\, \psi_1(x)\, dx \qquad \text{[III.3]}$$

Neglecting end effects, which is valid for this very long cylinder, shock-wave excitation is also independent of x. Thus, $f_1(x, t) = f_1(t)$ comes out of the integral in Equation [III.3] so that, by Equation [III.2], $F_1(t)$ vanished, prohibiting the excitation of such a mode. Therefore our $n = 1$ motion consists only of the two-dimensional rigid body response of the shell.

It is important to note that if the area density is a function of x (a more realistic assumption), $n = 1$ whipping modes would be significantly excited. Since these whipping modes are characterized by very low *invacuo* natural frequencies, their responses could never resonance-excite an oscillator possessing a much higher fixed-base natural frequency. Hence their importance arises from their constructive or destructive interference with rigid body motion at early times.

Modern submarines are characterized by a mass per unit length which is large amidships and small fore and aft. Thus it is clear that the motions of the whipping modes subtract from the rigid body motion amidships and add to the rigid body motion fore and aft. Neglecting the whipping modes, then, tends to overestimate the response of an oscillator located amidships and tends to underestimate the response of an oscillator located fore or aft. A similar argument applies to the rigid body rotational response of a submarine whose mass per unit length is not symmetric about its amidships compartment, i.e., neglecting the rotational mode tends to overestimate the response of an oscillator located on one side of the submarine center of gravity and tends to underestimate the response of an oscillator located on the other side.

The Lagrangian equation for $n = 1$, two-dimensional rigid body motion of the cylinder consists only of the kinetic energy term T_1, since the potential energy term V_1 vanishes, and is given by*

$$L_1 = T_1 = \pi\rho_0 a\mathfrak{L}hA\dot{w}_1^2 \qquad \text{[III.4]}$$

The generalized force for radial forcing is

$$Q_1(t) = \mathfrak{L} \int_{-\pi}^{\pi} f_r(\theta, t)\, a \cos\theta\, d\theta \qquad \text{[III.5]}$$

*The factor A accounts for the mass of the ring stiffeners in the orthotropic cylinder (Appendix B).

Using the Mindlin-Bleich[8] approximation to account for the presence of the fluid has the effect of introducing the additional generalized force

$$R_1(t) = -\pi\rho c \mathfrak{L} a \dot{w}_1 \qquad \text{[III.6]}$$

and of producing, for the Heaviside shock wave:

$$f_r(\theta, t) = (1 + \cos\theta) \begin{cases} 0\ , -\pi \le \theta \le \pi,\ t \le 0 \\ p_0, -\alpha \le \theta \le \alpha \\ 0\ , \alpha \le \theta \le 2\pi - \alpha \\ p_0, -\pi \le \theta \le \pi,\ t \ge 2a/c \end{cases} \quad \begin{matrix} \\ \\ \\ \\ \end{matrix} \quad 0 \le t \le 2a/c \qquad \text{[III.7]}$$

in which $\alpha = \cos^{-1}(1 - ct/a)$.

Using Equation [III.7] in Equation [III.5], performing the integration, and using the result with Equations [III.4] and [III.6] in connection with the Lagrange equation

$$\frac{d}{dt}\left(\frac{\partial L}{\partial \dot{w}}\right) - \frac{\partial L}{\partial w} = Q + R \qquad \text{[III.8]}$$

where $L = T - V$, we obtain for $n = 1$ motion

$$2\pi\rho_0 hA\ddot{w}_1 + \pi\rho c\dot{w}_1 = p_0 \begin{cases} \alpha + 2\sin\alpha + \sin\alpha\cos\alpha, & 0 \le t \le \dfrac{2a}{c} \\ \pi\ , & t \ge \dfrac{2a}{c} \end{cases} \qquad \text{[III.9]}$$

For $t < 2a/c$, the solution to Equation [III.9] must be obtained numerically. This is avoided by approximating the right side of Equation [III.9] for $0 \le t \le 2a/c$ as follows (Appendix A):

$$\alpha + 2\sin\alpha + \sin\alpha\cos\alpha \approx 3.357 \left(1 - 0.936e^{-7.3\,ct/a} - 0.064\cos\pi\frac{ct}{a}\right) \qquad \text{[III.10]}$$

The resulting approximate solution for zero initial conditions, $0 \le t \le 2a/c$:

$$w_1(t) = \frac{p_0 a^2}{1.872\rho_0 hAc^2}\left[\frac{\tau}{z_1} - \frac{1}{z_1^2} - \frac{0.936}{7.3z_1} + \left(\frac{1}{z_1^2} + \frac{0.936}{z_1(7.3-z_1)} - \frac{0.064}{z_1^2+\pi^2}\right) e^{-z_1\tau}\right.$$

$$\left. - \frac{0.936}{7.3(7.3-z_1)} e^{-7.3\tau} - \frac{0.064}{z_1^2+\pi^2}\left(\frac{z_1}{\pi}\sin \pi\tau - \cos \pi\tau\right)\right] \qquad \text{[III.11]}$$

in which $\tau = ct/a$ and $z_1 = \rho a/2\rho_0 hA$. Figure 2 compares this solution with the exact solution to Equation [III.9] by Mindlin-Bleich and with the exact rigid body motion solution by Murray for $z_1 = 1$, i.e., for a neutrally buoyant shell.

B. n = 0 MODES

Since the bulkheads separating the compartments are assumed rigid, this motion must vanish at the bulkheads. Appropriate boundary conditions for the orthotropic cylinder constituting the region $0 \leq x \leq \ell$, therefore, might be

$$\begin{aligned} u_n(0, t) &= u_n(\ell, t) = 0 \\ v_n(0, t) &= v_n(\ell, t) = 0 \\ w_n(0, t) &= w_n(\ell, t) = 0 \\ \frac{\partial w_n}{\partial x}(0, t) &= \frac{\partial w_n}{\partial x}(\ell, t) = 0 \end{aligned} \qquad \text{[III.12]}$$

with $n = 0$.

Even a solution of the *invacuo* equations of motion for an isotropic cylindrical shell subject to these boundary conditions is relatively involved. Furthermore, the boundary conditions for an actual submarine compartment lie "between" these "clamped clamped" boundary conditions and the "simply supported" boundary conditions

$$\begin{aligned} \frac{\partial u_n}{\partial x}(0, t) &= \frac{\partial u_n}{\partial x}(\ell, t) = 0 \\ v_n(0, t) &= v_n(\ell, t) = 0 \\ w_n(0, t) &= w_n(\ell, t) = 0 \\ \frac{\partial^2 w_n}{\partial x^2}(0, t) &= \frac{\partial^2 w_n}{\partial x^2}(\ell, t) = 0 \end{aligned} \qquad \text{[III.13]}$$

with $n = 0$. These facts induce us to substitute Equations [III.13] for Equations [III.12] as the cylinder boundary conditions.

This substitution is justified further by the following: (1) the essential character of $n = 0$ motion is preserved since each set of boundary conditions produces two groups of modes, one group symmetric about $x = \ell/2$ and the other group antisymmetric about $x = \ell/2$ and (2) for nontorsional ($w_0 \neq 0$) motion, the free vibrations of a thin cylindrical shell subject to Equations [III.13] involve very simple eigenfunction solutions—changing the boundary conditions from Equations [III.13] to Equations [III.12] produces perturbations in these eigenfunctions which are very small except near the ends of the cylinder.[21]

The eigenfunctions appropriate to Equations [III.13] yield

$$u_n = \sum_{m=1}^{\infty} u_{mn} \cos \frac{m\pi x}{\ell}$$

$$v_n = \sum_{m=1}^{\infty} v_{mn} \sin \frac{m\pi x}{\ell} \qquad \text{[III.14]}$$

$$w_n = \sum_{m=1}^{\infty} w_{mn} \sin \frac{m\pi x}{\ell}$$

with $n = 0$ so that the Lagrangian equation for $n = 0$ motion subject to Equations [III.13] is (Appendix B)

$$L_{m0} = \frac{\pi}{2} \rho_0 a\ell h A(\dot{u}_{m0}^2 + \dot{v}_{m0}^2 + \dot{w}_{m0}^2) - \frac{\pi}{2} \frac{E_0 \ell h}{(1-\nu^2/A)a} \left\{\lambda^2 u_{m0}^2 + A w_{m0}^2 + 2\nu\lambda u_{m0} w_{m0}\right.$$

$$\left. + \frac{1}{2}\left(\frac{1-\nu^2/A}{1+\nu}\right) \lambda^2 v_{m0}^2 + \frac{h^2}{12a^2}\left[\lambda^4 w_{m0}^2 + \frac{1}{2}\left(\frac{1-\nu^2/A}{1+\nu}\right)(1+\hat{r})^2 \lambda^2 v_{m0}^2\right]\right\} \qquad \text{[III.15]}$$

in which $\lambda = m\pi a/\ell$. Applying the Lagrange equation with no forcing shows that one $n = 0$ mode is given by $u_{m0} = w_{m0} = 0$ (Appendix B). This is the torsional mode involving v_{m0} motion only; since $w_{m0} = 0$, radial forcing cannot excite this mode. Due to orthogonality, the two remaining modes, which are excited by radial forcing, must have $v_{m0} = 0$. For a given $n = 0$ mode shape $(U/W)_{m0}$, our $n = 0$ Lagrangian equation then becomes

$$L_{m0} = \frac{\pi}{2}\rho_0 a\ell hA \left[1 - \left(\frac{U}{W}\right)_{m0}^2\right] \dot{w}_{m0}^2$$

$$- \frac{\pi}{2} \frac{E_0 \ell h}{(1-\nu^2/A)a} \left\{\lambda^2 \left(\frac{U}{W}\right)_{m0}^2 + A + 2\nu\lambda \left(\frac{U}{W}\right)_{m0} + \frac{h^2}{12a^2}\lambda^4\right\} w_{m0}^2 \qquad \text{[III.16]}$$

The generalized force for radial forcing is

$$Q_{mn}(t) = \begin{cases} 0 \ , & m = 2, 4, \ldots \\ \dfrac{2a\ell}{m\pi} \displaystyle\int_{-\pi}^{\pi} f_r(\theta, t) \cos n\theta \, d\theta \ , & m = 1, 3, 5 \ldots \end{cases} \qquad \text{[III.17]}$$

with $n = 0$. Using the Mindlin-Bleich approximation to account for the presence of the fluid has the effect of introducing the additional generalized force

$$R_{mn}(t) = - \frac{\pi\rho c}{\epsilon_n} a\ell \, \dot{w}_{mn} \qquad \text{[III.18]}$$

with $n = 0$ and of producing for $f_r(\theta, t)$, Equation [III.7].

Using Equation [III.7] in Equation [III.17], performing the integration, and using the result with Equations [III.16] to [III.18] in connection with the Lagrange equation, Equation [III.8], we obtain for $n = 0$ motion with $m = 1, 3, 5 \ldots$

$$\pi\rho_0 a\ell hA \left[1 + \left(\frac{U}{W}\right)_{m0}^2\right] \ddot{w}_{m0} + \pi\rho ca\ell \dot{w}_{m0} + \pi \frac{E_0 \ell h}{(1-\nu^2/A)a} \left[\lambda^2 \left(\frac{U}{W}\right)_{m0}^2 + A + 2\nu\lambda \left(\frac{U}{W}\right)_{m0}\right.$$

$$\left. + \frac{h^2}{12a^2}\lambda^4\right] w_{m0} = \frac{4a\ell}{m\pi} p_0 \left[\begin{array}{ll} \alpha + \sin\alpha, & 0 \le t \le 2a/c \\ \pi, & t \ge 2a/c \end{array}\right] \qquad \text{[III.19]}$$

We see that this is the equation of (forced) motion for a linear single degree-of-freedom system.

As in the $n = 1$ case, the solution to Equation [III.19] for $t < 2a/c$ must be obtained numerically. This is avoided by approximating the right side of Equation [III.19] for $0 \le t \le 2a/c$ as follows (Appendix A)

$$\alpha + \sin\alpha \approx \pi\,(1 - e^{-2ct/a}) \qquad \text{[III.20]}$$

The resulting approximate solution for greater than critical damping with zero initial conditions is, for $0 \leq t \leq 2a/c$:

$$w_{m0}(t) = \frac{1.273\, p_0 a^2}{m\rho_0 h A \mu_{m0} c^2} \left[\frac{1}{z_{m0}\bar{z}_{m0}} - \frac{1}{(z_{m0}-2)(\bar{z}_{m0}-2)} e^{-2\tau}\right.$$

$$- \frac{2}{z_{m0}(2-z_{m0})(\bar{z}_{m0}-z_{m0})} e^{-z_{m0}\tau}$$

$$\left. - \frac{2}{\bar{z}_{m0}(2-\bar{z}_{m0})(z_{m0}-\bar{z}_{m0})} e^{-\bar{z}_{m0}\tau}\right] \qquad \text{[III.21]}$$

in which

$$\tau = \frac{ct}{a}$$

$$\mu_{m0} = 1 + \left(\frac{U}{W}\right)^2_{m0}$$

$$z_{m0} = \omega_{m0}\,\frac{a}{c}\left(\beta_{m0} + \sqrt{\beta_{m0}^2 - 1}\right) \qquad \text{[III.22]}$$

$$\bar{z}_{m0} = \omega_{m0}\,\frac{a}{c}\left(\beta_{m0} - \sqrt{\beta_{m0}^2 - 1}\right)$$

where, using the equivalent plate velocity $c_h^2 = \dfrac{E_0}{\rho_0(1-\nu^2/A)}$

$$\omega_{m0} = \frac{c_h}{a(\mu_{m0}A)^{1/2}}\left[\lambda^2\left(\frac{U}{W}\right)^2_{m0} + A + 2\nu\lambda\left(\frac{U}{W}\right)_{m0} + \frac{h^2}{12a^2}\lambda^4\right]^{1/2} \qquad \text{[III.23]}$$

$$\beta_{m0} = \frac{\rho c}{2\rho_0 h A \mu_{m0}\omega_{m0}}$$

The approximate solution for less than critical damping with zero initial conditions is, for $0 \leq t \leq 2a/c$:

$$w_{m0}(t) = \frac{1.273\, p_0 a^2}{m\rho_0 h A \mu_{m0} c^2} \left[\frac{1}{\alpha_{m0}^2 + \gamma_{m0}^2} - \frac{1}{(\alpha_{m0}-2)^2 + \gamma_{m0}^2} e^{-2\tau} \right.$$

$$-2 \frac{\alpha_{m0}(2-\alpha_{m0}) + \gamma_{m0}^2}{\gamma_{m0}(\alpha_{m0}^2+\gamma_{m0}^2)\,[(2-\alpha_{m0})^2 + \gamma_{m0}^2]} e^{-\alpha_{m0}\tau} \sin \gamma_{m0}\tau$$

$$\left. -4 \frac{(1-\alpha_{m0})}{(\alpha_{m0}^2 + \gamma_{m0}^2)\,[(2-\alpha_{m0})^2 + \gamma_{m0}^2]} e^{-\alpha_{m0}\tau} \cos \gamma_{m0}\tau \right] \qquad \text{[III.24]}$$

in which

$$\alpha_{m0} = \beta_{m0}\, \omega_{m0}\, \frac{a}{c}$$

$$\gamma_{m0} = \omega_{m0}\, \frac{a}{c} \sqrt{1 - \beta_{m0}^2} \qquad \text{[III.25]}$$

where ω_{m0} and β_{m0} are given by Equations [III.23].

C. n ≥ 2 MODES

Since the bulkheads separating the compartments are assumed rigid, this motion must also vanish at the bulkheads. Appropriate boundary conditions for the orthotropic cylinder constituting the region $0 \leq x \leq \ell$, therefore, might be Equations [III.12] with $n \geq 2$. For the same reasons as those stated for the $n = 0$ modes, we substitute for Equations [III.12] with $n \geq 2$ the boundary conditions Equations [III.13] with $n \geq 2$. The justifications for this step are essentially the same as those offered for the $n = 0$ modes. Investigations carried out by Arnold and Warburton[22] indicate that this substitution has a small effect on the response characteristics of the cylinder.

The eigenfunctions appropriate to Equations [III.13] with $n \geq 2$ yield Equations [III.14] with $n \geq 2$ so that the Lagrangian equation for $n \geq 2$ motion subject to Equations [III.13] is (Appendix B)

$$L_{mn} = \frac{\pi}{4}\rho_0 a\ell h A(\dot{u}_{mn}^2 + \dot{v}_{mn}^2 + \dot{w}_{mn}^2) - \frac{\pi}{4}\frac{E_0\ell h}{(1-\nu^2/A)a}\left\{\lambda^2 u_{mn}^2\right.$$

$$+ A(w_{mn} - nv_{mn})^2 + 2\nu\lambda u_{mn}(w_{mn} - nv_{mn}) + \frac{1}{2}\left(\frac{1-\nu^2/A}{1+\nu}\right)(\lambda v_{mn} - nu_{mn})^2$$

$$+ \frac{h^2}{12a^2}\left[\lambda^4 w_{mn}^2 + A\hat{r}^2 n^2 (nw_{mn} - v_{mn})^2 + 2\hat{r}\nu n\lambda^2 w_{mn}(nw_{mn} - v_{mn})\right.$$

$$\left.\left. + \frac{1}{2}\left(\frac{1-\nu^2/A}{1+\nu}\right)(1+\hat{r})^2\,\lambda^2(nw_{mn} - v_{mn})^2\right]\right\} \qquad \text{[III.26]}$$

again in which $\lambda = m\pi a/\ell$. Using the predominantly radial mode shape for any $n \geq 2$ given in Appendix B,* our $n \geq 2$ Lagrangian equation becomes

$$L_{mn} = \frac{\pi}{4}\rho_0 a\ell h A\left\{1 + \frac{n^2}{n^4 + [2A + (2A-1)\nu]^{-2}\lambda^4}\right\}\dot{w}_{mn}^2$$

$$- \frac{\pi}{4}\frac{E_0\ell h}{(1-\nu^2/A)a}\left[\frac{(A-\nu^2)\,\lambda^4}{An^4 + 2[A(1+\nu) - \nu]\,n^2\lambda^2 + \lambda^4}\right. \qquad \text{[III.27]}$$

$$\left. + \frac{h^2}{12a^2}\left\{A\hat{r}^2(n^2-1)^2 + \left[2\hat{r}\nu + \frac{1}{2}\left(\frac{1-\nu^2/A}{1-\nu}\right)(1+\hat{r})^2\right]\,(n^2-1)\lambda^2 + \lambda^4\right\}\right] w_{mn}^2$$

The generalized force for radial forcing is given by Equation [III.17] with $n \geq 2$. Using the Mindlin-Bleich approximation to account for the presence of the fluid has the effect of introducing the additional generalized force given by Equation [III.18] with $n \geq 2$ and of producing for $f_r(\theta, t)$, Equation [III.7].

Using Equation [III.7] in Equation [III.17], performing the integration, and using the result with Equations [III.27] and [III.18] in connection with the Lagrange equation, Equation [III.8], we obtain for $n \geq 2$ motion with $m = 1, 3, 5 \ldots$

---

*Since the two other modes for any m when $n \geq 2$ have such large generalized masses and such high frequencies (see Reference 23), they are negligibly excited by the shock wave.

$$\frac{\pi}{2}\rho_0 a\ell hA\left\{1+\frac{n^2}{n^4+[2A+(2A-1)\nu]^{-2}\lambda^4}\right\}\ddot{w}_{mn}+\frac{\pi}{2}\rho c\,a\ell\dot{w}_{mn}$$

$$+\frac{\pi}{2}\frac{E_0\ell h}{(1-\nu^2/A)a}\left[\frac{(A-\nu^2)\lambda^4}{An^4+2[A(1+\nu)-\nu]n^2\lambda^2+\lambda^4}\right. \qquad \text{[III.28]}$$

$$\left.+\frac{h^2}{12a^2}\left\{[A\hat{r}^2(n^2-1)^2]+\left[2\hat{r}\nu+\frac{1}{2}\left(\frac{1-\nu^2/A}{1-\nu}\right)(1+\hat{r})^2\right](n^2-1)\lambda^2+\lambda^4\right\}\right]w_{mn}$$

$$=\frac{2a\ell}{m\pi}p_0\begin{cases}\dfrac{1}{n-1}\sin(n-1)\alpha+\dfrac{2}{n}\sin n\alpha+\dfrac{1}{n+1}\sin(n+1)\alpha, & 0\le t\le 2a/c\\ 0, & t\ge 2a/c\end{cases}$$

This is again the equation of motion for a linear single degree-of-freedom system.

As before, the solutions to Equation [III.28] for $t < 2a/c$ must be obtained numerically. We avoid this by specializing Equation [III.28] to the cases $n = 2$ and $n = 3$ for which we make the approximations (Appendix A)

$$\sin\alpha+\sin 2\alpha+\frac{1}{3}\sin 3\alpha\approx 18.03\,\frac{ct}{a}e^{-3.414\,ct/a} \qquad \text{[III.29]}$$

$$\frac{1}{2}\sin 2\alpha+\frac{2}{3}\sin 3\alpha+\frac{1}{4}\sin 4\alpha\approx 0.253\left(104\,\frac{ct}{a}e^{-7.21\,ct/a}+\cos\pi\,\frac{ct}{a}-1\right)$$

The resulting approximate solution for $n = 2$ with greater than critical damping and with zero initial conditions is, for $0 \le t \le 2a/c$

$$w_{m2}(t)=\frac{7.307\,p_0a^2}{m\rho_0hA\mu_{m2}c^2}\left[\frac{1}{(z_{m2}-3.414)(\bar{z}_{m2}-3.414)}\tau e^{-3.414\tau}\right.$$

$$+\frac{6.828-(z_{m2}+\bar{z}_{m2})}{(z_m-3.414)^2(\bar{z}_{m2}-3.414)^2}e^{-3.414\tau} \qquad \text{[III.30]}$$

$$\left.+\frac{1}{(3.414-z_{m2})^2(\bar{z}_{m2}-z_{m2})}e^{-z_{m2}\tau}+\frac{1}{(3.414-\bar{z}_{m2})^2(z_{m2}-\bar{z}_{m2})}e^{-\bar{z}_{m2}\tau}\right]$$

The approximate solution for $n = 3$ with greater than critical damping and with zero initial conditions is, for $0 \leq t \leq 2a/c$

$$w_{m3}(t) = \frac{0.1025\, p_0 a^2}{m\rho_0 h A \mu_{m3} c^2} \left[-\frac{1}{z_{m3}\bar{z}_{m3}} + \frac{104}{(z_{m3}-7.21)(\bar{z}_{m3}-7.21)} \tau e^{-7.21\tau} \right.$$

$$+ 104 \frac{14.42-(z_{m3}+\bar{z}_{m3})}{(z_{m3}-7.21)^2 (\bar{z}_{m3}-7.21)^2} e^{-7.21\tau}$$

$$+ \frac{1}{(z_{m3}^2+\pi^2)(\bar{z}_{m3}^2+\pi^2)} [\pi(z_{m3}+\bar{z}_{m3}) \sin \pi\tau + (z_{m3}\bar{z}_{m3}-\pi^2) \cos \pi\tau] \qquad \text{[III.31]}$$

$$+ \left[\frac{104}{(\bar{z}_{m3}-z_{m3})(7.21-z_{m3})^2} - \frac{z_{m3}}{(\bar{z}_{m3}-z_{m3})(z_{m3}^2+\pi^2)} + \frac{1}{z_{m3}(\bar{z}_{m3}-z_{m3})} \right] e^{-z_{m3}\tau}$$

$$\left. + \left[\frac{104}{(z_{m3}-\bar{z}_{m3})(7.21-\bar{z}_{m3})} - \frac{\bar{z}_{m3}}{(z_{m3}-\bar{z}_{m3})(\bar{z}_{m3}^2+\pi^2)} + \frac{1}{\bar{z}_{m3}(z_{m3}-\bar{z}_{m3})} \right] e^{-\bar{z}_{m3}\tau} \right]$$

In Equations [III.30] and [III.31]

$$\mu_{mn} = 1 + \frac{n^2}{n^4 + [2A+(2A-1)\nu]^{-2}\lambda^4}$$

$$z_{mn} = \omega_{mn} \frac{a}{c} (\beta_{mn} + \sqrt{\beta_{mn}^2 - 1}) \qquad \text{[III.32]}$$

$$\bar{z}_{mn} = \omega_{mn} \frac{a}{c} (\beta_{mn} - \sqrt{\beta_{mn}^2 - 1})$$

where $\beta_{mn} = \rho c/2\rho_0 h A \mu_{mn} \omega_{mn}$ and where ω_{mn} is given in Appendix B. The approximate solution for $n = 2$ with less than critical damping and with zero initial conditions is, for $0 \leq t \leq 2a/c$:

$$w_{m2}(t) = \frac{7.307\, p_0 a^2}{m\rho_0 hA\mu_{m2}c^2}\left[\frac{1}{\alpha_{m2}^2+\gamma_{m2}^2-6.828\alpha_{m2}+(3.414)^2}\tau e^{-3.414\tau}\right.$$

$$+\frac{2(3.414-\alpha_{m2})}{[\alpha_{m2}^2+\gamma_{m2}^2-6.828\alpha_{m2}+(3.414)^2]^2}e^{-3.414\tau}$$

$$+\frac{\alpha_{m2}^2-\gamma_{m2}^2-6.828\alpha_{m2}+(3.414)^2}{\gamma_{m2}[\alpha_{m2}^2+\gamma_{m2}^2-6.828\alpha_{m2}+(3.414)^2]^2}e^{-\alpha_{m2}\tau}\sin\gamma_{m2}\tau$$

$$\left.+\frac{2(\alpha_{m2}-3.414)}{[\alpha_{m2}^2+\gamma_{m2}^2-6.828\alpha_{m2}+(3.414)^2]^2}e^{-\alpha_{m2}\tau}\cos\gamma_{m2}\tau\right] \qquad \text{[III.33]}$$

The approximate solution for $n = 3$ with less than critical damping and with zero initial conditions is, for $0 \leq t \leq 2a/c$:

$$w_{m3}(t) = \frac{0.1025\, p_0 a^2}{m\rho_0 hA\mu_{m3}c^2}\left[-\frac{1}{\alpha_{m3}^2+\gamma_{m3}^2}+\frac{104}{(\alpha_{m3}-7.21)^2+\gamma_{m3}^2}\tau e^{-7.21\tau}\right.$$

$$+\frac{208(7.21-\alpha_{m3})}{[(\alpha_{m3}-7.21)^2+\gamma_{m3}^2]^2}e^{-7.21\tau}+\frac{1}{[\alpha_{m3}^2+(\pi+\gamma_{m3})^2][\alpha_{m3}^2+(\pi-\gamma_{m3})^2]}[2\pi\alpha_{m3}\sin\pi\tau$$

$$+(\alpha_{m3}^2+\gamma_{m3}^2-\pi^2)\cos\pi\tau]+\frac{104\{(7.21-\alpha_{m3})^2-\gamma_{m3}^2\}}{\gamma_{m3}[(7.21-\alpha_{m3})^2+\gamma_{m3}^2]^2}$$

$$-\frac{(\alpha_{m3}^2+\gamma_{m3}^2+\pi^2)\alpha_{m3}/\gamma_{m3}}{[\alpha_{m3}^2+(\pi+\gamma_{m3})^2][\alpha_{m3}^2+(\pi-\gamma_{m3})^2]}+\frac{\alpha_{m3}/\gamma_{m3}}{\alpha_{m3}^2+\gamma_{m3}^2}\Bigg]e^{-\alpha_{m3}\tau}\sin\gamma_{m3}\tau$$

$$-\left[\frac{208(7.21-\alpha_{m3})}{[(7.21-\alpha_{m3})^2+\gamma_{m3}^2]^2}+\frac{\alpha_{m3}^2+\gamma_{m3}^2-\pi^2}{[\alpha_{m3}^2+(\pi+\gamma_{m3})^2][\alpha_{m3}^2+(\pi-\gamma_{m3})^2]}\right.$$

$$\left.\left.-\frac{1}{\alpha_{m3}^2+\gamma_{m3}^2}\right]e^{-\alpha_{m3}\tau}\cos\gamma_{m3}\tau\right] \qquad \text{[III.34]}$$

In Equations [III.33] and [III.34], μ_{mn} is given by the first of Equations [III.32] and

$$\alpha_{mn} = \beta_{mn}\,\omega_{mn}\,\frac{a}{c}$$

$$\gamma_{mn} = \omega_{mn}\,\frac{a}{c}\,\sqrt{1-\beta_{mn}^{\,2}} \qquad \text{[III.35]}$$

We terminate our cylinder response solutions at $n = 3$, assuming that the contributions to oscillator response of the $n > 3$ modes are negligible. The validity of this step will be examined by observing oscillator response to forcing appropriate to each value of n.

IV. OSCILLATOR RESPONSE

We now examine oscillator motion by expressing it in terms of the input impedance of the hull and the fluid beyond as seen from the point of oscillator attachment (Figure 3).

A. GOVERNING EQUATIONS

First we break the radial displacement into two components at the point of oscillator attachment w_0. This is possible, of course, because our problem is linear. Letting the term "bare hull" denote the hull with the oscillator removed, the first component w_s is the response of the bare hull at that point due to shock-wave forcing. The second component w_{0sc} is the response of the bare hull at that point due to forcing produced by the oscillator moving with the (unknown) motion it undergoes in the complete interaction. Thus we have

$$w_0(t) = w_s(t) + w_{0sc}(t) \qquad \text{[IV.1]}$$

Then we write a force balance at interface (1) in Figure 3 to obtain:

$$M\ddot{w}_M + R(\dot{w}_M - \dot{w}_0) + K(w_M - w_0) = 0 \qquad \text{[IV.2]}$$

Finally we write a Fourier-transformed force balance at interface (2) in Figure 3 to obtain

$$j\omega R(\tilde{w}_M - \tilde{w}_0) + K(\tilde{w}_M - \tilde{w}_0) = j\omega Z_H(\omega)\,\tilde{w}_{0sc} \qquad \text{[IV.3]}$$

For Z_H known, Equations [IV.1], [IV.2], and [IV.3] can in principle be combined to solve for the motion of the oscillator mass. In practice, however, the complexity of Z_H renders an exact solution virtually impossible. Thus we seek a way to simplify Z_H.

B. OSCILLATOR RESPONSE AT EARLY TIMES

The transient reaction exerted by the oscillator on the hull excites a large number of elastic wave modes in the hull. However, because this force is normal to the hull and because of the predominance of relatively low frequencies in the spectrum of this force, hull response will be comprised mainly of response in the lowest antisymmetric, or flexural mode. The group velocity dispersion curve of this mode has a maximum value equal to the shear velocity c_s.[24, 25] Hence, no significant portion of the elastic energy will travel at speeds in excess of the shear velocity. From this fact, it is apparent from Figure 1 that the earliest time the energy generated at the point of oscillator attachment at $t = 0$ can return to that point is

$$t_\ell = \frac{\ell}{c_s} \approx \frac{2\pi a}{c_s} \qquad \text{[IV.4]}$$

Now the time required for the shock wave to travel across the hull from $\theta = 0$ to $\theta = \pi$, the envelopment time, is

$$t_e = \frac{2a}{c} \qquad \text{[IV.5]}$$

Combining Equations [IV.4] and [IV.5] and remembering that for a steel hull in water, $c_s \gtrsim \pi\, c$, we obtain

$$t_\ell \gtrsim t_e \qquad \text{[IV.6]}$$

Thus for $t < t_e$, the oscillator "sees" energy generated at its point of attachment traveling away into an apparently infinite fluid-backed orthotropic curved plate, since the finite nature of the hull cannot be detected during $t < t_e$.

If one models a typical submarine hull in water as a fluid-backed orthotropic plate, one finds that the contribution of the fluid to the total impedance during early times is small.* Because of this and because the curvature of the hull is unimportant for early times,* we take the hull impedance for $t < t_e$ to be that of an infinite orthotropic plate given by Heckl[26] as

$$Z_{He}(\omega) \approx R_H = 8(\rho_0 hA)^{1/2}\,(D_x\, D_\theta)^{1/4} \qquad \text{[IV.7]}$$

---

*See Appendix A.

where D_x and D_θ are the x- and θ-bending stiffnesses, respectively. In the notation of Appendix B, Equation [IV.7] becomes

$$Z_{He}(\omega) \approx R_H = \frac{4}{3}\sqrt{3}\ A^{3/4}\hat{\rho}^{1/2}\rho_0 c_h h^2 \qquad [IV.8]$$

We see that R_H is frequency independent, the hull acting like a dashpot.

Using Equation [IV.8], Equation [IV.3] can be inverse transformed to yield

$$R(\dot{w}_M - \dot{w}_0) + K(w_M - w_0) = R_H \dot{w}_{0sc} \qquad [IV.9]$$

Combining Equations [IV.2] and [IV.9] then yields

$$\dot{w}_{0sc} = -\frac{M}{R_H}\ \ddot{w}_M \qquad [IV.10]$$

Integrating Equation [IV.10] with the initial conditions that $w_{0sc} = \dot{w}_M = 0$ at $t = 0$ and combining the result with Equations [IV.1], [IV.2], and [IV.10] gives

$$\ddot{w}_M + 2\beta_e\omega_e\dot{w}_M + \omega_e^2 w_M = F_e(t) \qquad [IV.11]$$

in which:

$$\omega_e = \frac{\omega_0}{\left(1 + \dfrac{2M\beta_0\omega_0}{R_H}\right)^{1/2}}$$

$$\beta_e = \frac{\beta_0 + \dfrac{M\omega_0}{2R_H}}{\left(1 + \dfrac{2M\beta_0\omega_0}{R_H}\right)^{1/2}} \qquad [IV.12]$$

$$F_e(t) = \frac{1}{\left(1 + \dfrac{2M\beta_0\omega_0}{R_H}\right)}\ [\omega_0^2 w_s(t) + 2\beta_0\omega_0\dot{w}_s(t)]$$

where $\omega_0 = (K/M)^{1/2}$ is the fixed-base undamped natural circular frequency of the oscillator,

$\beta_0 = R/2M\omega_0$ is the fixed-base critical damping ratio of the oscillator, and

w_s and $\dot{w}_s$ are the displacement and velocity response at the point of oscillator attachment of the bare hull to shock-wave excitation.

Since this point is at $\theta = 0$, $x = \ell/2$

$$w_s(t) = w_1(t) + \sum_{n=0,2,3..}^{\infty} \sum_{m=1,3,5..}^{\infty} (-1)^{1/2(m-1)}\, w_{mn}(t) \qquad [IV.13]$$

giving for $F_e(t)$

$$F_e(t) = \frac{1}{\left(1 + \dfrac{2M\beta_0\omega_0}{R_H}\right)} \left\{\omega_0^2 w_1(t) + 2\beta_0\omega_0\dot{w}_1(t) + \sum_{n=0,2,3..}^{\infty} \sum_{m=1,3,5..}^{\infty} (-1)^{1/2(m-1)}[\omega_0^2 w_{mn}(t) + 2\beta_0\omega_0\dot{w}_{mn}(t)]\right\} \qquad [IV.14]$$

Another quantity of interest is relative displacement between the oscillator mass and the oscillator attachment point. From Equation [IV.2] this is given by the equation

$$\frac{2\beta_0}{\omega_0}\dot{w}_R + w_R = -\frac{1}{\omega_0^2}\ddot{w}_M \qquad [IV.15]$$

C. OSCILLATOR RESPONSE AT LATE TIMES

To investigate the nature of Z_H for $t >> t_e$, let us consider the following experiment. An impedance head is attached to a submarine hull; at $t = 0$, a force is suddenly exerted on the hull by the impedance head. Let the force be a sine wave with frequency ω. We now ask what the measured impedance of the hull will look like as a function of time.

For times less than the envelopment time, it is clear from the above that the impedance will essentially resemble that of an infinite orthotropic plate. For very long times (after the transients have been damped out), the impedance will take on its steady-state value. Experiments have shown that lightly damped submarine equipment vibrates for a considerable length of time after shock-wave excitation of the hull and that this motion is characterized by low frequencies. Thus one can picture the motion of such equipment at late time as rather low-frequency motion (below 200 cps) to which the hull presents its low-frequency impedance.

Steady-state impedance measurements on present-day hulls have shown that, for this frequency range, hull impedance is approximately given by[27]

$$Z_{Hr} \approx \frac{K_H}{j\omega} \qquad \text{[IV.16]}$$

We see that Z_{Hr} is inversely proportional to frequency, the hull acting like a spring.* Using Equation [IV.16], Equation [IV.3] can be inverse-transformed to yield:

$$R(\dot{w}_M - \dot{w}_0) + K(w_M - w_0) = K_H w_{0sc} \qquad \text{[IV.17]}$$

Combining Equations [IV.2] and [IV.17] then yields

$$w_{0sc} = -\frac{M}{K_H}\ddot{w}_M \qquad \text{[IV.18]}$$

Differentiating Equation [IV.18] and combining the result with Equations [IV.1], [IV.2], and [IV.18] gives:

$$R\frac{M}{K_H}\dddot{w}_M + M\left(1 + \frac{K}{K_H}\right)\ddot{w}_M + R\dot{w}_M + Kw_M = Kw_s + R\dot{w}_s \qquad \text{[IV.19]}$$

For $t >> t_e$, $\ddot{w}_s$ has decayed to virtually zero, so that assuming the first term of Equation [IV.19] to be negligible, we obtain for $t >> t_e$

$$w_M \approx c_1 + c_2 t + c_3 e^{-\beta_r \omega_r t} \sin(\omega_r \sqrt{1-\beta_r^2}\, t + \phi_r) \qquad \text{[IV.20]}$$

in which

$$\omega_r = \frac{\omega_0}{\left(1 + \frac{M\omega_0^2}{K_H}\right)^{1/2}} \qquad \beta_r = \frac{\beta_0}{\left(1 + \frac{M\omega_0^2}{K_H}\right)^{1/2}} \qquad \text{[IV.21]}$$

---

*The reason why a system with many resonances below 200 cps should respond in a springlike fashion is that the admittance of a localized region excited by a point force (or a distributed force satisfying Equations [A.14] to [A.16]) is much smaller than the admittance of the hull compartment modes, even at their resonance frequencies; thus the modal structure of the compartment is not observed.

where $\omega_0 = (K/M)^{1/2}$ is again the fixed-base undamped natural circular frequency of the oscillator and $\beta_0 = R/2M\omega_0$ is again its fixed-base critical damping ratio. Using Equations [IV.20] and [IV.21], we find that the ratio of first to the second term in the left side of Equation [IV.19] is, for $\beta_r < \beta_0 << 1$

$$\frac{R\dfrac{M}{K_H}\ddot{w}_M}{M\left(1+\dfrac{M\omega_0^2}{K_H}\right)\ddot{w}_M} = \frac{R\omega_r}{K_H + M\omega_0^2} < \frac{R\omega_r}{M\omega_0^2} < 2\beta_0 \qquad \text{[IV.22]}$$

Since $\beta_0 \sim 10^{-2}$, we see that neglecting the first term in Equation [IV.19] is justified.

Thus we obtain for $t >> t_e$

$$\ddot{w}_M + 2\beta_r\omega_r\dot{w}_M + \omega_r^2 w_M = F_r(t) \qquad \text{[IV.23]}$$

in which:

$$F_r(t) = \omega_r^2 w_s(t) + 2\beta_r\omega_r\dot{w}_s(t) \qquad \text{[IV.24]}$$

Using Equation [IV.13], Equation [IV.24] becomes:

$$F_r(t) = \omega_r^2 w_1(t) + 2\beta_r\omega_r\dot{w}_1(t)$$

$$+ \sum_{n=0,2,3..}^{\infty} \sum_{m=1,3,5..}^{\infty} (-1)^{1/2(m-1)} [\omega_r^2 \omega_{mn}(t) + 2\beta_r\omega_r\dot{w}_{mn}(t)] \qquad \text{[IV.25]}$$

From Equation [IV.2] we see that relative displacement for $t >> t_e$ is still given by Equation [IV.15] but with w_M determined by Equations [IV.23] and [IV.25], and by certain initial conditions.

D. OSCILLATOR RESPONSE AT INTERMEDIATE TIMES

The time region $t \gtrsim t_e$ presents great problems in precisely determining oscillator response. It is during this time that coupling between the x-dependent bare hull modes is significant and that transients generated by the impedance head described in the previous section would detect significant transient hull motion resulting from the suddenly started sine wave forcing. It is possible, however, to describe certain characteristics of the motion during this time.

First, whatever motions occur for either the bare hull or the hull-oscillator system, hull motion will approach a new equilibrium state. This state (in the absence of buckling) is characterized by a new constant deflection of the hull at the oscillator attachment point due to the increase in hydrostatic pressure on the hull and by the constant velocity term in the hull $n = 1$ solution. In real situations, however, no shock wave is truly a Heaviside pulse, so that the final equilibrium state in a real situation is the same as that obtained before the incidence of the shock wave except for a net translation.

Second, the problem posed for $t \gtrsim t_e$ is largely an initial value problem since the incident and scattered pressures on the hull due to the shock wave become very small. Thus the coupled bare hull modes would be free, in the absence of the oscillator, to respond on their own in a highly incoherent manner about some coherent (time-varying mean) motion which approaches the new equilibrium state.

Third, the hull transients generated by the impedance head in the previous section would tend to produce highly incoherent response signals for detection by the impedance head because of the vary large number of hull modes excited.

Finally, experimental records have shown that little change occurs in the nature of the relative motion between the oscillator mass and its attachment point from $t \gtrsim t_e$ to $t >> t_e$.[17]

From the above observations, we make the following approximations:

1. Because hull transients excited by point impulsive forcing superpose at that point to form highly incoherent, and thus largely self-canceling motion and because experimental records have shown that little change occurs in the nature of the oscillator motion from $t \gtrsim t_e$ to $t >> t_e$, Equations [IV.23] and [IV.25] apply for $t \gtrsim t_e$ as well as for $t >> t_e$.

2. Because the incoherent x-dependent bare hull motions at the point of oscillator attachment for $t \gtrsim t_e$ will tend to be largely self-canceling and because experimental records have shown that little change occurs in the nature of the oscillator motion from $t \gtrsim t_e$ to $t >> t_e$, the effect of the incoherent, x-dependent bare hull motions on oscillator response is negligible.

Taking oscillator motion for $t > t_e$ to be given by Equations [IV.23] and [IV.25], and neglecting the incoherent x-dependent bare hull motions in Equation [IV.25] yields, for a Heaviside shock wave

$$\ddot{w}_M + 2\beta_r\omega_r\dot{w}_M + \omega_r^2 w_M = \omega_r^2 w_1 + 2\beta_r\omega_r\dot{w}_1 + \omega_r^2 w_c + 2\beta_r\omega_r\dot{w}_c \qquad \text{[IV.26]}$$

in which $w_c(t)$ represents the coherent displacement at the point of oscillator attachment which approaches the constant deflection portion of the new equilibrium state.

Now relative displacement for $t > t_e$ is, neglecting incoherent motion

$$w_R = w_M - (w_1 + w_c) \qquad \text{[IV.27]}$$

so that using Equation [IV.27] in Equation [IV.26] we obtain

$$\ddot{w}_R + 2\beta_r \omega_r \dot{w}_R + \omega_r^2 w_R = -(\ddot{w}_1 + \ddot{w}_c) \qquad \text{[IV.28]}$$

The assumption is now made that for $t > t_e$, both $\ddot{w}_1$ and $\ddot{w}_c$ are very low-frequency, small-amplitude motions so that the right side of Equation [IV.28] can be set equal to zero in determining the relative response of the oscillator. Under this condition, it is conservative to neglect the damping term ($\beta_r \lesssim 10^{-2}$) so that, from the initial conditions at $t = t_e$, maximum relative displacement for $t > t_e$ is given by

$$(w_R)_{max} = \left[w_R^2(t_e) + \frac{1}{\omega_r^2}\dot{w}_R^2(t_e)\right]^{1/2} \qquad \text{[IV.29]}$$

In addition, neglecting the damping term in Equation [IV.2] ($\beta_0 \lesssim 10^{-2}$also), maximum absolute acceleration of the oscillator mass for $t > t_e$ is given by

$$(\ddot{w}_M)_{max} = \omega_0^2 (w_R)_{max} \qquad \text{[IV.30]}$$

E. SOLUTION TO EQUATIONS

We now have the equations required to obtain the solutions for oscillator peak relative displacement and peak absolute acceleration. The steps taken to obtain these equations are depicted in Figure 4. The coupled interaction for $t < t_e$, represented by (*a*) in the figure, was transformed into two uncoupled interactions, represented by (*b*), with the output of one interaction constituting the input of the other; this was accomplished by approximating the point impedance of the submerged hull for $t < t_e$ by that of a dashpot. The completely coupled interaction for $t > t_e$, represented by (*c*), was similarly transformed into two uncoupled interactions by approximating the point impedance of the submerged hull for $t > t_e$ by that of a spring.

To obtain the desired oscillator motions for $t < t_e$, we use Equations [III.11], [III.21], and/or [III.24]; [III.30] and/or [III.33]; and [III.31] and/or [III.34] in Equation [IV.14]. Letting $\hat{w}_M = w_M/a$, $\tau = ct/a$, $\hat{\omega}_e = \omega_e\, a/c$ and $\hat{F}_e = F_e\, a/c^2$, Equation [IV.11] then yields for dimensionless oscillator acceleration when $\beta_e < 1$

$$\frac{d^2\hat{w}_M}{d\tau^2}(\tau) = \hat{F}_e(\tau) - \frac{1}{\gamma_e}(\gamma_e^2 - \alpha_e^2)\int_0^\tau \hat{F}_e(\tau_1)\, e^{-\alpha_e(\tau-\tau_1)} \sin \gamma_e(\tau-\tau_1)\, d\tau_1$$

$$- 2\alpha_e \int_0^\tau \hat{F}_e(\tau_1)\, e^{-\alpha_e(\tau-\tau_1)} \cos \gamma_e(\tau-\tau_1)\, d\tau_1 \qquad \text{[IV.31]}$$

where $\alpha_e = \beta_e\hat{\omega}_e$ and $\gamma_e = \hat{\omega}_e(1 - \beta_e^2)^{1/2}$. For $\beta_e = 1$, Equation [IV.11] yields for oscillator acceleration

$$\frac{d^2\hat{w}_M}{d\tau^2}(\tau) = \hat{F}_e(\tau) - 2\hat{\omega}_e \int_0^\tau \hat{F}_e(\tau_1)\, e^{-\hat{\omega}_e(\tau-\tau_1)}\, d\tau_1$$

$$+ \omega_e^2 \int_0^\tau \hat{F}_e(\tau_1)\, e^{-\hat{\omega}_e(\tau-\tau_1)}\, [\tau-\tau_1]\, d\tau_1 \qquad \text{[IV.32]}$$

and for $\beta_e > 1$, Equation [IV.11] yields for oscillator acceleration

$$\frac{d^2\hat{w}_M}{d\tau^2}(\tau) = \hat{F}_e(\tau) + \frac{1}{z_e - \bar{z}_e}\int_0^\tau \hat{F}_e(\tau_1)\, [\bar{z}_e^2\, e^{-\bar{z}_e(\tau-\tau_1)}$$

$$- z_e^2\, e^{-z_e(\tau-\tau_1)}]\, d\tau_1 \qquad \text{[IV.33]}$$

where $z_e = \hat{\omega}_e(\beta_e + \sqrt{\beta_e^2 - 1})$ and $\bar{z}_e = \hat{\omega}_e(\beta_e - \sqrt{\beta_e^2 - 1})$. Oscillator relative displacement is then obtained using Equation [IV.15] which yields, letting $\hat{w}_R = w_R/a$, $\hat{\omega}_0 = \omega_0\, a/c$

$$\hat{w}_R(\tau) = -\frac{1}{2\beta_0\hat{\omega}_0}\int_0^\tau \frac{d^2\hat{w}_M}{d\tau^2}(\tau_1)\, e^{-(\hat{\omega}_0/2\beta_0)(\tau-\tau_1)}\, d\tau_1 \qquad \text{[IV.34]}$$

Since $\hat{\omega}_0/2\beta_0 \gg 1$ for the situations to be considered, performing the integration in Equation [IV.34] numerically would require a very fine mesh in time; to avoid this we proceed as follows. We write Equation [IV.34] as

$$\hat{w}_R(\tau) = -\frac{1}{\hat{\omega}_0^2}\int_{e^{-\eta\tau}}^{1}\frac{d^2\hat{w}_M}{d\tau^2}\left(\tau+\frac{\ell n\, u}{\eta}\right)du \qquad \text{[IV.35]}$$

in which $\eta = \hat{\omega}_0/2\beta_0$ and $u = e^{-\eta(\tau-\tau_1)}$. We then expand $d^2\hat{w}_M/d\hat{\tau}^2$ in a Taylor series about $\hat{\tau}$ to obtain

$$\frac{d^2\hat{w}_M}{d\tau^2}\left(\tau+\frac{\ell n\, u}{\eta}\right) = \frac{d^2w_M}{d\tau^2}(\tau) + \frac{\ell n\, u}{\eta}\,\frac{d^3\hat{w}_M}{d\tau^3}(\tau) + \frac{1}{2}\left(\frac{\ell n\, u}{\eta}\right)^2\frac{d^4\hat{w}_M}{d\tau^4} + \ldots \qquad \text{[IV.36]}$$

Using this in Equation [IV.35] yields

$$\hat{w}_R(\tau) = -\frac{1}{\hat{\omega}_0^2}\,\frac{d^2\hat{w}_M}{d\tau^2}(\tau)\,[1-e^{-\eta\tau}] - \frac{1}{\eta\hat{\omega}_0^2}\,\frac{d^3\hat{w}_M}{d\hat{\tau}^3}(\tau)\int_{e^{-\eta\tau}}^{1}\ell n\, u\, du$$

$$-\frac{1}{2\eta^2\hat{\omega}_0^2}\,\frac{d^4\hat{w}_M}{d\tau^4}(\tau)\int_{e^{-\eta\tau}}^{1}(\ell n\, u)^2\, du - \ldots \qquad \text{[IV.37]}$$

Evaluating the integrals then gives

$$\hat{w}_R(\tau) = -\frac{1}{\hat{\omega}_0^2}\,\frac{d^2\hat{w}_M}{d\tau^2}(\tau)\,[1-e^{-\eta\tau}] + \frac{1}{\eta\hat{\omega}_0^2}\,\frac{d^3\hat{w}_M}{d\tau^3}(\tau)\,[1-(1+\eta\tau)e^{-\eta\tau}]$$

$$-\frac{1}{\eta^2\hat{\omega}_0^2}\,\frac{d^4\hat{w}_M}{d\tau^4}(\tau)\,\left[1-\frac{1}{2}\,(2+2\eta\tau+\eta^2\tau^2)\,e^{-\eta\tau}\right] + \ldots \qquad \text{[IV.38]}$$

It can be shown that this series converges if the derivatives are bounded. Sample calculations have shown that for all except very early times ($\tau < 0.2$), convergence is uniformly very rapid. Thus the right side of Equation [IV.38] was truncated after the third term.

Looking back to Equation [IV.29], we see that the relative velocity at envelopment time is needed. This is most easily obtained by differentiating Equation [IV.15] to obtain

$$\frac{d\hat{w}_R}{d\tau}(\tau) = -\frac{1}{2\beta_0\hat{\omega}_0}\int_0^{\tau}\frac{d^3\hat{w}_M}{d\tau^3}(\tau_1)\, e^{-(\hat{\omega}_0/2\beta_0)/(\tau-\tau_1)}\, d\tau_1 \qquad \text{[IV.39]}$$

This equation is of exactly the same form as Equation [IV.34] so that the development used for that equation yields for Equation [IV.39]

$$\frac{d\hat{w}_R}{d\tau}(\tau) \approx -\frac{1}{\hat{\omega}_0^2}\frac{d^3\hat{w}_M}{d\tau^3}(\tau)\,[1-e^{-\eta\tau}] + \frac{1}{\eta\hat{\omega}_0^2}\frac{d^4\hat{w}_M}{d\tau^4}(\tau)\,[1-(1+\eta\tau)\,e^{-\eta\tau}]$$

$$-\frac{1}{\eta^2\hat{\omega}_0^2}\frac{d^5\hat{w}_M}{d\tau^5}(\tau)\,\left[1-\frac{1}{2}(2+2\eta\tau+\eta^2\tau^2)\,e^{-\eta\tau}\right] \qquad \text{[IV.40]}$$

The derivatives $d^3\hat{w}_M/d\tau^3$, $d^4\hat{w}_M/d\tau^4$, and $d^5\hat{w}_M/d\tau^5$ in Equations [IV.38] and [IV.40] were obtained by numerically differentiating $d^2\hat{w}_M/d\tau^2$ given by Equations [IV.31] to [IV.33]; mesh width was small enough to insure good accuracy in determining $\hat{w}_R(\tau)$ and $\frac{d\hat{w}_R}{d\tau}(\tau)$ for $\tau > 0.2$. Sample calculations have shown that $\hat{w}_R(\tau)$ never reaches its peak during $0 < \tau < 0.2$.

Dimensionless peak acceleration and peak relative displacement for the oscillator are then given ~~rather~~ either by their maximum values for $\tau \leq 2$ or, from Equations [IV.29] and [IV.30], by

$$(\hat{w}_R)_{max} = \left\{\hat{w}_R^2(2) + \frac{1}{\hat{\omega}_r^2}\left[\frac{d\hat{w}_R}{d\tau}(2)\right]^2\right\}^{1/2} \qquad \text{[IV.41]}$$

$$\left(\frac{d^2\hat{w}_M}{d\tau^2}\right)_{max} = \hat{\omega}_0^2\,(\hat{w}_R)_{max}$$

V. COMPUTATIONS AND RESULTS

A. COMPUTATIONS PERFORMED

Dimensionless peak accelerations and peak relative displacements for 39 oscillators with critical damping ratios of $\beta_0 = 0.02$ are computed for total forcing, i.e., for forcing appropriate to bare-hull motion resulting from the combined responses at the oscillator attachment point of all the hull modes considered ($n = 0$, 2, or 3 and $m = 1$, 3, 5, or 7 modes, and $n = 1$ rigid body mode) (Table 1). Separate computations are made for each of the three cases described in Chapter I; thus, 117 *general computations* are performed. The hull parameters appropriate to the three cases are presented in Table 2. To produce neutral buoyancy of the hull in Cases 2 and 3, an effective hull material density ρ_0' is introduced. For the PERMIT-Class hull, this density is found to be $\rho_0' = 4.525\ \rho_0$. The generalized masses of the hull in Case 2 are thus (ρ_0'/ρ_0) times the corresponding generalized masses in Case 1, and the undamped natural frequencies and critical damping ratios in Case 2 are $(\rho_0/\rho_0')^{1/2}$ times the corresponding parameters in Case 1. The generalized masses of the hull in Case 3 are also (ρ_0'/ρ_0) times the corresponding generalized masses in Case 1, but the undamped natural frequencies remain the same as those in Case 1, and the critical damping ratios are (ρ_0/ρ_0') times those in Case 1. The R_H-values for Cases 2 and 3 are $(\rho_0'/\rho_0)^{1/2}$ and (ρ_0'/ρ_0) times the R_H-value in Case 1, respectively, (see Equation [IV.7]; the K_H-value remains the same in all three cases since K_H is an empirical parameter apparently associated with the response of the hull plating between frames.

The responses of eight of the oscillators (Table 1) are investigated in depth by performing *special computations* of dimensionless oscillator peak acceleration and peak relative displacement in all three cases for:

1. Forcing caused separately by $n = 0$, $n = 1$, $n = 2$, and $n = 3$ bare-hull motions with $\beta_0 = 0.02$ and for forcing caused by the combined bare-hull motions of the $m = 7$, $n = 0$, 2, and 3 hull modes with $\beta_0 = 0.02$; this is done to determine the relative importance of the various hull modes and to examine convergence of hull mode forcing with respect to peak oscillator response.

2. Forcing caused separately by $n = 0$, $n = 1$, $n = 2$, and $n = 3$ bare-hull motions with $\beta_0 = 0.0001$ and for forcing caused by the combined bare-hull motions of the $m = 7$, $n = 0$, 2, and 3 hull modes with $\beta_0 = 0.0001$; this is done to examine the importance of oscillator damping.

3. Total forcing with $\beta_0 = 0.001$ and $\beta_0 = 0.05$; this is also done to examine the importance of oscillator damping.

4. Total forcing with R_H at first decreased by 20 percent and then increased by 20 percent; this is done to determine the sensitivity of the results to changes in the values of R_H and K_H.

5. Total forcing with $t_e = 1.5\ a/c$ instead of $2\ a/c$; this is done to determine the sensitivity of the results to changes in the value of the somewhat arbitrary parameter t_e.

In addition to these data, oscillator response time histories are obtained in a special computation (1 above) and in the general computations for the eight oscillators considered in the special computations. It is seen that a total of 360 special computations are performed.

B. RESULTS OF GENERAL COMPUTATIONS

The results of the general computations are presented in Figures 5 through 16. Since peak oscillator response occurs when $t \geq t_e$ for the majority of the oscillators, dimensionless peak acceleration and dimensionless peak relative displacement are related by $\hat{\omega}_0^2$.* Thus it is convenient to describe peak oscillator response as that to a step velocity input at the point of oscillator attachment given by

$$\hat{V}_0 = \hat{\omega}_0 \, \hat{w}_{R_{max}} = 1/\hat{\omega}_0 \, d^2\hat{w}_M/d\tau^2 \Big|_{max} \qquad [V.1]$$

Even for those few oscillators whose peak responses occur when $t < t_e$, it is found that Equation [V.1] applies with excellent accuracy, an expected result in view of Equation [IV.38]. Therefore all peak oscillator response data are presented in terms of $\hat{V}_0$. We will discuss plots of the results in terms of the maximum deviation of the furthest point from the mean of the ordinate values of the data points appropriate to a fixed value of the abscissa; this maximum deviation will be referred to as "zero to peak scatter" and will be expressed as a percentage of the mean.

Figure 5 shows $\hat{V}_0$ plotted as a function of dimensionless oscillator mass $\hat{M}_0 = (M/K_H)\,(c/a)^2$** for various values of dimensionless oscillator natural frequency $\hat{\omega}_0(a/c)$** with $\beta_0 = 0.02$ in Case 1. Figure 6 shows $\hat{V}_0$ plotted as a function of dimensionless oscillator natural frequency for various values of oscillator mass with $\beta_0 = 0.02$ in Case 1. Figures 7 and 9 are like Figure 5 except that they pertain to Cases 2 and 3, respectively. Similarly, Figures 8 and 10 are like Figure 6 except that they pertain to Cases 2 and 3, respectively.

---

*We remember that Equation [IV.41] neglects damping in the oscillator; it will be seen that peak oscillator response is very insensitive to changes in (small) oscillator damping.

**For the PERMIT-Class hull, $\hat{M}_0 = 1$ corresponds to a weight of 7600 lb, and $\hat{\omega}_0 = 1$ corresponds to a frequency of 51 cps.

Figure 5 shows that in Case 1 $\hat{V}_0$ can be considered independent of $\hat{\omega}_0$ within 15 to 25 percent of zero to peak scatter about the mean. Figure 6, however, shows that for greater accuracy, the value of $\hat{\omega}_0$ must be considered, especially for large values of $\hat{M}_0$. In addition, it appears from the locations of the peaks of the curves in Figure 6 that peak response can be conservatively stated as $\hat{V}_0 \approx 1.1\ \hat{\omega}_0$, independent of $\hat{M}_0$. Figure 7 shows that from 20 to 35 percent of zero to peak scatter must be tolerated to neglect $\hat{\omega}_0$ as a parameter in Case 2, and Figure 8 shows a significant downward trend in $\hat{V}_0$ for increasing $\hat{\omega}_0$, even for small values of $\hat{M}_0$. Figure 9 shows that 20 to 35 percent of zero to peak scatter must be tolerated to neglect $\hat{\omega}_0$ as a parameter in Case 3 also. Figure 10, like Figure 8, shows a significant downward trend in $\hat{V}_0$ for increasing $\hat{\omega}_0$, even for small values of $\hat{M}_0$.

Finally, a comparison of Figures 5, 7, and 9 shows that the general decrease in $\hat{V}_0$ with increasing $\hat{M}_0$ is significantly more pronounced in Case 1 than in Cases 2 and 3, and that it is more pronounced in Case 2 than in Case 3.

It has been suggested that peak oscillator response data can be correlated more simply in terms of a parameter equal to the product of oscillator mass and the cube of the oscillator natural frequency.[17] The peak oscillator response parameter suggested for this correlation is $\hat{V}_0/\hat{\omega}_0^{1/2}$. Figure 11 shows a plot of the Case 1 data in accordance with this suggestion; we see that the data correlate reasonably well in this way, the zero to peak scatter about the mean value of the data points appropriate to a fixed value of $\hat{M}_0\hat{\omega}_0^3$ ranging from 5 to 30 percent of the mean. In contrast, the plot of $\hat{V}_0$ versus $\hat{M}_0\hat{\omega}_0^3$ in Figure 12 shows a zero to peak scatter ranging from 20 to 50 percent. Comparison of the trends of the data in the two figures indicates that a peak oscillator response parameter given by $\hat{V}_0/\hat{\omega}_0^{2/3}$ or $\hat{V}_0/\hat{\omega}^{3/4}$ would correlate the data best, involving less than about 15 percent zero to peak scatter.

Figure 13 shows a plot of $\hat{V}_0/\hat{\omega}_0^{1/2}$ versus $\hat{M}_0\hat{\omega}_0^3$ in Case 2, and Figure 14 shows a plot of $\hat{V}_0$ versus $\hat{M}_0\hat{\omega}_0^3$. Again it appears that the peak response parameter $\hat{V}_0/\hat{\omega}_0^{1/2}$ produces a better correlation of the data than does $\hat{V}_0$; zero to peak scatter ranges from 10 to 20 percent in Figure 13 and from 5 to 30 percent in Figure 14. Comparison ~~of~~ the trends of the data in the two figures indicates that a peak oscillator response parameter given by $\hat{V}_0/\hat{\omega}_0^{1/3}$ of $\hat{V}/\hat{\omega}_0^{1/4}$ would correlate the data best, involving less than about 10 percent zero to peak scatter.

Figure 15 shows a plot of $\hat{V}_0/\hat{\omega}_0^{1/2}$ versus $\hat{M}_0\hat{\omega}_0^3$ in Case 3 and Figure 16 shows a plot of $\hat{V}_0$ versus $\hat{M}_0\hat{\omega}_0^3$. In this case, the data are better correlated by $\hat{V}_0$ than by $\hat{V}_0/\hat{\omega}_0^{1/2}$; zero to peak scatter ranges from 5 to 20 percent in Figure 16 and from 20 to 35 percent in Figure 15. A comparison of the trends of the data in the two figures indicates that a peak oscillator response parameter given by $\hat{\omega}_0^{1/4}\hat{V}_0$ or $\hat{\omega}_0^{1/3}\hat{V}_0$ would correlate the data best, involving less than 15 percent of zero to peak scatter.

Looking back to Chapter I, it seems that the Case 1 results might characterize experimental data from model-scale shock tests of simulated equipment in the UERD shell if one assumes that peak response of an oscillator to $n = 1$ motion is not grossly affected by the presence of the end bells used to effect neutral buoyancy of the UERD shell. In addition, the Case 2 results might characterize experimental data obtained from full-scale shock tests on operational PERMIT-Class submarines since in a rough sense, Case 2 accounts for the presence of submarine equipment other than the oscillator. Finally, the Case 3 results might characterize experimental data obtained from shock tests of deep-diving hulls since in a rough sense, Case 3 accounts for increases in hull stiffness as well as for increases in effective hull mass.

C. RESULTS OF SPECIAL COMPUTATIONS

Because of the voluminous amount of data generated by the special computations and because the individual data points themselves are not of particular interest, the results of the special computations will be presented in summary form.

Data from special computation (1) indicate that in Case 1, an oscillator peak response to forcing caused only by $n = 1$ bare-hull motion is from 50 to 75 percent of that caused by total forcing; in Case 2, peak response to $n = 1$ forcing is from 75 to 115 percent of that to total forcing; and in Case 3, that of $n = 1$ is 94 to 102 percent of that to total forcing. Thus, $n = 1$ bare-hull motion is clearly the dominant bare-hull motion as far as oscillator response is concerned; in all three cases, the response caused only by $n = 3$ bare-hull motion is from 20 to 60 percent of that caused only by $n = 2$ forcing, indicating adequate convergence in n. Adequate convergence in m is also observed; in neither case, however, can convergence be termed rapid for all the oscillators.

Data from special computation (2) indicate that peak oscillator response to forcing of a basically oscillatory nature is highly sensitive to the value of β_0, e.g., that caused only by $n = 0$ bare-hull motion in Case 2 varies $\sim$100 percent for some oscillators when β_0 changes from 0.02 to 0.0001. Conversely, the response varies only slightly for basically exponential forcing, e.g., that caused only by $n = 1$ bare-hull motion in Cases 2 and 3 varies less than 5 percent when β_0 changes from 0.02 to 0.0001.

Data from special computation (3) indicate that peak oscillator response to total forcing varies 1 to 10 percent as β_0 changes from 0.02 to 0.0001, or as β_0 changes from 0.02 to 0.05, with peak response generally varying inversely with β_0.

Data from special computation (4) indicate that peak oscillator response varies as much as +14 or −17 percent as R_H is increased or decreased, respectively, by 20 percent. For Case 1 response is most sensitive to changes in R_H, with variations averaging +10 and −8 percent for +20 and −20 percent changes in R_H, respectively. In Case 2, data vary about

+6 and −7 percent for +20 and −20 percent changes in R_H, respectively. Case 3 data shows the least sensitivity to changes in R_H, averaging +3 and −4 percent for +20 and −20 percent changes in R_H, respectively. Thus we observe that although peak oscillator response is very insensitive to changes in β_0, it is only moderately insensitive to changes in R_H.

It is seen from the equations in Chapter IV that a 25-percent increase in K_H is equivalent to a 20-percent decrease in both oscillator mass and R_H and that a 16.7-percent decrease is equivalent to a 20-percent increase in both oscillator mass and R_H. Since decreases (increases) in oscillator mass tend to increase (decrease) peak oscillator response, and since decreases (increases) in R_H tend to decrease (increase) peak oscillator response, it is clear that peak oscillator response is less sensitive to changes in K_H than to changes in R_H.

Data from special computation (5) show that peak oscillator response to total forcing ranges from −15 to +15 percent for a 25-percent decrease in t_e, indicating that peak oscillator response is moderately insensitive to changes in t_e; this is fortunate since, as pointed out earlier, the point at which the envelopment period ends and the reverberant period begins is somewhat arbitrary.

Each of the eight oscillator acceleration time histories when $t \leq t_e$ can be roughly described as a $\sin(C\omega_0 t - \pi/8)$ function starting at $t = 3\pi/8\ C\omega_0$ which is connected smoothly at $t = 3\pi/8C\omega_0$ to a curve starting at $t = 0$ with zero slope. In Case 1, $C \sim 1$ for the high-frequency, small-mass oscillators, while for the low-frequency, large-mass oscillators, $C \sim 2$. In Cases 2 and 3, $C \sim 1/2$ for the high-frequency, small-mass oscillators, while for the low-frequency, large-mass oscillators, $C \sim 1$. From Chapter IV, oscillator response when $t > t_e$ is taken as sinusoidal with circular frequency ω_r.

VI. CONCLUSIONS AND POSSIBLE DIRECTIONS OF FUTURE STUDY

A. CONCLUSIONS

From the results presented above, the following conclusions are drawn:

1. The analytical technique and the rather crude mathematical model developed in this study are capable of predicting the principal trends in experimental shock spectra obtained from model-scale shock tests on the UERD shell containing simulated submarine equipment (Case 1 of this study) and full-scale tests on operational hulls (Case 2 of this study); in addition, shock spectra predictions pertaining to deep-diving hulls are presented (Case 3 of this study).

2. Within reasonable accuracy limits, peak oscillator response for lightly damped, linear oscillators in a given hull can be predicted in terms of $\hat{V}_0$, $\hat{M}_0$, and $\hat{\omega}_0$, i.e., without considering β_0.

3. $\hat{V}_0$ decreases uniformly with increasing $\hat{M}_0$ for a fixed value of $\hat{\omega}_0$.

4. Especially for large $\hat{M}_0$, $\hat{\omega}_0$ is an important parameter, with an increase in $\hat{\omega}_0$ producing a decrease in $\hat{V}_0$ for Cases 2 and 3. For Case 1, the shock spectra display a mild maximum at a value of $\hat{\omega}_0$ which decreases with increasing $\hat{M}_0$.

5. A given increase in $\hat{M}_0$ causes a greater decrease in $\hat{V}_0$ in a light hull (Case 1) than it does in a heavy hull (Cases 2 and 3), showing that differences among hulls are significant.

6. Model tests should produce oscillator response data which differ significantly from those obtained on operational submarines; the model-scale data should exceed the full-scale data for small values of oscillator mass but should be less than or about equal to the full-scale data for large values of oscillator mass. This is, in fact, the trend observed in Reference 17.

7. Model-scale shock tests are, however, useful for fundamental investigations of the shock problem since the essential nature of the interaction problem remains the same in both cases.

8. Correlation of peak oscillator response data in terms of the oscillator parameter $\hat{M}_0\,\hat{\omega}_0^3$ and a peak response parameter given by $\hat{V}_0$ times some (positive or negative) fractional power of $\hat{\omega}_0$ provides a simple and reasonably accurate way to present the data.

9. This peak response parameter decreases with increasing $\hat{M}_0\,\hat{\omega}_0^3$ for all three cases.

10. Beam response of the hull (i.e., $n = 1$ motion) constitutes the major bare-hull input for determining oscillator shock spectra in the manner outlined in this report. At a "hard spot" of the hull, namely, at a station corresponding to a deep floor, $n = 1$ beam response can be expected to be of even greater importance relative to the $n = 0$, 2, and 3 bare-hull responses, which involve deformation of the hull circumference. The differences between the responses of oscillators located on a small frame and on a deep floor should therefore arise mainly from the differences in the hull impedance at the oscillator attachment points.

B. POSSIBLE DIRECTIONS OF FUTURE STUDY

This study has used numerous simplifications and approximations in an attempt to understand the basic nature of this shock problem. It is clear that much work remains to be done. Two main lines of development appear promising.

1. Use of the basic analytical technique and mathematical model developed in this study to explore the following:

a. Varying the direction of attack and the oscillator location.*
The present study corresponds only to the simplest of geometries, although it may be easily extended to investigate the situation where the oscillator is mounted directly across the hull from its position in this study. For oscillator locations off the plane of θ-symmetry with respect to the shock-wave propagation vector, rotational response of the oscillator would be considered.

b. Mounting the oscillator on a hard spot (namely, a deep floor).
The hull input would be limited to the beam modes which, however, should be analyzed more realistically to include the responses of the whipping modes of the hull. The hull impedance at the oscillator attachment point for $t < t_e$ would be that of an infinite beam rather than of an infinite orthotropic plate.

c. The effect of the presence of other equipment.
The present technique (in a modified form) would be used for two adjoining oscillators; the oscillator-hull interaction analysis would take cognizance of the transfer impedance between the two oscillators.

d. The response of extended systems.
The present technique (in a modified form) would be used for systems supported at widely separated points on the hull; the oscillator-hull analysis would take cognizance of transfer impedances.

e. The response of a multidegree-of-freedom system attached to the hull.
The present study would be repeated for two and three degree-of-freedom systems.

f. The overall dynamic characteristics of various hulls.
This study would seek to explain the effect observed in model tests[17] that deep-submergence hulls tend to deliver a more severe shock input to the equipment than do present-day operational hulls.

2. Experimental study supplemented by analytical work.

a. Obtain experimental hull response time histories for shock-wave excitation (perferably on model scale) in the absence of a heavy oscillator whose peak response is to be predicted.

b. Make hull input impedance measurements on the above hull or hulls at the points at which the response time histories to shock-wave excitation were obtained; it may be necessary to neglect some of the fine detail of such measurements in succeeding steps so that idealization of the experimental data may be required.

c. Using the method described in Chapter IV, predict the peak responses of various oscillators using the information obtained in (a) and (b).

d. Perform shock tests identical to those in (a) only with the oscillators of (c) installed in the hull or hulls.

---

*This was included in the original proposal regarding this study but was not carried out because of the considerable effort required by the development of the present analytical technique. Another analytical development, which would involve more than a mere extension of the present analysis, would be an analysis of the response of an infinite cylindrical shell to an axially propagating shock wave, not requiring the use of the rather unnecessary approximations mentioned in connection with References 12-15.

e. Compare the peak oscillator responses predicted in (c) with those obtained in (d).

If a method such as this proves successful, it will serve as a first step toward more accurately determining shock-resistance requirements for heavy equipment in submarines by idealizing data obtained from these submarines in the absence of that heavy equipment.

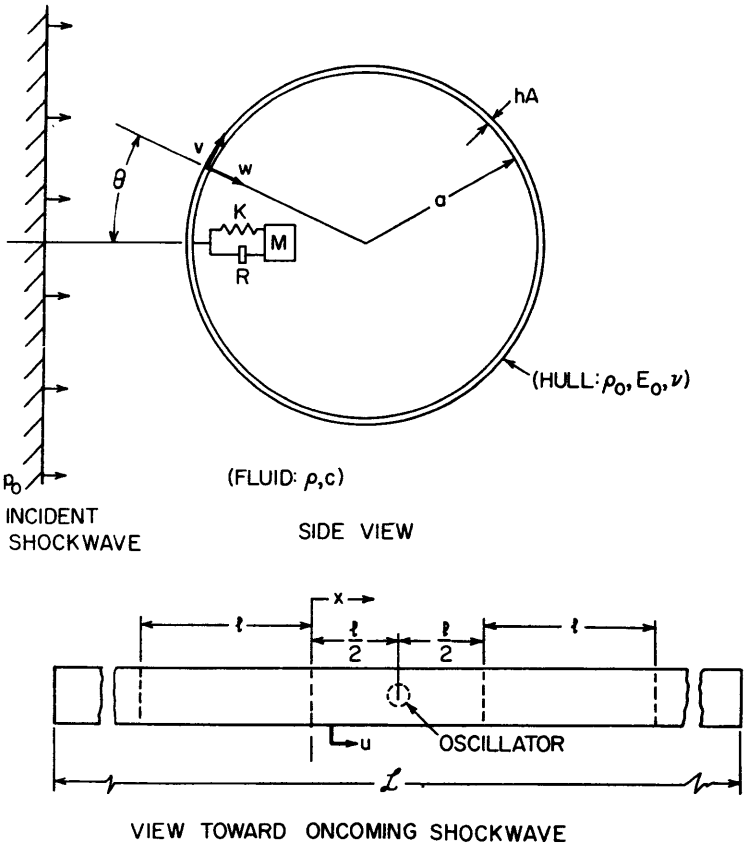

Figure 1 – Mathematical Model

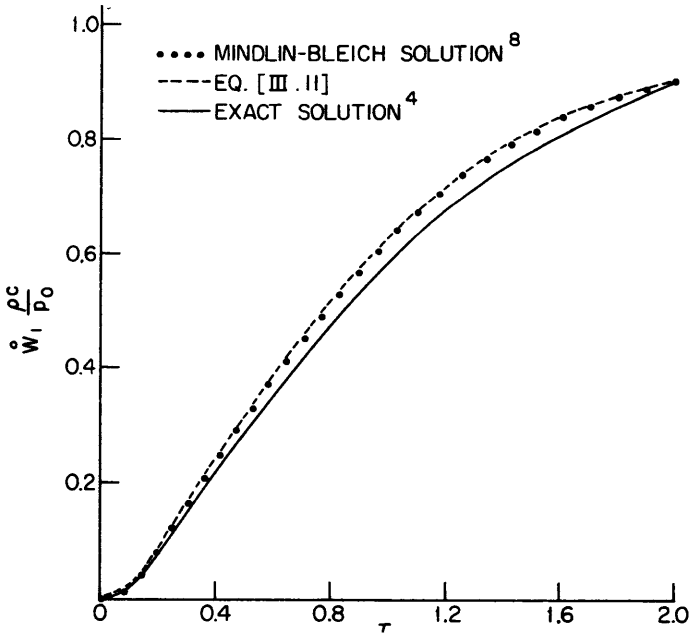

Figure 2 – $n = 1$ Velocity Solutions

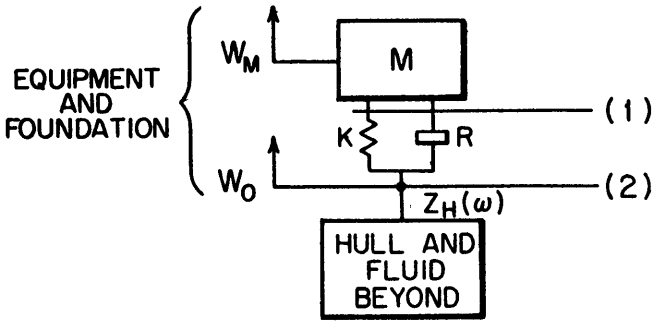

Figure 3 – Point-Attached Oscillator

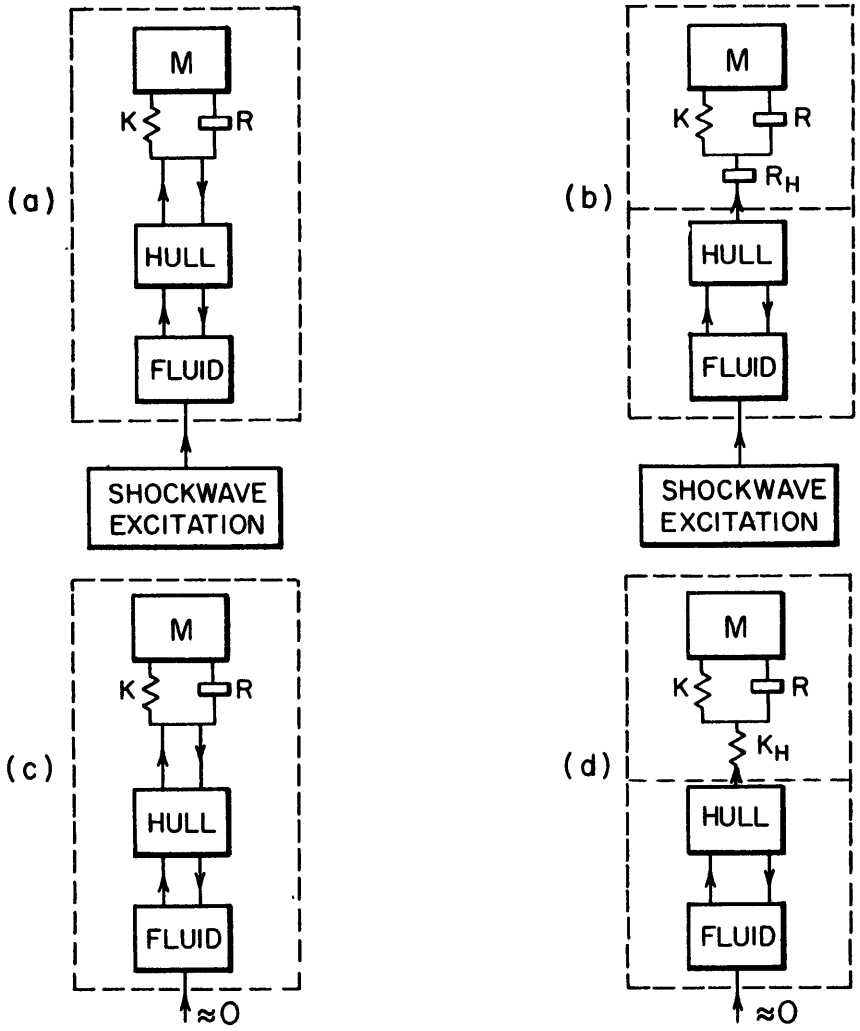

Figure 4 – Oscillator-Hull-Fluid Interactions

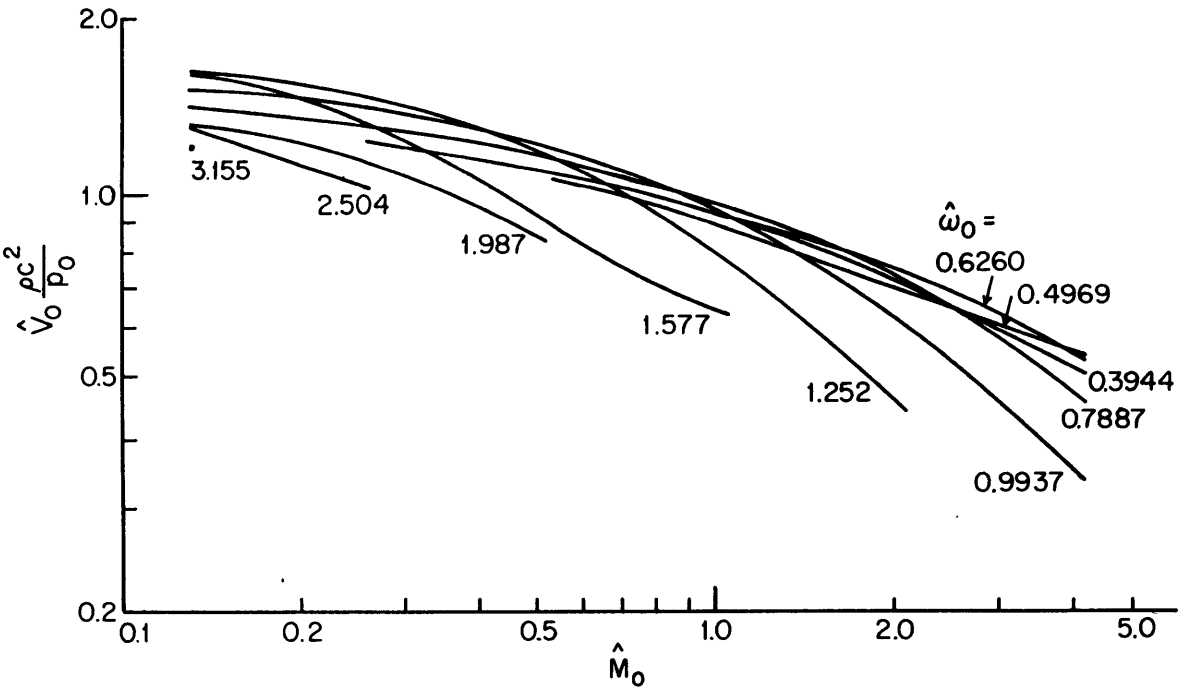

Figure 5 – Case 1 Peak Response versus Oscillator Mass

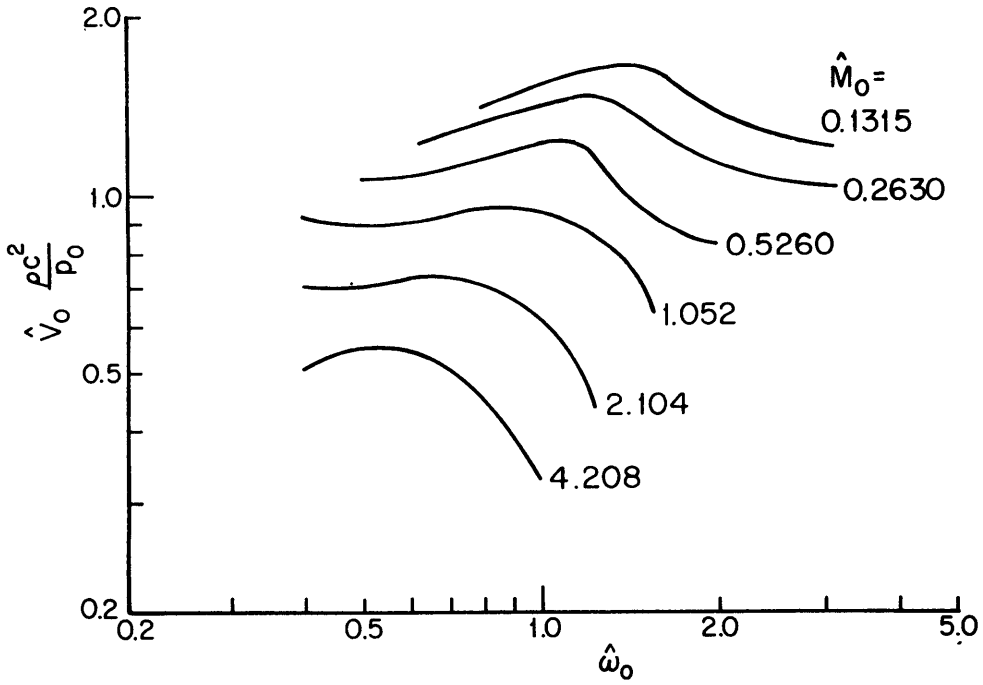

Figure 6 – Case 1 Peak Response versus Oscillator Frequency

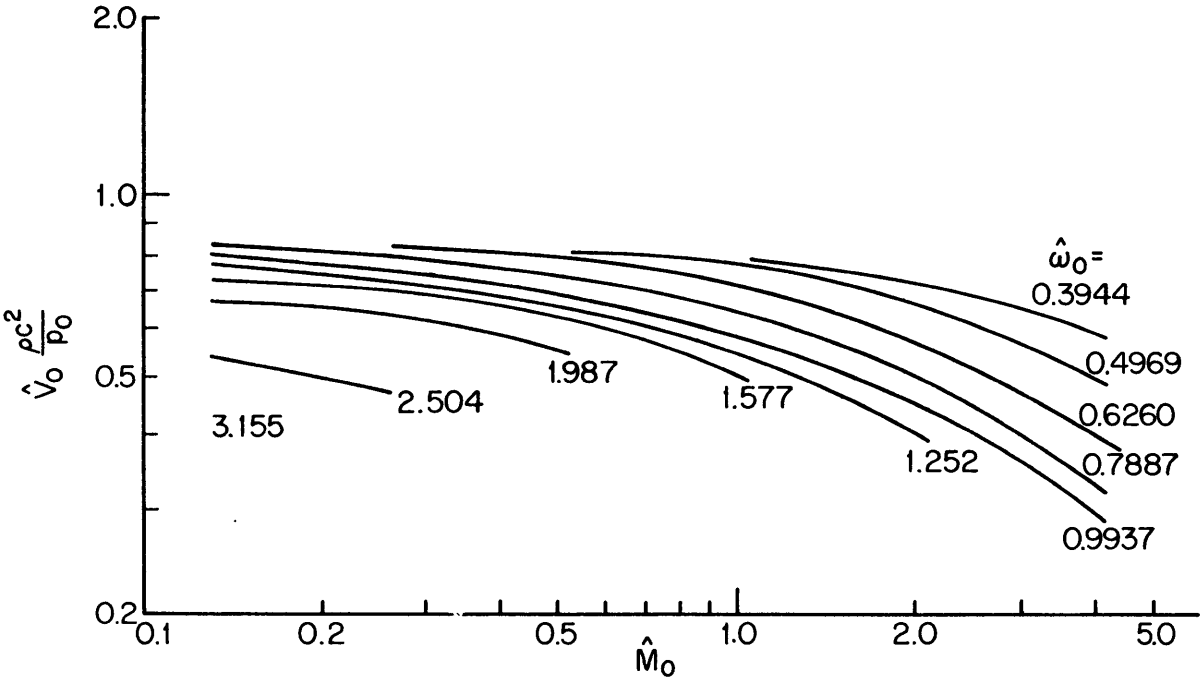

Figure 7 – Case 2 Peak Response versus Oscillator Mass

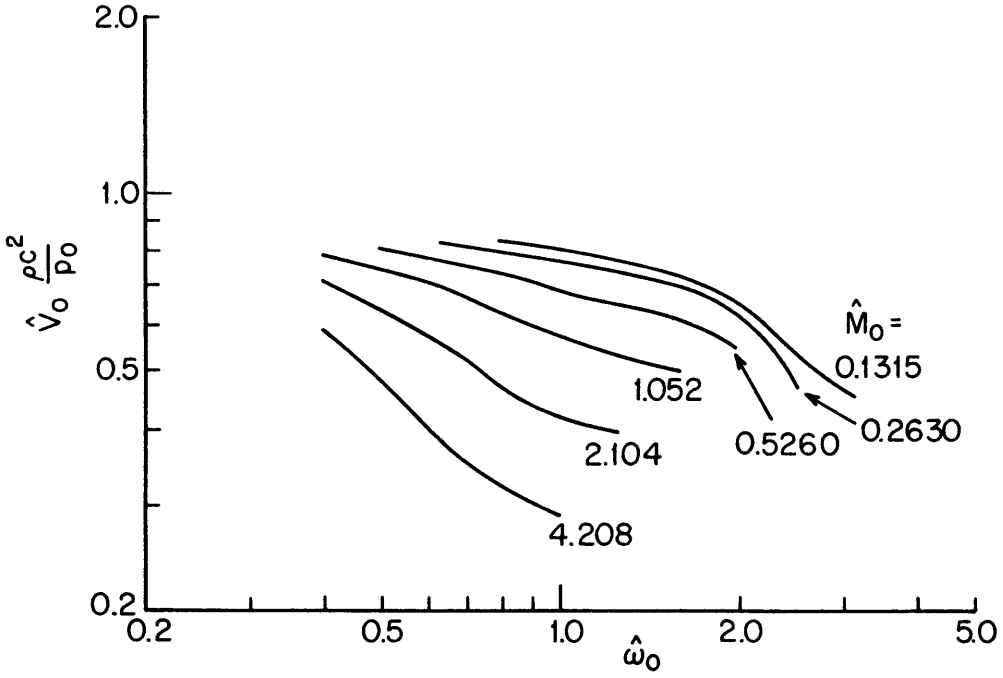

Figure 8 – Case 2 Peak Response versus Oscillator Frequency

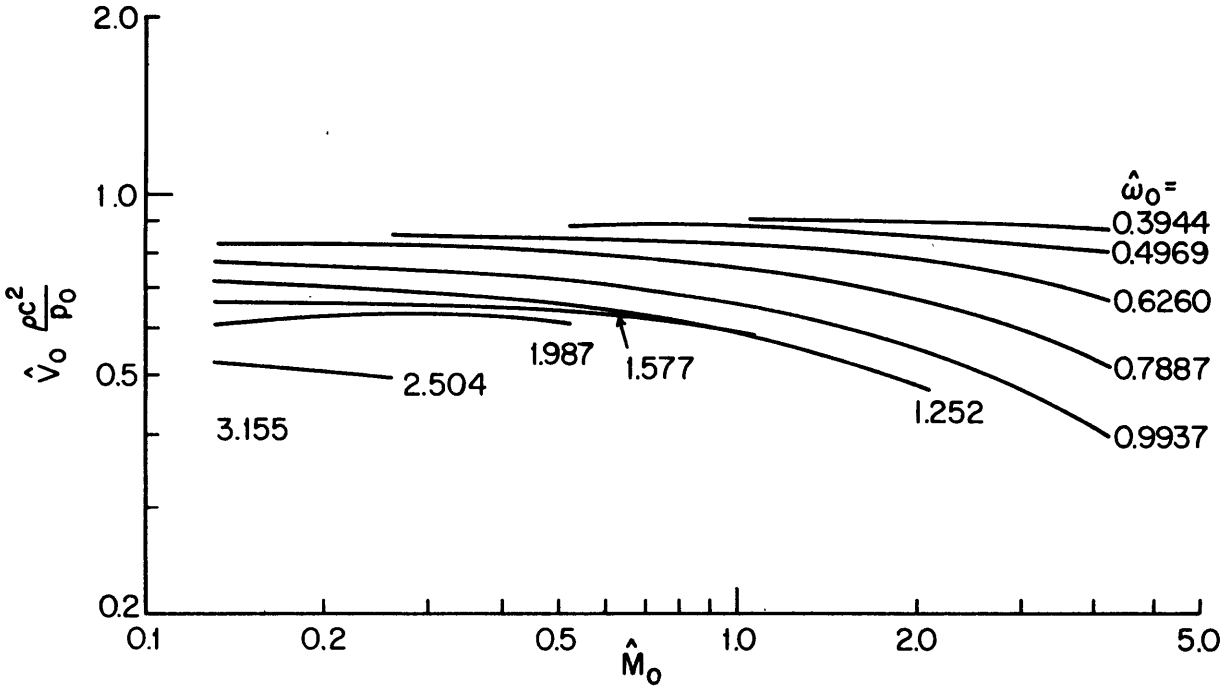

Figure 9 – Case 3 Peak Response versus Oscillator Mass

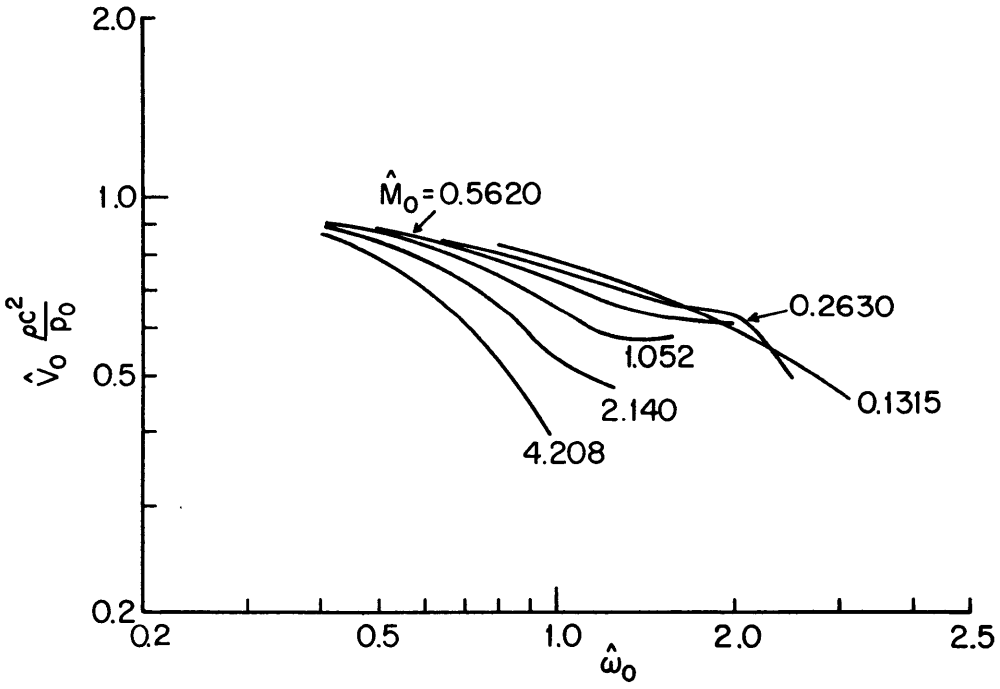

Figure 10 – Case 3 Peak Response versus Oscillator Frequency

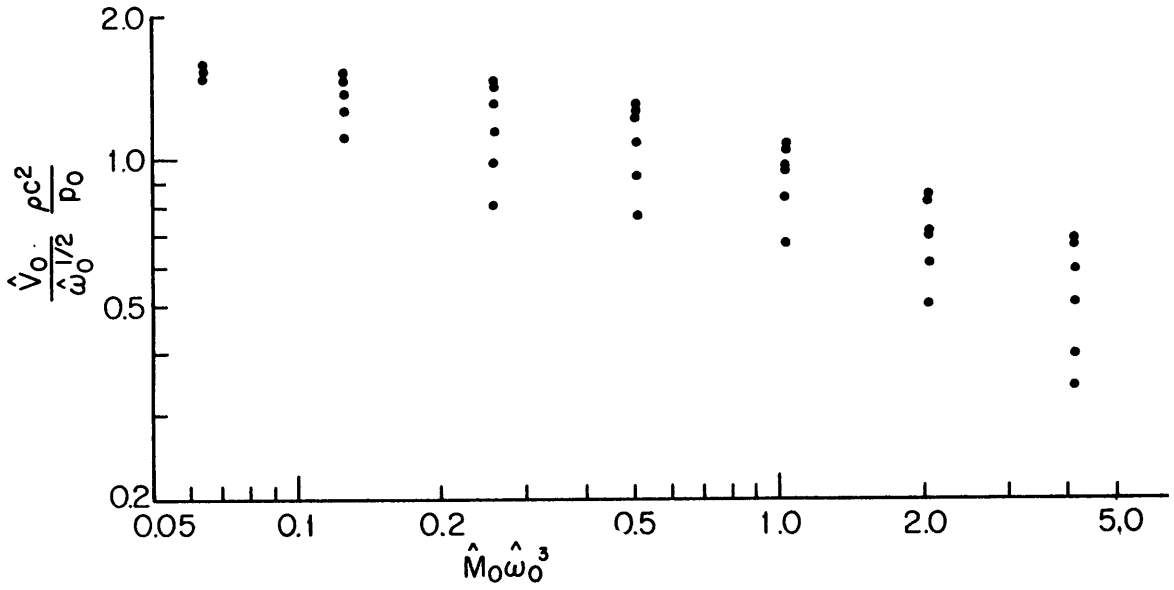

Figure 11 – First Correlation of Case 1 Peak Response Data

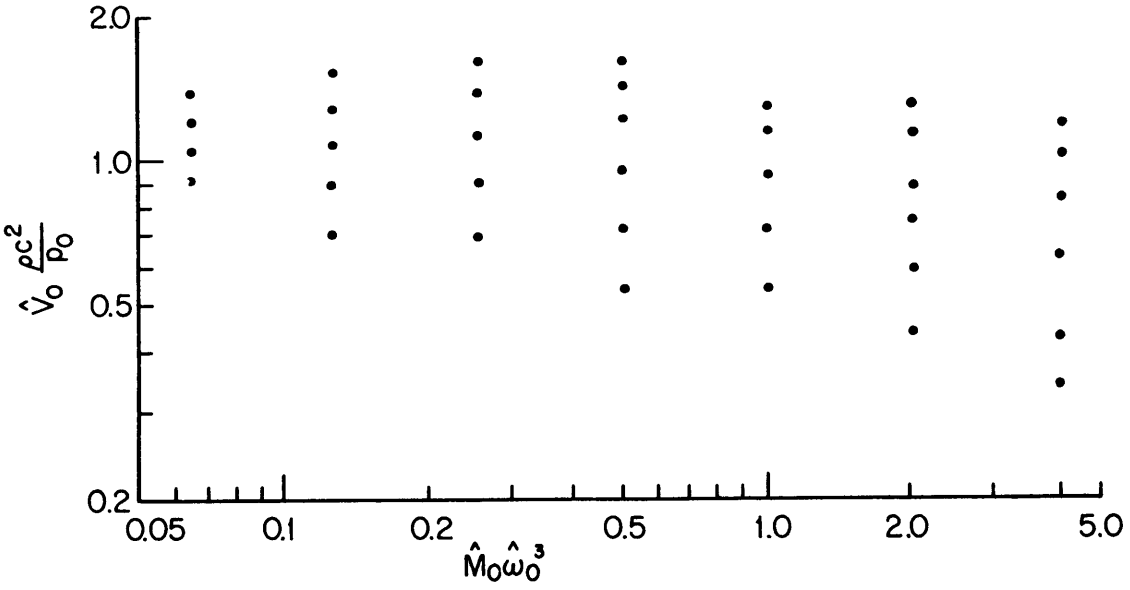

Figure 12 – Second Correlation of Case 1 Peak Response Data

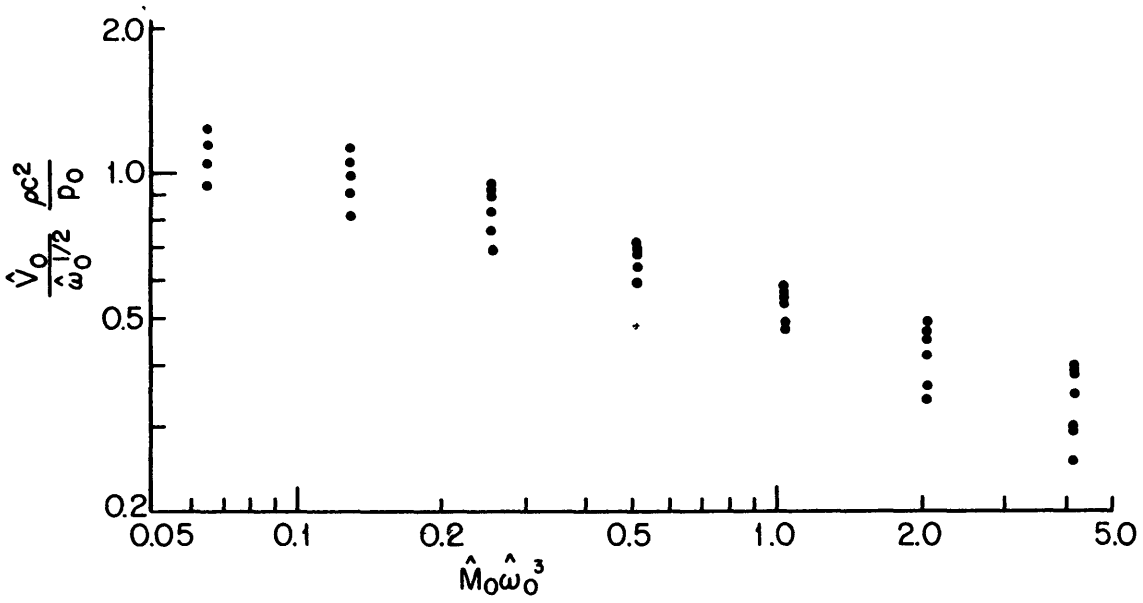

Figure 13 – First Correlation of Case 2 Peak Response Data

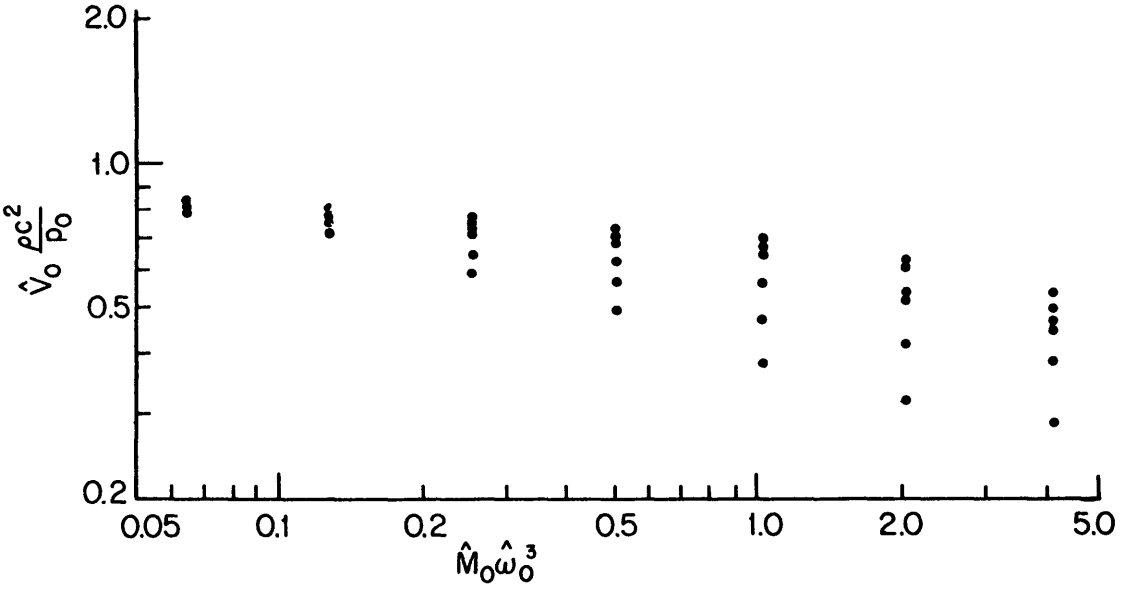

Figure 14 – Second Correlation of Case 2 Peak Response Data

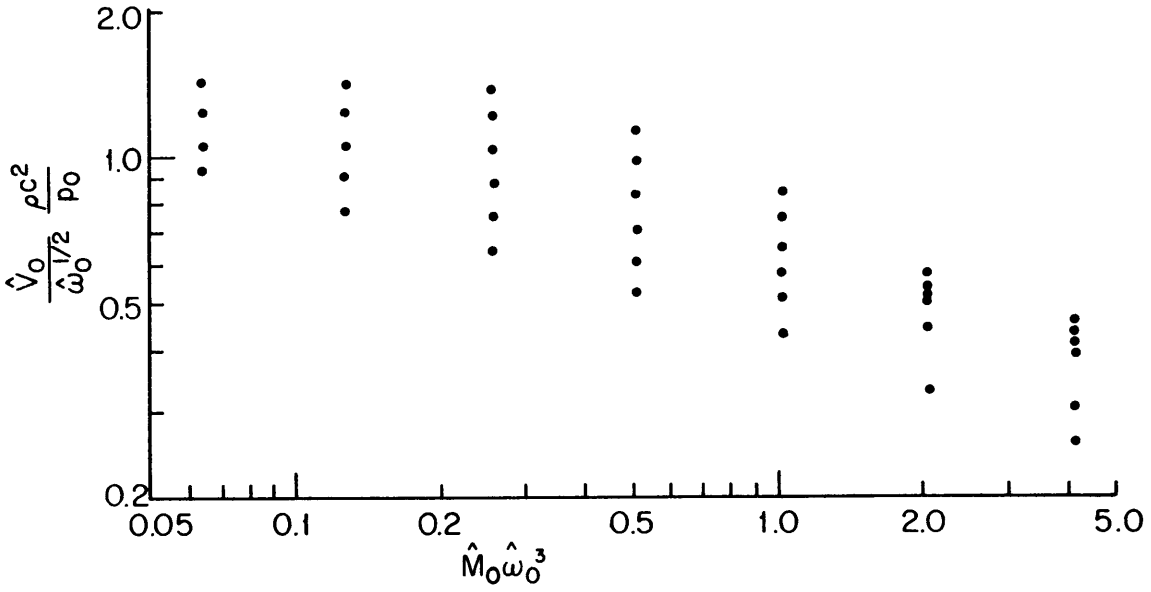

Figure 15 – First Correlation of Case 3 Peak Response Data

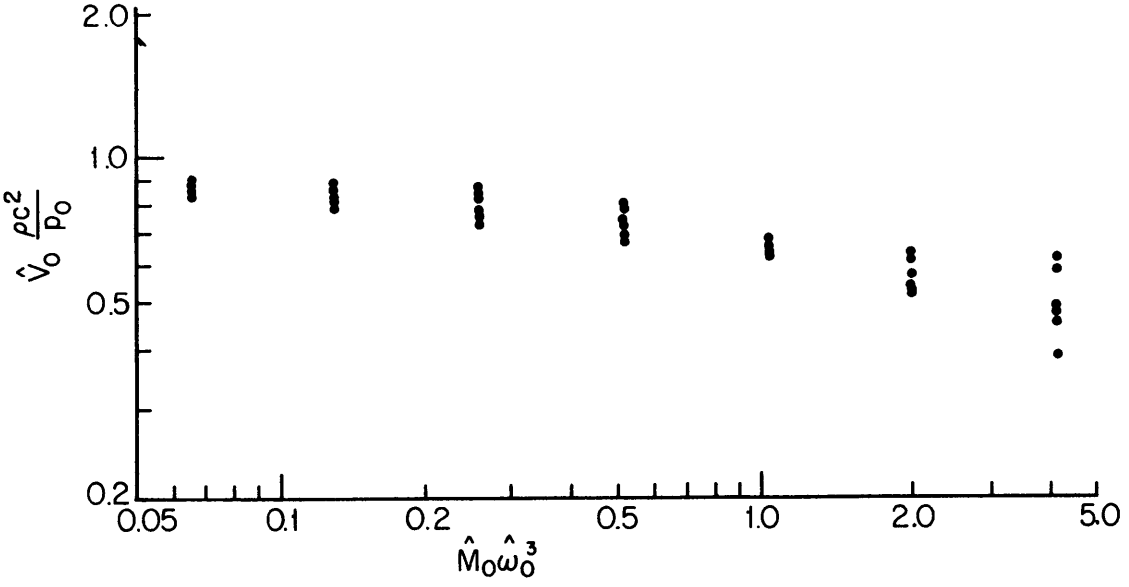

Figure 16 – Second Correlation of Case 3 Peak Response Data

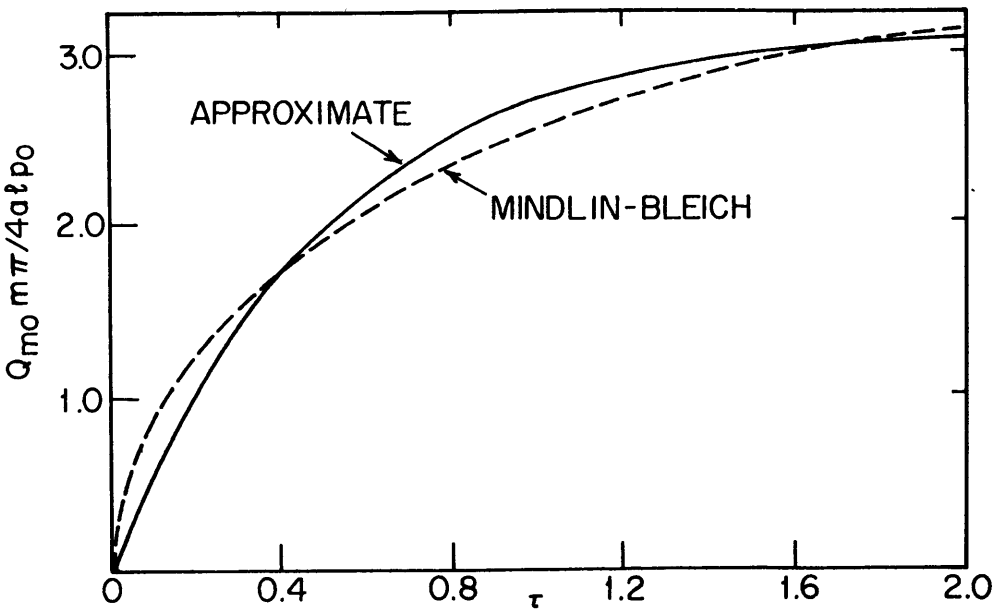

Figure 17 – $n = 0$ Generalized Forces

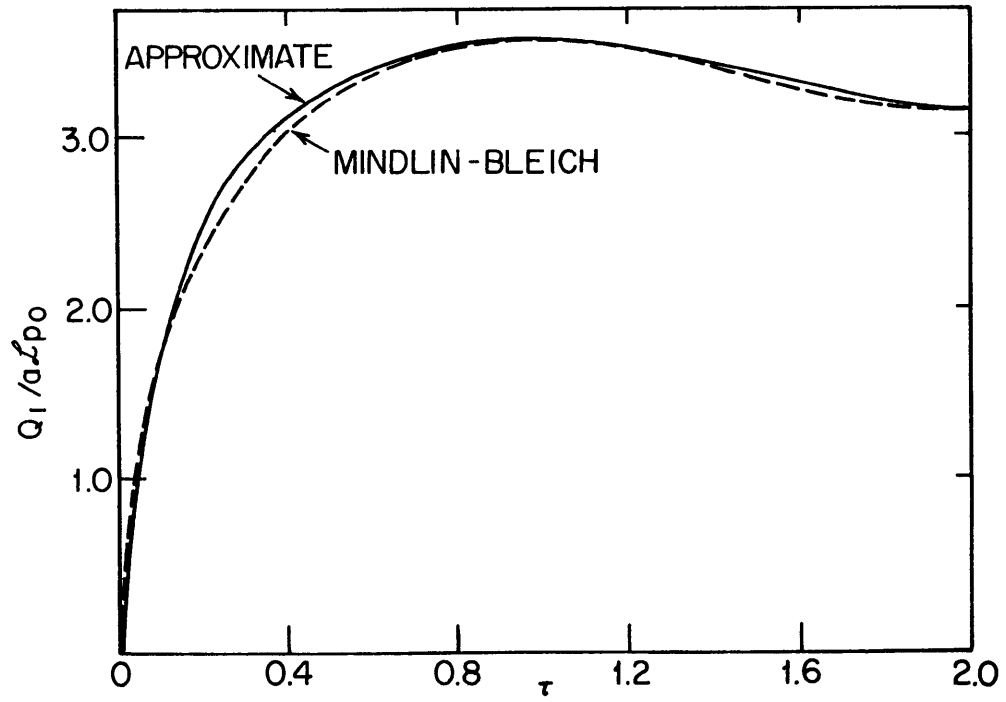

Figure 18 – $n = 1$ Generalized Forces

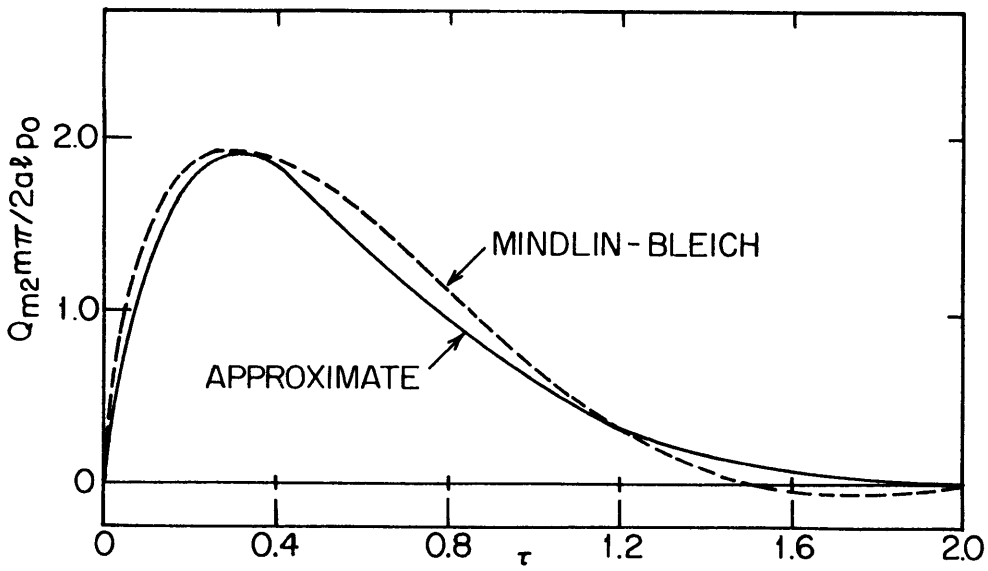

Figure 19 – $n = 2$ Generalized Forces

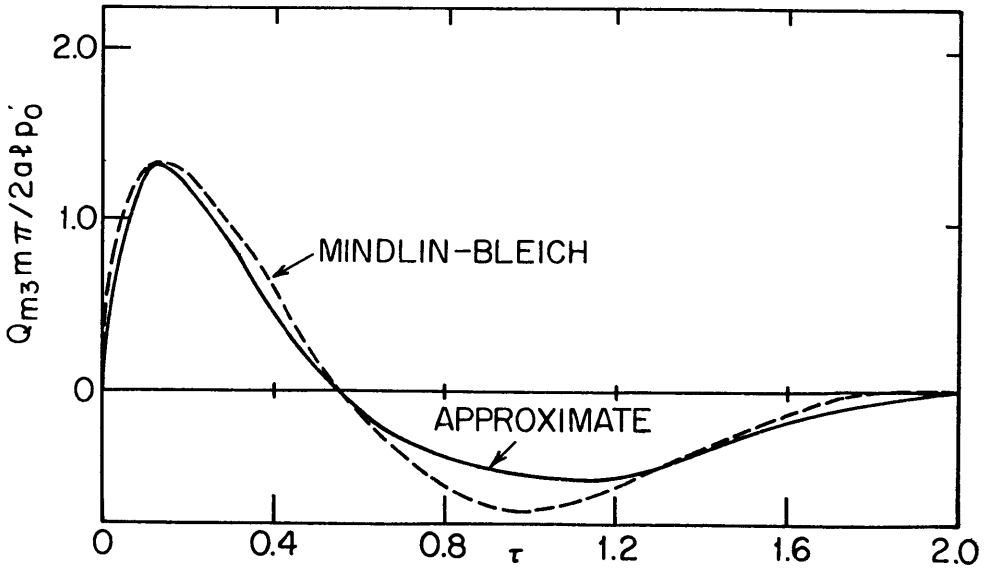

Figure 20 – $n = 3$ Generalized Forces

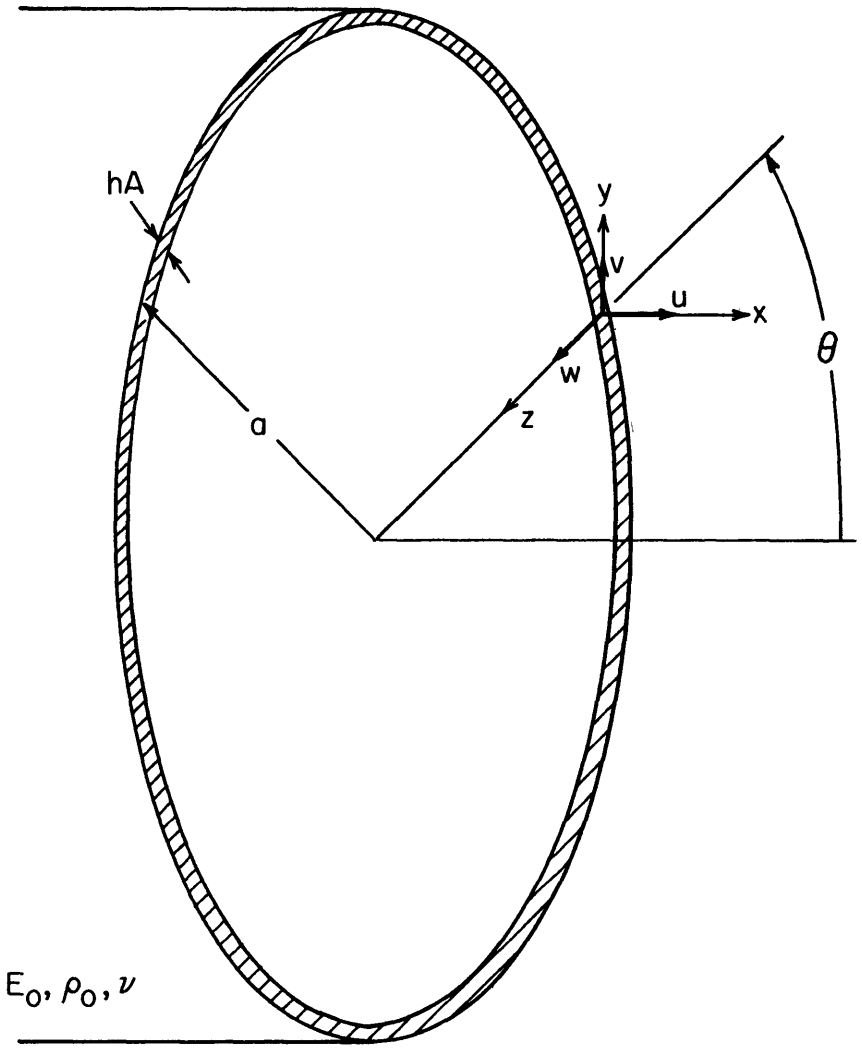

Figure 21 – Orthotropic Cylindrical Shell

TABLE 1

Oscillator Parameters

$\hat{M}_0$ \ $\hat{\omega}_0$	0.3944	0.4969	0.6260	0.7887	0.9937	1.252	1.577	1.987	2.504	3.155
0.1315				X	X	⊗	X	⊗	X	X
0.2630			X	X	X	X	X	X	X	
0.5260		X	X	⊗	X	⊗	X	X		
1.052	X	X	⊗	X	⊗	X	X			
2.104	X	X	X	X	X	X				
4.208	⊗	X	⊗	X	X					

X Denotes an oscillator included in the general computations.

⊗ Denotes an oscillator included in both the general and the special computations.

For the PERMIT-Class hull, $\hat{M}_0 = 1$ corresponds to a weight of 7600 lb.

For the PERMIT-Class hull, $\hat{\omega}_0 = 1$ corresponds to a frequency of 51 cps.

TABLE 2

Hull Parameters

	Case 1			Case 2			Case 3		
m	$\omega_{m0}\frac{a}{c}$	$\omega_{m2}\frac{a}{c}$	$\omega_{m3}\frac{a}{c}$	$\omega_{m0}\frac{a}{c}$	$\omega_{m2}\frac{a}{c}$	$\omega_{m3}\frac{a}{c}$	$\omega_{m0}\frac{a}{c}$	$\omega_{m2}\frac{a}{c}$	$\omega_{m3}\frac{a}{c}$
1_a	3.631	0.3076	0.7535	1.707	0.1446	0.3542	3.631	0.3076	0.7535
3	3.311	0.9699	0.9511	1.557	0.4560	0.4471	3.311	0.9699	0.9511
5	3.381	1.676	1.400	1.590	0.7877	0.6582	3.381	1.676	1.400
7	3.409	2.206	1.865	1.603	1.037	0.8765	3.409	2.206	1.865
1_b	1.725			0.8109			1.725		
m	β_{m0}	β_{m2}	β_{m3}	β_{m0}	β_{m2}	β_{m3}	β_{m0}	β_{m2}	β_{m3}
1_a	1.197	11.77	5.697	0.5629	5.532	2.678	0.2646	2.601	1.259
3	1.247	3.751	4.514	0.5861	1.764	2.122	0.2755	0.8291	0.9976
5	1.314	2.236	2.926	0.6176	1.051	1.373	0.2903	0.4942	0.6453
7	1.327	1.799	2.318	0.6239	0.8457	1.090	0.2933	0.3976	0.5122
1_b	0.1028			0.04833			0.0227		
m	μ_{m0}	μ_{m2}	μ_{m3}	μ_{m0}	μ_{m2}	μ_{m3}	μ_{m0}	μ_{m2}	μ_{m3}
1_a	1.041	1.250	1.111	4.710	5.656	5.028	4.710	5.656	5.028
3	1.096	1.244	1.111	4.959	5.627	5.025	4.959	5.627	5.025
5	1.019	1.208	1.107	4.609	5.464	5.008	4.609	5.464	5.008
7	1.000	1.140	1.096	4.525	5.159	4.960	4.525	5.159	4.960
1_b	25.51			115.4			115.4		

APPENDIX A

DISCUSSION OF VARIOUS APPROXIMATIONS

1. REACTION AT OSCILLATOR ATTACHMENT POINT

Chapter IV indicated that during the envelopment period, i.e., for $0 \leq t \leq t_e$, the shell responds to forcing at the oscillator attachment point as a point-loaded, fluid-backed, infinite orthotropic plate. The point impedance of an infinite orthotropic plate is frequency-independent, at least in the frequency range of interest where the thin-plate theory of flexural waves applies.* It is assumed in Chapter IV that the contribution of the radiation loading to the point impedance of the orthotropic plate is negligible during the envelopment phase. This approximation greatly simplified the shell-oscillator interaction problem because it preserves the frequency-independence of the point impedance. We shall now examine this approximation.

Gutin[28] computes the contribution of radiation loading to the point impedance of an infinite isotropic plate exposed to fluid on one side. The effect of radiation loading is expressed in terms of a complex factor χ as follows:

$$Z_H(\omega) = \frac{R_H}{\chi(\omega)} \qquad [A.1]$$

Here, as in Chapter IV, R_H is the frequency-independent, purely resistive impedance of an infinite plate *in vacuo*; Z_H is the actual impedance, which includes radiation loading. χ is actually a function of the ratio ω/ω_c, where ω_c is the coincidence frequency in radians per second, i.e., the frequency above which the wavelength of straight-crested flexural waves exceeds the wavelength in the acoustic medium.** In an isotropic plate, this frequency is given by

$$\omega_c = \frac{c^2}{c_0 r_g} \qquad [A.2]$$

---

*The frequency range where this approximation is valid is discussed in Section A.2.

**This concept is important to acousticians because flexural waves in large plates radiate sound effectively above, but not below this frequency. For orthotropic plates, i.e., for the situation relevant to this study, expressions for the two coincidence frequencies corresponding to the two flexural rigidities are given in Reference 26 together with the geometric mean of these two frequencies which determines the driving-point impedance of the plate.

where r_g is the radius of gyration of the plate cross section, i.e., 0.289 h (h being the thickness of the isotropic plate);

$c_0 = [E_0/\rho_0(1-\nu^2)]^{1/2}$ is the "plate velocity," i.e., the low-frequency phase velocity of compressive waves in the plate (211,000 in./sec for steel); and

c is the sound velocity in the fluid medium (59,050 in./sec for water).

The Gutin results for an isotropic plate indicate that χ tends to unity with increasing values of (ω/ω_c); for (ω/ω_c) equal to unity, χ equals (0.982-j 0.055). The high-frequency limit of the radiation loading is therefore zero rather than being proportional to ρc, as in the case of the shell modes discussed in Chapter II. It is to be expected that even though this conclusion is based on an isotropic plate analysis, it also applied to an orthotropic plate, namely, the stiffened hull. We see from Equations [IV.7] and [IV.8] that the approximate radius of gyration for the orthotropic plate is the geometric mean of the radii of gyration characterizing, respectively, the circumferential and the axial bending stiffnesses of the hull. This yields for an effective radius of gyration.

$$r_g = \hat{r}^{1/2}(0.289\ h) \qquad [A.3]$$

In addition, an effective plate velocity for the stiffened plate given by $c_h = [E_0/\rho_0(1-\nu^2/A)]^{1/2}$ replaces c_0 in Equation [A.2] (Appendix B). Equations [A.2] and [A.3] then produce an effective coincidence frequency which, in dimensionless form, i.e., multiplied by ~~alternating current~~ a/c, is given by

$$\hat{\omega}_c = 3.46\ \hat{r}^{-1/2}(c/c_h)\,(a/h) \qquad [A.4]$$

With the parameters used in Chapter IV, we find a coincidence frequency $\hat{\omega}_c$ of 32.5 (f_c = 1650 c/s for the PERMIT-Class hull). This frequency is intermediate between the coincidence frequency corresponding to the axial flexural waves ($\hat{\omega}_{cx}$ = 104, f_c = 5250 c/s) and the coincidence frequency for circumferential flexural waves ($\hat{\omega}_{c\theta}$ = 10.2, f_c = 515 c/s).

We see that setting χ equal to unity in Chapter IV amounts to using a high-frequency approximation for the radiation loading in our analysis of the oscillator-hull interaction during the envelopment period. This is consistent with the high-frequency assumption of a ρc-radiation loading in the analysis of the hull-shockwave interaction in Chapter II. It does not seem justified to refine the radiation loading in the oscillator-hull interaction analysis without effecting a corresponding refinement in the fluid-hull interaction analysis.

2. FLEXURAL WAVE CONSIDERATIONS RELEVANT TO OSCILLATOR-HULL INTERACTION

This section deals with three topics: (1) the region of validity for approximating the point impedance of an "infinite" curved plate by that of an infinite flat plate; (2) the maximum oscillator-hull attachment interface for which the hull presents a mechanical impedance essentially equal to the impedance sensed by a point force, as given in Equations [IV.7] and [IV.16]; and (3) the frequency range in which thin-plate theory is valid for the hull. Two parameters which arise in the discussion of these topics are the wavelength of a flexural wave in the shell and the wavelength of a compressional wave in the acoustic medium. The flexural wavelength in an isotropic plate varies inversely as $\omega^{1/2}$, and the acoustic wavelength in the acoustic medium varies inversely as ω. By definition, the acoustic wavelength equals the flexural wavelength at the coincidence frequency (Equation [A.2]) and exceeds the flexural wavelength at lower frequencies. Hence a convenient way of writing the flexural wavelength λ_f in terms of the acoustic wavelength λ_{ac} is as follows:*

$$\lambda_f = \lambda_{ac}(\hat{\omega}/\hat{\omega}_c)^{1/2}$$

$$\frac{\lambda_f}{2\pi a} = (\hat{\omega}\ \hat{\omega}_c)^{-1/2} \qquad \text{[A.5]}$$

In Chapter IV, the point impedance of the hull during the envelopment phase was taken to be that of an infinite orthotropic plate. This mathematical model is valid if (1) the duration of the envelopment phase is too short to permit the flexural waves radiated from the oscillator-hull attachment point to form standing waves and (2) if during this short time interval, the curvature of the shell has a negligible effect on the equations of motion of the hull. In Chapter IV, Condition (1) was shown to be satisfied. We will now show that Condition (2) is also satisfied. In comparing the elastic terms in the equations of motion of the cylindrical shell and the flat plate, we will ignore membrane stresses and focus our attention on flexural stresses. The reason for this is that for small deflections of plates transiently excited by transverse forces, the ~~membrane stresses become important only after standing waves are established.~~ membrane stresses are not produced, the response of the plate being inextensional. If we prove that the effect of curvature in the cylindrical plate is small, i.e., that the shell behaves like a plate during this early time interval, we will also have shown that our assumption of inextensionality was justified. The flexural potential energy per unit area of the plate or shell is

$$V = \frac{E_0 h^3}{24(1-\nu^2)}\left[(\kappa_1+\kappa_2)^2 - 2(1-\nu)\,(\kappa_1\kappa_2-\kappa_{12}^2)\right] \qquad \text{[A.6]}$$

* The second of these equations follows from the first since $\lambda_{ac} = 2\pi c/\omega = 2\pi \cdot a/\hat{\omega}$.

where κ_1, κ_2, and κ_{12} are the changes in curvature.[29] For flat plates, the changes in curvature are:

$$\begin{aligned} \kappa_1 &= \partial^2 w/\partial x^2 \\ \kappa_2 &= \partial^2 w/\partial y^2 \\ \kappa_{12} &= \partial^2 w/\partial x \partial y \end{aligned} \qquad [A.7]$$

For cylindrical shells,

$$\begin{aligned} \kappa_1 &= \partial^2 w/\partial x^2 \\ \kappa_2 &= \frac{1}{a^2}\frac{\partial^2 w}{\partial \theta^2} + \frac{1}{a^2}\frac{\partial v}{\partial \theta} \\ \kappa_{12} &= \frac{1}{a}\frac{\partial^2 w}{\partial x \partial \theta} + \frac{1}{a}\frac{\partial v}{\partial x} \end{aligned} \qquad [A.8]$$

Since the operator $(1/a)\ \partial/\partial\theta$ is equivalent to $\partial/\partial y$, the expressions for the cylinder tend to those for the flat plate as the radius, a, of the cylinder tends to infinity. For our purposes, we must show that the two terms which do not have their equivalent in the plate expressions of $(1/a^2)\ (\partial v/\partial\theta)$ and $(1/a)\ (\partial v/\partial x)$ are negligible compared to those components which are common to the cylinder and the flat plates:

$$\begin{aligned} \frac{1}{a^2}\frac{\partial v}{\partial \theta} &\ll \frac{1}{a^2}\frac{\partial^2 w}{\partial \theta^2} \\ \frac{1}{a}\frac{\partial v}{\partial x} &\ll \frac{1}{a}\frac{\partial^2 w}{\partial x \partial \theta} \end{aligned} \qquad [A.9]$$

Differentiating the second of these inequalities with respect to θ and integrating it with respect to x yields the first of Equations [A.9]; the two requirements are therefore equivalent. Consistent with our assumption of inextensionality we set

$$\frac{\partial v}{\partial \theta} = w$$

$$\frac{\partial v}{\partial x} = -\frac{1}{a}\frac{\partial u}{\partial \theta} \qquad [A.10]$$

$$\frac{\partial u}{\partial x} = 0$$

If we exclude the type of inextensional motion which involves a linear dependence of v and w on x, the inextensionality conditions require that u be a function of θ, but independent of x, thus making the derivative in the last of Equations [A.10] equal to zero. Using the first of Equations [A.10] in the first of Equations [A.9], this inequality becomes

$$\frac{w}{a^2} \ll \frac{1}{a^2}\frac{\partial^2 w}{\partial \theta^2} \qquad [A.11]$$

We note that the operation indicated by $(1/a)\,(\partial/\partial\theta)$ is equivalent to multiplying by $(2\pi/\lambda_{f\theta})$, just as the differentiation $\partial/\partial x$ amounts to multiplying by $(2\pi/\lambda_{fx})$. Equation [A.11] can therefore be written as

$$\left(\frac{2\pi a}{\lambda_{f\theta}}\right)^2 \gg 1 \qquad [A.12]$$

Substituting Equation [A.5], we see that the inequality requires

$$\hat{\omega}\,\hat{\omega}_{c\theta} \gg 1$$

or [A.13]

$$\hat{\omega} \gg (10.2)^{-1}$$

This inequality is obviously satisfied for all of the significant frequency range of the oscillator-shell interaction spectrum. It is consistent with the restriction that circumferential standing waves are not formed during envelopment, a fact which, incidentally, is expressed by Equation [A.12]. Before leaving this subject, we note that if the two terms peculiar to the cylinder satisfy the conditions in Equations [A.9], these terms are automatically negligible compared to κ_1, which is smaller than either κ_2 or κ_{12} in Equation [A.7]. The reason for this

is that the operation indicated by $\partial^2/\partial x^2$, which is equivalent to multiplication by $(2\pi/\lambda_{fx})^2$, gives rise to a term which is larger than $(1/a)\partial^2/\partial x \partial\theta$ or $(1/a)^2\partial^2/\partial\theta^2$ because λ_{fx} is smaller than $\lambda_{f\theta}$.

The second point to be explored is whether the assumption of a point force impedance at the oscillator-hull interface is a valid approximation for foundation columns or stanchions which, of course, extend over a finite attachment area. For an isotropic plate subjected to a load acting over a circular area of diameter d, the shear force per unit circumferential length tends to infinity as d^{-1} for vanishing values of d for a unit transverse velocity of the plate section.[30] The *resultant* force obtained by multiplying the shear forces by πd tends to the point impedance, i.e., to the finite, frequency-independent quantity in Equation [IV.8]. Now, in contrast to the impedance-per-unit circumferential length, the mechanical impedance associated with a distributed load increases only slowly above the mechanical impedance of a point load with increasing d. It can be verified that the deviation is no more than 25 percent for $d \leq 0.4\ \lambda_f$. Because test calculations have shown that the oscillator is relatively insensitive to changes in Z_H, even a large error in Z_H results in small errors in the shock spectrum. It is convenient to express the 25-percent-error requirement in terms of the area A_0 over which the distributed load acts, giving

$$A_0 \leq 0.126\ \lambda_f^2 \qquad [A.14]$$

We will now make our usual assumption that this relation holds for an orthotropic plate if we use the effective (i.e., the mean) flexural wavelength obtained by combining Equations [A.4] and [A.5]. Substituting the latter in Equation [A.4], the condition for the maximum permissible distributed load area becomes

$$A_0 \leq 4.96\ a^2/\hat{\omega}\ \hat{\omega}_c \qquad [A.15]$$

In terms of the full-scale hull parameters, this requirement is

$$A_0(\text{sq in.}) \leq \frac{2.67 \times 10^5}{f} \qquad [A.16]$$

where f is in cycles per second. From the predominantly low-frequency content of the computed oscillator response,* it appears consistent with other approximations made in this study to truncate the oscillator-hull interaction spectrum by introducing a low-pass cutoff

*See Chapter V.

frequency. This cutoff frequency is selected equal to $(2f_0)$, i.e., twice the fixed-based oscillator natural frequency. One thus obtains a relation between the maximum permissible interface area and the oscillator natural frequency. Additional insight into the practical range of validity of this study is obtained by relating the interface area to the weight of some equipment components in nuclear hulls. An examination of six direct-current emergency propulsion motors weighing between 48 and 130 kip yielded a value of 0.21 sq in./lb for the ratio of machinery base area to weight, the deviation from the mean being ± 18 percent. An examination of seven direct-coupled and geared ship service turbogenerator sets, weighing between 19 and 55 kip yielded a ratio of 0.37 sq in./lb, with a scatter of approximately ± 50 percent. If we average the direct-current motor and turbogenerator set ratios, we obtain an admittedly rather crude ratio of

$$\frac{A_0}{W_0} \approx 290 \text{ sq in./kip} \qquad \text{[A.17]}$$

with deviations of +66 percent and −57 percent. Combining this with Equation [A.16], and with our assumed $(2f_0)$ cutoff frequency for the oscillator-hull interaction spectrum, we finally arrive at the following requirement relating equipment component weight and oscillator natural frequency:

$$f_0(\text{cps}) \leq \frac{460}{W_0(\text{kip})} \qquad \text{[A.18]}$$

Thus, a piece of equipment weighing 5000 lb must have a natural frequency of 90 cps or less if the present analysis is to be applicable. A few of the numerical results in Section C for combinations of heavy equipment on very stiff springs do not satisfy this condition, but they are included in view of the highly approximate nature of Equation [A.18].

It is seen that the point attachment approximation to the foundation-hull interface is valid for many practical column foundations. The important practical situation not covered by this approximation is the deep-floor foundation. This foundation exerts a line load over approximately half of the shell circumference. The large compressive stiffness of the deep floor can be assumed to prevent any but transverse, whipping mode deformations over the lower half of the hull since, in contrast to the lobar and breathing modes, the whipping modes do not require an elastic deformation of the deep floors. A simple mathematical model for analyzing the shock damage to equipment on deep-floor foundations would therefore idealize the hull as a beam of variable mass and stiffness rather than as a shell. Such a model would therefore be simpler in that the breathing and lobar mode contributions need not be considered, but the transverse modes would have to be analyzed in a more refined fashion.

To conclude this section, we shall explore the frequency range of validity of the thin-plate approximation of flexural waves on which the impedance expressions (Equations [IV.2] and [A.8]) are based. For isotropic plates, Mindlin gives an upper frequency limit of

$$f \leq \frac{c_s}{20h}$$

where c_s is the shear velocity in the plate material* (1.26×10^5 in./sec in steel). Using an effective plate thickness of 17.5 in., which is representative of the larger of the two radii of gyration of the hull plating, i.e., which is related to $\lambda_{f\theta}$, we compute an upper frequency limit of 360 cps. This limitation is of the same order of magnitude as the larger values of cutoff frequencies ($2f_0$) computed for the oscillator-hull interaction spectrum when the oscillator has a relatively high natural frequency.

3. APPROXIMATIONS TO THE MINDLIN-BLEICH GENERALIZED FORCES ASSOCIATED WITH INCIDENT AND SCATTERED WAVES

To avoid numerical computation of the bare hull modal response, Chapter III used various approximations to the Mindlin-Bleich[8] generalized forces associated with the incident and scattered waves. The method used to obtain these approximations is described below; discrepancies between these approximations and the Mindlin-Bleich generalized forces are believed to be much smaller than errors associated with the use of the Mindlin-Bleich generalized forces themselves.

The technique used to obtain the approximations was simple curve fitting. For $n = 0$, Equation [III.20] constitutes a good approximation, as shown by Figure 17; the impulse (the integral over time) from $\tau = 0$ to $\tau = 2$ for the approximate force differs from that for the Mindlin-Bleich force by 0.6 percent. For $n = 1$, Equation [III.10] constitutes a very good approximation, as shown by Figure 18; the values and slopes of the approximate force are virtually identical to those of the Mindlin-Bleich force at $\tau = 1$ and $\tau = 2$, and the impulse from $\tau = 0$ to $\tau = 2$ for the approximate force matches that for the Mindlin-Bleich force. For $n = 2$, the first of Equations [III.29] constitutes a good approximation, as shown by Figure 19; the value and slope of the approximate force matches those of the Mindlin-Bleich force at $\tau = 0.293$ and the impulse from $\tau = 0$ to $\tau = 2$ for the approximate force matches that for the Mindlin-Bleich force. For $n = 3$, the second of Equations [III.29] constitutes a fairly good approximation, as shown by Figure 20; the value and slope of the approximate force matches those of the Mindlin-Bleich force at $\tau = 0.134$, and the impulse from $\tau = 0$ to $\tau = 2$ for the approximate force matches that for the Mindlin-Bleich force.

---

*Mindlin's criterion ($\Omega < 10^{-1}$) has been translated into the notation of this report by noting that his Ω is twice the ratio of the plate thickness to the wavelength of shear waves.

It is emphasized that these approximations serve only to simplify the computations leading to determination of oscillator response. It is seen that they constitute good approximations to the Mindlin-Bleich forces for $n = 0$ through $n = 3$, so that the chief uncertainty associated with their use is the result of employing the Mindlin-Bleich approximation to account for the scattered pressure loading on the shell.

APPENDIX B

DYNAMIC PARAMETERS OF THE HULL COMPARTMENT

A ring-stiffened cylindrical shell with a large number of equally spaced ring stiffeners should lend itself to accurate modeling as an orthotropic shell. Hoppmann[31] has formulated a method by which experimentally obtained orthotropic plate parameters can be used to determine approximate natural frequencies for a stiffened cylinder. Relatively rigorous analytical approaches, such as that of Gondikas,[32] are characterized by extensive analytical and computational efforts. Approximate analytical approaches of varying complexity (and thus of varying accuracy) have been presented by Bleich,[33] Galletly,[34] Greenspon,[35] and Garnett and Goldberg,[36] but even these require numerical computations which may be considered too extensive for many approximate analyses. Thus a highly simplified approach is needed which gives reasonably good values for parameters describing the lower shell modes.

Such an approach has been developed by one of the authors.[37] It is based on a systematic development of approximate constitutive relations and of approximate strain-displacement relations by analyzing the overall effects of the ring stiffeners on the shell. The approximate constitutive relations thus obtained are (Figure 21)

$$\sigma_x = \frac{E_0}{1-\nu^2/A}(\epsilon_x + \nu\,\epsilon_y)$$

$$\sigma_y = \frac{E_0}{1-\nu^2/A}(A\,\epsilon_y + \nu\,\epsilon_x) \qquad \text{[B.1]}$$

$$\sigma_{xy} = \frac{E_0}{2(1+\nu)}\,\epsilon_{xy}$$

where A is the ratio of the longitudinal cross-sectional area of the stiffened shell to that of the unstiffened shell. The approximate strain displacement relations obtained are

$$\epsilon_x = \partial u/\partial x - z(\partial^2 w/\partial x^2)$$

$$\epsilon_y = (1/a)\,(\partial v/\partial\theta) - w/a - (\hat{r}z/a^2)\,(\partial^2 w/\partial\theta^2 + \partial v/\partial\theta) \qquad \text{[B.2]}$$

$$\epsilon_z = \partial v/\partial x + (1/a)\,(\partial u/\partial\theta) - (1+\hat{r})\,(z/a)\,(\partial^2 w/\partial x\partial\theta + \partial v/\partial x)$$

In this equation, $\hat{r}$ is an effective ratio of the radius of gyration of the stiffened longitudinal cross section to that of the unstiffened longitudinal cross section and is given by

$$\hat{r} = \left(\frac{1}{A}\ \frac{I_S}{I_U}\right)^{1/2} \qquad [B.3]$$

where I_U is the area moment of inertia (about the centroidal axis) of the unstiffened cross section of the cylinder with length ℓ_S (the distance between stiffeners), and I_S is the area moment of inertia about the centroidal axis of the stiffened shell cross section consisting of one ring stiffener and an effective length of shell given by Bleich[33] as

$$\ell_E = \frac{1.52}{(1-\nu^2)^{1/4}}\sqrt{ah} \qquad [B.4]$$

Following Arnold and Warburton,[38] the following approximate expression for the cylinder potential energy is used

$$V = \int_0^{2\pi}\int_0^{\ell}\int_{-h/2}^{h/2} \frac{1}{2}\left[\sigma_x \epsilon_x + \sigma_y \epsilon_y + \sigma_{xy}\epsilon_{xy}\right] a\, d\theta dx dz \qquad [B.5]$$

Neglecting inter-ring deformation, the eigenfunctions appropriate to the free vibrations of a simply supported unstiffened shell are introduced. This yields

$$u(\theta, x, t) = \sum_{n=0}^{\infty}\sum_{m=1}^{\infty} u_{mn}(t)\cos n\theta \cos\frac{m\pi x}{\ell}$$

$$v(\theta, x, t) = \sum_{m=1}^{\infty} v_{m0}(t)\sin\frac{m\pi x}{\ell} + \sum_{n=1}^{\infty}\sum_{m=1}^{\infty} v_{mn}(t)\sin n\theta \sin\frac{m\pi x}{\ell} \qquad [B.6]$$

$$w(\theta, x, t) = \sum_{n=0}^{\infty}\sum_{m=1}^{\infty} w_{mn}(t)\cos n\theta \sin\frac{m\pi x}{\ell}$$

Equations [B.1], [B.2], and [B.6] are then used in Equation [B.5] and the integrations are performed to yield for the Lagrangian equation of the orthotropic (stiffened) cylinder

$$L = \frac{\pi}{2\epsilon_n}\rho_0 a\ell hA \sum_{n=0}^{\infty}\sum_{m=1}^{\infty}\left(\dot{u}_{mn}^2 + \dot{v}_{mn}^2 + \dot{w}_{mn}^2\right)$$

$$- \frac{\pi E_0 \ell h}{2\epsilon_n a(1-\nu^2/A)} \sum_{n=0}^{\infty}\sum_{m=1}^{\infty}\Bigg[\lambda^2 u_{mn}^2 + A(w_{mn}-nv_{mn})^2$$

$$+ 2\nu\lambda u_{mn}(w_{mn}-nv_{mn}) + \frac{1}{2}\left(\frac{1-\nu^2/A}{1+\nu}\right)(\lambda v_{mn}-nu_{mn})^2$$

$$+ \frac{h^2}{12a^2}\Big\{\lambda^4 w_{mn}^2 + 2\nu\hat{r}n\lambda^2 w_{mn}(nw_{mn}-v_{mn})$$

$$+ \left[A\hat{r}^2n^2 + \frac{1}{2}\left(\frac{1-\nu^2/A}{1+\nu}\right)(1+\hat{r})^2\lambda^2\right](nw_{mn}-v_{mn})^2\Big\}\Bigg] \qquad \text{[B.7]}$$

Applying the Lagrange equation with no forcing and letting $c_h^2 = E_0/\rho_0(1-\nu^2/A)$, $\delta = \frac{1}{2}(1-\nu^2/A)/(1+\nu)$ produces the dynamic equations

$$\frac{a^2}{c_h^2}\ddot{u}_{mn} + (\delta n^2+\lambda^2)u_{mn} - (\nu+\delta)n\lambda\, v_{mn} + \nu\lambda w_{mn} = 0$$

$$\frac{a^2}{c_h^2}\ddot{v}_{mn} - (\nu+\delta)n\lambda u_{mn} + \left[An^2 + \delta\lambda^2 + \frac{h^2}{12a^2}\{A\hat{r}^2n^2 + \delta(1+\hat{r})^2\lambda^2\}\right] v_{mn}$$

$$- n\left[A + \frac{h^2}{12a^2}\{A\hat{r}^2n^2 + \nu\hat{r}\lambda^2 + \delta(1+\hat{r})^2\lambda^2\}\right] w_{mn} = 0 \qquad \text{[B.8]}$$

$$\frac{a^2}{c_h^2}\ddot{w}_{mn} + \nu\lambda u_{mn} - n\left[A + \frac{h^2}{12a^2}\{A\hat{r}^2n^2 + \nu\hat{r}\lambda^2 + \delta(1+\hat{r})^2\lambda^2\}\right] v_{mn}$$

$$+ \left[A + \frac{h^2}{12a^2}\{\lambda^4 + A\hat{r}^2n^4 + 2\nu\hat{r}n^2\lambda^2 + \delta(1+\hat{r})^2n^2\lambda^2\}\right] w_{mn} = 0$$

For a given m-n combination, Equations [B.8] produce three modes of vibration, each vibrating sinusoidally in time. The mode shapes are obtained by first setting the determinant of the coefficient matrix multiplying the displacement column matrix equal to zero. A cubic equation results which yields three natural frequencies of vibration for that m-n vibration configuration. Substituting each of the frequencies into two of Equations [B.8] yields the mode shapes for the three orthogonal modes of vibration.

For radial forcing, the mode of greatest interest is that in which radial motion predominates; it is assumed that this mode is the lowest frequency mode for any specified m-n combination. This assumption is later checked and verified in all cases for $n \neq 0$ and when $\lambda >> \nu$ for $n = 0$. The inertia terms and all terms multiplied by $h^2/12a^2$ in the first two of Equations [B.8] are then neglected to obtain the approximate mode shapes

$$\left(\frac{U}{W}\right)_{mn} \approx \lambda \frac{A(n^2+\lambda^2) - (A+\nu)\lambda^2}{An^4 + 2(A+A\nu-\nu)n^2\lambda^2 + \lambda^4}$$

$$\left(\frac{V}{W}\right)_{mn} \approx n \frac{A(n^2+\lambda^2) + (A+2A\nu-\nu)\lambda^2}{An^4 + 2(A+A\nu-\nu)n^2\lambda^2 + \lambda^4} \qquad [B.9]$$

These approximate mode shapes are then used in the various terms of Equation [B.7] for the purpose of obtaining the Rayleigh quotient since, because of the stationary property of the Lagrangian for a true mode of vibration of the cylinder, errors in Equations [B.9] of order ϵ will produce errors in the Rayleigh quotient only of order ϵ^2.[39] This is preferable to using these approximate mode shapes in the third of Equations [B.8] with $\ddot{w}_{mn} = -\omega_{mn}{}^2 w_{mn}$; here, errors in Equations [B.9] of order ϵ will produce errors in $\omega_{mn}{}^2$ or order ϵ also.

At this point, $n \neq 0$ and $n = 0$ motions are investigated separately. For $n \neq 0$ motions, the bending potential energy (the terms multiplied by $h^2/12a^2$) and the kinetic energy in Equation [B.7] are simplified by using approximate expressions which neglect unimportant complicating terms in the original expressions. This yields for the dynamic parameters of the shell when $n \neq 0$

$$\mu_{mn} = 1 + \frac{n^2}{n^4 + (2A+2A\nu-\nu)^{-2}\lambda^4}$$

$$\frac{\omega_{mn}a}{c_h} = \left[1 + \frac{n^2}{n^4 + (2A+2A\nu-\nu)^{-2}\lambda^4}\right]^{-1/2} \left[\frac{(1-\nu^2/A)\lambda^4}{An^4 + 2(A+A\nu-\nu)n^2\lambda^2+\lambda^4}\right. \qquad [B.10]$$

$$\left. + \frac{1}{A}\frac{h^2}{12a^2}\left\{A\hat{r}^2(n^2-1)^2 + \left[2\nu\hat{r} + \frac{1}{2}\left(\frac{1-\nu^2/A}{1+\nu}\right)(1+\hat{r})^2\right](n^2-1)\lambda^2 + \lambda^4\right\}\right]^{1/2}$$

where $\mu_{mn} = m_{mn}\epsilon_n/\pi\rho_0 a\ell hA$ is the dimensionless generalized mass and $\omega_{mn}a/c_h$ is the dimensionless natural frequency for the primarily radial mode for a given m and a given (nonzero) n.

For $n = 0$ motion, it is seen from Equations [B.8] that for a given m, one mode involves purely circumferential motion. By orthogonality, the other two have $v_{m0} = 0$. For $\lambda >> \nu \sim 0.3$, Equations [B.9] apply, and the shell dynamic parameters for $n = 0$ are found to be

$$\mu_{m0} = 1$$

$$\frac{\omega_{mn}a}{c_h} = \left[1 - \nu^2/A + \frac{1}{A}\,\frac{h^2}{12a^2}\,\lambda^4\right]^{1/2} \qquad [B.11]$$

For $\lambda < \nu \sim 0.3$, Equations [B.9] do not apply; instead it is found that $\left(\frac{U}{W}\right)_{m0} \approx \nu\lambda$, and the dynamic parameters of the shell for $n = 0$ are found to be

$$\mu_{m0} = 1$$

$$\frac{\omega_{m0}a}{c_h} = 1 \qquad [B.12]$$

The approximate theory cannot be used for $\nu < \lambda < 10\nu$, but from Equations [B.11] and [B.12] it is concluded that for $n = 0$ motion, for all practical purposes the parameters for an orthotropic (stiffened) cylindrical shell can be obtained from those for the unstiffened cylinder merely by multiplying the generalized mass for the unstiffened cylinder by A. Using this modification, the Baron and Bleich tables[23] can be used for $n = 0$ motion when $\nu < \lambda < 10\nu$.

The above approximate relations are used to determine the dynamic parameters for the Underwater Explosions Research Division experimental hull. For this hull, $A = 1.51$, $r = 10.2$, $\ell/a = 6.14$, and $h/a = 9.5 \times 10^{-3}$, where a is the distance from the axis of the cylinder to the centroid of the longitudinal cross section of the shell about which I_S is taken. In addition, $\nu = 0.3$, $E_0 = 30 \times 10^6$ lb/in.^{2}, $\rho_0 = 7.4 \times 10^{-4}$ lb-sec^2/in.^{4}, $c = 59{,}000$ in./sec, and $\rho = 9.6 \times 10^{-5}$ lb-sec^2/in.^{4} are used.

The parameters required in Chapter III for $n = 0$, $n = 2$, and $n = 3$ are shown in Table 2. As explained in Chapter I, three cases are considered. All parameters are calculated for $m = 1$ through $m = 7$, even though (Chapter II) the Mindlin-Bleich approximation for $n = 0$

should start to fail for $m \geq 3$. Shell responses for all $m \leq 7$ are included, however, since the Mindlin-Bleich[8] approximation holds for all m at very early times, and since it is found that the $m \geq 3$, $n = 0$ modes contribute little to oscillator response anyway, especially at later times. Note that both $n = 0$, $m = 1$, $v_{m0} = 0$ modes are included since the Baron and Bleich tables suggest that both might be significantly excited.

From Equation [IV.8] the full-scale orthotropic plate impedance appropriate to the Underwater Explosions Research Division hull is $R_H = 4780$ lb-sec/in. The full-scale value of K_H used for the hull is $K_H = 2 \times 10^6$ lb/in.

REFERENCES

1. Belsheim, R.O. and O'Hara, G.J., "Shock Design of Shipboard Equipment, Part I – Dynamic Design-Analysis Method," NAVSHIPS 250-423-30,(May 1961); also Naval Research Laboratory Report 5545 (Sep 1960).

2. O'Hara, G.J. and Belsheim, R.O., "Shoc k Design of Shipboard Equipment, Part II – Interim Design Inputs for Submarine and Surface Ship Equipment (U)," NAVSHIPS 250-423-31 (Jan 1962); superseded by Naval Research Laboratory Memo Report 1396.

3. Sette, W.J., "The Pressure Produced on a Rigid Circular Cylinder by a Step Pulse (U)," Fourth Conference on Research on Ship Protection against Underwater Explosions, Navy Department NAVSHIPS Report 250-423-14 (Jul 1952).

4. Murray, W.W., "Interaction of a Spherical Acoustic Wave with a Beam of Circular Cross Section," Underwater Explosions Research Division Report 1-55, (Jan 1955).

5. Payton, R.G., "Transient Interaction of an Acoustic Wave with a Circular Cylindrical Elastic Shell," Journal of the Acoustical Society of America 32, 722-729 (1960).

6. Peralta, L.A. and Raynor, S., "Initial Response of a Fluid-Filled, Elastic, Circular Cylindrical Shell to a Shock Wave in Acoustic Medium," Journal of the Acoustical Society of America 36, 476-488 (1964).

7. Friedlander, F.G., "Diffraction of Pulses by a Circular Cylinder," Communications on Pure and Applied Mathematics 7, 705-732 (1954).

8. Mindlin, R.D. and Bleich, H.H., "Response of an Elastic Cylindrical Shell to a Transverse, Step Shock Wave," Journal of Applied Mechanics 20, 189 (1953).

9. Haywood, J.H., "Response of an Elastic Cylindrical Shell to a Pressure Pulse," Quarterly Journal of Mechanics and Applied Mathematics 11, 129 (1958).

10. Herman, H. and Klosner, J.M., "Transient Response of a Periodically Supported Cylindrical Shell Immersed in a Fluid Medium," Journal of Applied Mechanics 32, 562 (1965).

11. Junger, M.C., et al., "The Response of an Elastic Cylindrical Shell and of the Elastic Structures Therein to a Spherical Shock Wave," CAA, Inc. Report U-138-102, Contract NObs-84491 (May 1962).

12. Forrestal, M.J. and Herrmann, G., "Response of a Submerged Cylindrical Shell to an Axially Propagating Step Wave," Journal of Applied Mechanics Paper 65-APM-19.

13. Bhuta, P.G., "Transient Response of a Thin Elastic Cylindrical Shell to a Moving Shock Wave," Journal of the Acoustical Society of America 35, 25-30 (1963).

14. Brogan, W.L., "Radial Vibrations of a Thin Cylindrical Shell," Journal of the Acoustical Society of America 33, 1778-1781 (1961).

15. Cottis, M.G., "Green's-Function Technique in the Dynamics of a Finite Cylindrical Shell," Journal of the Acoustical Society of America 37, 31-42 (1965).

16. Cohen, D.S., "Vibration and Sound Radiation Measurements of Stiffened Cylindrical Shells (U)," Underwater Explosions Research Division Report C-1305, David Taylor Model Basin (Apr 1962).

17. Geers, T.L., "Shock Tests of Simulated Equipment in Model Submarine Pressure Hulls (U)," David Taylor Model Basin Report C-1731 (Mar 1965).

18. Chertock, G., "Resonant Scattering of Explosive Sound by Submarines," United States Navy Journal of Underwater Acoustics 14, 93-100 (1964).

19. Goodier, J.N. and McIvor, I.K., "The Elastic Cylindrical Shell under Nearly Uniform Radial Impulse," Journal of Applied Mechanics 31, 259-266 (1964).

20. McIvor, I.K., "The Elastic Cylindrical Shell under Radial Impulse," San Bernardino Operations, Aerospace Corp. Report TDR-469(S5810-12)-1 (Aug 1964).

21. Forsberg, K., "Influence of Boundary Conditions on the Model Characteristics of Thin Cylindrical Shells," American Institute of Aeronautics and Astronautics Journal 2, 2150-2157 (1964).

22. Arnold, R.N. and Warburton, G.B., "The Flexural Vibrations of Thin Cylinders," Journal of Proceedings of the Institution of Mechanical Engineers, London, 167, 62-74 (1953).

23. Baron, M.L. and Bleich, H.H., "Tables for Frequencies and modes of Free Vibration of Infinitely Long Thin Cylindrical Shells," Journal of Applied Mechanics 21, 178-184 (1954).

24. Ewing, W.M., et al., "Elastic Waves in Layered Media," McGraw-Hill Book Company, New York (1957), pp. 285-286.

25. "Proceedings of the First Symposium on Naval Structural Mechanics," Edited by Goodier and Hoff, Pergamon Press, New York (1960), "Waves and Vibrations in Isotropic, Elastic Plates," (R.D. Mindlin) pp. 199-232.

26. Heckl, M., "Untersuchungen an Orthotropen Platten," Acustica 10, 109-115 (1960). See also United States Navy Underwater Sound Reference Laboratory Translation No. 10, "Studies in Orthotropic Plates."

27. Wright, D.V. and Hagg, A.C., "Practical Calculation and Control of Vibration Transmission through Resilient Mounts and Basic Foundation Structures," Westinghouse Research Laboratories, 405 Fd 208-R2, Contract NObs 72326, Dec 1959, p. 6, Fig. 3.

28. Gutin, L. Ya., "Sound Radiation from an Infinite Plate Excited by a Normal Point Force," Soviet Physics: Acoustics 10, 369 (1965). The numerical results were actually quoted by Gutin from a Soviet paper by Tamm, et al., (Gutin Reference 1) which is relatively inaccessible.

29. Love, A.E.H., "A Treatise on the Mathematical Theory of Elasticity," 4th Edition, Dover Publications, New York (1944), p. 530. For changes in curvature of a flat plate see p. 464, and for those of a cylindrical shell se p. 543.

30. Thomas, D.A., "Characteristic Impedances for Flexure Waves in Thin Plates," Journal of the Acoustical Society of America 30, 220 (1958), gives a plot of this shear force versus $\omega d/2c_f$.

31. Hoppmann II, W.H., "Some Characteristics of the Flexural Vibrations of Orthogonally Stiffened Cylindrical Shells," Journal of the Acoustical Society of America 30, 77 (1958).

32. Gondikas, P.C., "Vibrations of Ring-Stiffened Cylindrical Shells," Columbia University Report 13, Contract Nonr-266(08) (Mar 1955).

33. Bleich, H.H., "Approximate Determination of the Frequencies of Ring Stiffened Cylindrical Shells," Columbia University Report 14, Contract Nonr-266(08) (Mar 1955).

34. Galletly, G.D., "On the In-Vacuo Vibrations of Simply Supported Ring-Stiffened Cylindrical Shells," Proceedings of the Second United States National Congress of Applied Mechanics (Jun 1954).

35. Greenspon, J.G., "Random Loading and Radiation from Stiffened and Sandwich Type Cylindrical Shell Structures," J G Engineering Research Associates Report 7, Contract Nonr-2733(00) (Sep 1962).

36. Garnet, H. and Goldberg, M.A., "Free Vibrations of Ring-Stiffened Shells," Grumman Aircraft Engineering Corporation Report 2, Contract Nonr-3465(00) (Mar 1962).

37. Geers, T.L., "An Approximate Analysis of the Vibrations of Stiffened Plates and Stiffened Cylindrical Shells," Ph.D. Unpublished Thesis Proposal, Department of Mechanical Engineering, Massachusetts Institute of Technology (Sep 1965).

38. Arnold, R.N. and Warbuton, G.B., "Flexural Vibrations of the Walls of Thin Cylindrical Shells Having Freely Supported Ends," Proceedings of the Royal Society (London) Series A, 197, 238 (1949).

39. Crandall, S.H., Engineering Analysis, McGraw-Hill Book Company, New York (1956).

INITIAL DISTRIBUTION

Copies

- 13 CHBUSHIPS
  - 2 Ship Protect (Code 423)
  - 2 Tech Lib (Code 210L)
  - 1 Ch Scientist for R&D (Code 305)
  - 1 Lab Mgt (Code 320)
  - 1 App Res (Code 340)
  - 1 Shock Coordinator (Code 641A)
  - 1 Prel Des (Code 420)
  - 1 Mach Sci (Code 436)
  - 1 Hull Des (Code 440)
  - 1 Sci & Res (Code 442)
  - 1 Sub Br (Code 525)
- 1 CHNAVMAT
- 2 CHBUWEPS
  - 1 Tech Lib (Code DLI-3)
  - 1 Physical Sci Consultant (Code RR23)
- 2 CHONR
  - 1 Attn: Dr. H. Leibowitz
- 1 DASA
- 1 CO & DIR, USNASL
- 1 CO & DIR, USNEL
- 1 CO & DIR, USNMDL
- 1 CO & DIR, USNMEL
- 1 CO & DIR, USNUSL
- 1 CO & DIR, RADLDEFLAB
- 1 CDR, USNOL, White Oak
- 1 CDR, USNOTS, China Lake
- 2 DIR, USNRL
  - 1 (Code 6260)
  - 1 (Code 2020)
- 1 CDR, USNWEPLAB
- 1 CO, USNUOS
- 1 O in C, PGSCOL, Webb
- 1 SUPT, PGSCOL, Monterey

Copies

- 1 CO, USNROTC & NAVADMINUMIT (Post Graduate School)
- 2 Cambridge Acoustical Assoc
  - 1 Dr. M. C. Junger
  - 1 Mr. Thomas L. Geers
- 20 CDR, DDC

UNCLASSIFIED

Security Classification

DOCUMENT CONTROL DATA - R&D

(Security classification of title, body of abstract and indexing annotation must be entered when the overall report is classified)

1. ORIGINATING ACTIVITY (Corporate author)	2a REPORT SECURITY CLASSIFICATION
Department of the Navy David Taylor Model Basin Washington, D.C. 20007	UNCLASSIFIED
	2b GROUP

3. REPORT TITLE

TRANSIENT RESPONSE OF A DAMPED MECHANICAL OSCILLATOR ATTACHED TO A SHOCK-WAVE-EXCITED, SUBMERGED CYLINDRICAL SHELL

4. DESCRIPTIVE NOTES (Type of report and inclusive dates)

Final Report

5. AUTHOR(S) (Last name, first name, initial)

Geers, Thomas L. and Junger, Miguel C.

6. REPORT DATE	7a TOTAL NO. OF PAGES	7b. NO. OF REFS
March 1966	88	39

8a. CONTRACT OR GRANT NO.	9a. ORIGINATOR'S REPORT NUMBER(S)
N600(167)60523(X)FBM b. PROJECT NO.	2142
c Req. No. 00167-3-000139 d.	9b. OTHER REPORT NO(S) (Any other numbers that may be assigned this report) Cambridge Acoustical Associates, Inc. U-209-150

10. AVAILABILITY/LIMITATION NOTICES

Distribution of this document is unlimited.

11. SUPPLEMENTARY NOTES	12. SPONSORING MILITARY ACTIVITY
Report was prepared by by Cambridge Acoustical Associates, Inc. 129 Mount Auburn Street Cambridge, Massachusetts 02138	Department of the Navy David Taylor Model Basin Washington, D.C. 20007

13. ABSTRACT

This report presents a simple analytical technique for investigating the response of a linear single degree-of-freedom mechanical oscillator mounted in a frame-stiffened cylindrical compartment of a shock-wave-excited submarine hull. Computations are performed to explore the dependence of peak oscillator response on oscillator fixed-base natural frequency, mass, and damping. It is found that damping is not a significant variable for lightly damped oscillators and that peak oscillator response can be correlated with reasonable accuracy in terms of two simple parameters. The general characteristics of experimental shock spectra measured in model tests and in tests on operational submarines are found to be predictable by means of two different mathematical models. Suggestions are made for further use of the analytical technique developed here, possibly in combination with experimental studies.

DD FORM 1 JAN 64 1473

UNCLASSIFIED

Security Classification

14. KEY WORDS	LINK A		LINK B		LINK C	
	ROLE	WT	ROLE	WT	ROLE	WT
Shock Submarine Hulls Submarine Equipment Underwater Explosion Effects Theory Cylindrical Shells Stiffened Shells						

INSTRUCTIONS

1. ORIGINATING ACTIVITY: Enter the name and address of the contractor, subcontractor, grantee, Department of Defense activity or other organization *(corporate author)* issuing the report.

2a. REPORT SECURITY CLASSIFICATION: Enter the overall security classification of the report. Indicate whether "Restricted Data" is included. Marking is to be in accordance with appropriate security regulations.

2b. GROUP: Automatic downgrading is specified in DoD Directive 5200.10 and Armed Forces Industrial Manual. Enter the group number. Also, when applicable, show that optional markings have been used for Group 3 and Group 4 as authorized.

3. REPORT TITLE: Enter the complete report title in all capital letters. Titles in all cases should be unclassified. If a meaningful title cannot be selected without classification, show title classification in all capitals in parenthesis immediately following the title.

4. DESCRIPTIVE NOTES: If appropriate, enter the type of report, e.g., interim, progress, summary, annual, or final. Give the inclusive dates when a specific reporting period is covered.

5. AUTHOR(S): Enter the name(s) of author(s) as shown on or in the report. Enter last name, first name, middle initial. If military, show rank and branch of service. The name of the principal author is an absolute minimum requirement.

6. REPORT DATE: Enter the date of the report as day, month, year, or month, year. If more than one date appears on the report, use date of publication.

7a. TOTAL NUMBER OF PAGES: The total page count should follow normal pagination procedures, i.e., enter the number of pages containing information.

7b. NUMBER OF REFERENCES: Enter the total number of references cited in the report.

8a. CONTRACT OR GRANT NUMBER: If appropriate, enter the applicable number of the contract or grant under which the report was written.

8b, 8c, & 8d. PROJECT NUMBER: Enter the appropriate military department identification, such as project number, subproject number, system numbers, task number, etc.

9a. ORIGINATOR'S REPORT NUMBER(S): Enter the official report number by which the document will be identified and controlled by the originating activity. This number must be unique to this report.

9b. OTHER REPORT NUMBER(S): If the report has been assigned any other report numbers *(either by the originator or by the sponsor)*, also enter this number(s).

10. AVAILABILITY/LIMITATION NOTICES: Enter any limitations on further dissemination of the report, other than those imposed by security classification, using standard statements such as:

(1) "Qualified requesters may obtain copies of this report from DDC."

(2) "Foreign announcement and dissemination of this report by DDC is not authorized."

(3) "U. S. Government agencies may obtain copies of this report directly from DDC. Other qualified DDC users shall request through _____."

(4) "U. S. military agencies may obtain copies of this report directly from DDC. Other qualified users shall request through _____."

(5) "All distribution of this report is controlled. Qualified DDC users shall request through _____."

If the report has been furnished to the Office of Technical Services, Department of Commerce, for sale to the public, indicate this fact and enter the price, if known.

11. SUPPLEMENTARY NOTES: Use for additional explanatory notes.

12. SPONSORING MILITARY ACTIVITY: Enter the name of the departmental project office or laboratory sponsoring *(paying for)* the research and development. Include address.

13. ABSTRACT: Enter an abstract giving a brief and factual summary of the document indicative of the report, even though it may also appear elsewhere in the body of the technical report. If additional space is required, a continuation sheet shall be attached.

It is highly desirable that the abstract of classified reports be unclassified. Each paragraph of the abstract shall end with an indication of the military security classification of the information in the paragraph, represented as *(TS), (S), (C), or (U)*.

There is no limitation on the length of the abstract. However, the suggested length is from 150 to 225 words.

14. KEY WORDS: Key words are technically meaningful terms or short phrases that characterize a report and may be used as index entries for cataloging the report. Key words must be selected so that no security classification is required. Identifiers, such as equipment model designation, trade name, military project code name, geographic location, may be used as key words but will be followed by an indication of technical context. The assignment of links, roles, and weights is optional.